SUPPORTING INFORMATION (SI)

Non-Fullerene Acceptors with Direct and Indirect Hexa-fluorination Afford >17 % Efficiency in Polymer Solar Cells

Guoping Li [a,#], **Liang-Wen Feng** [a,#], **Subhrangsu Mukherjee** [b], **Leighton O. Jones** [a], **Robert M. Jacobberger** [a], **Wei Huang** [a], **Ryan M. Young** [a,*], **Robert M. Pankow** [a], **Weigang Zhu** [a,d], **Norman Lu** [a,f], **Kevin L. Kohlstedt** [a,*], **Vinod K. Sangwan**,[c,*] **Michael R. Wasielewski** [a,*], **Mark C. Hersam** [a,c,*], **George C. Schatz** [a,*], **Dean M. DeLongchamp** [b,*], **Antonio Facchetti** [a,e,*], **and Tobin J. Marks** [a,c,*]

[a] Department of Chemistry, the Center for Light Energy Activated Redox Processes (LEAP), and the Materials Research Center (MRC), Northwestern University, 2145 Sheridan Road, Evanston, Illinois 60208, United States

[b] Material Measurement Laboratory, National Institute of Standards and Technology, Gaithersburg, Maryland 20899, United States

[c] Department of Materials Science and Engineering, and the Materials Research Center (MRC), Northwestern University, Evanston, Illinois 60208, United States

[d] Tianjin Key Laboratory of Molecular Optoelectronic Sciences (TJ-MOS), Department of Chemistry, School of Science, Tianjin University, Tianjin 300072, China

[e] Flexterra Corporation, 8025 Lamon Avenue, Skokie, Illinois 60077, United States

[f] Institute of Organic and Polymeric Materials, and Research and Development Center for Smart Textile, National Taipei University of Technology, Taipei 106, Taiwan

[#] Guoping Li and Liang-Wen Feng contributed equally to this work.

*To whom correspondence should be addressed. E-mail:
ryan.young@northwestern.edu(R.M.Y.)
kkohlstedt@northwestern.edu (K.L.K.);
vinod.sangwan@northwestern.edu (V.K.S.);
m-wasielewshi@northwestern.edu (M.R.W.);
g-schatz@northwestern.edu (G.C.S.);
m-hersam@northwestern.edu (M.C.H);
dean.delongchamp@nist.gov (D.M.D.);
a-facchetti@northwestern.edu (A.F.);
t-marks@northwestern.edu (T.J.M.)

Contents

1. Materials and Methods

All reagents and chemicals were purchased from commercial sources and were used without further purification unless noted otherwise. **PNDIT-F3N,** and **D18-Cl** were purchased from He (Henry) Yan group at HKUST and the eFlexPV, Inc. All solvents were purified by a Pure Process Technology solvent purification system prior to using. Nuclear magnetic resonance (NMR) spectra were recorded on Bruker Avance III (FT, 500 MHz, ^{1}H; 470 MHz, ^{19}F, 126MHz ^{13}C) spectrometers at ambient temperature. The mass spectra of the samples were recorded on Bruker Impact-II high-resolution spectrometer using electrospray ionization (ESI) and atmospheric pressure photoionization ionization (APPI) with methanol as the eluent. Differential scanning calorimetry (DSC) measurements were performed on an In-calibrated TAInstruments DSC250. The samples (weight range 2.0 – 3.0 mg) were placed in lidded 40 µL Al-pans with a heating/cooling rate of 10 °C/min under an N_2 flow. All data shown in the text are reported from the first thermal cycle. Note that certain commercial equipment, instruments, or materials are identified in this paper to specify the experimental procedure adequately. Such identification is not intended to imply recommendation or endorsement by NIST, nor is it intended to imply that the materials or equipment identified are necessarily the best available for the purpose.

2. Materials Synthesis

Scheme S1. Synthesis of 3F-LIC, mix.
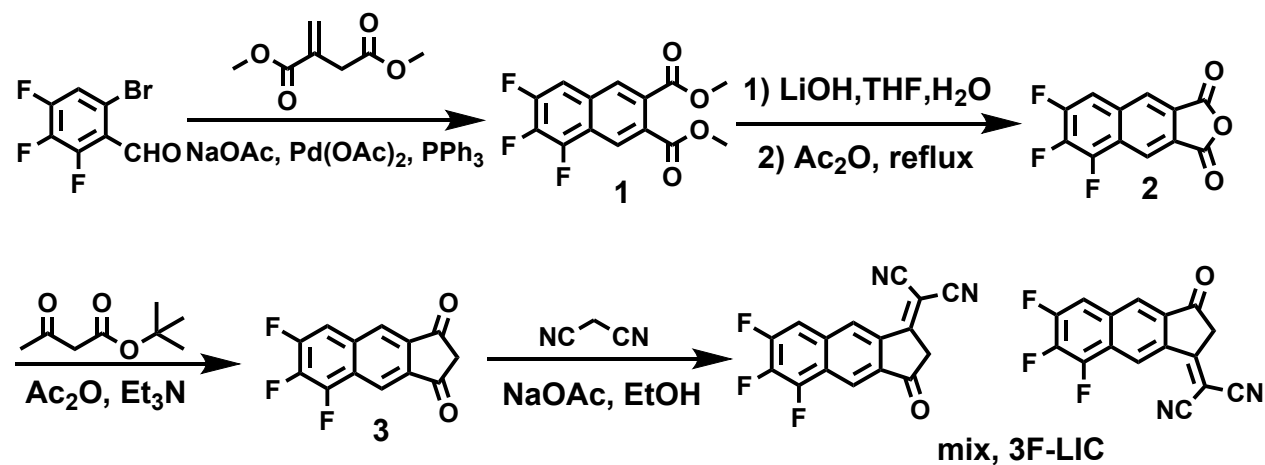
1: The regents 3,4,5-trifluoro-2-bromobenzaldehyde (4.0g, 16.3 mmol, 1 equiv), dimethyl itaconate (2.84 g, 18 mmol, 1.1 equiv), and sodium acetate (4.0 g, 49 mmol, 3 equiv) were mixed in 120 mL THF. The resulting solution was degassed by N_2 bubbling for 20 min. The Pd(OAc)$_2$ (183 mg, 0.82 mmol, 0.05 equiv) and PPh$_3$ (428 mg, 1.6 4 mmol, 0.1 equiv) was then added to the degassed the solution. The mixture was heated to 120 °C for 24h. The solution was then filtered to remove the precipitate, and the filtrate solvent was removed by evaporation. The residue was purified by column chromatography (EtOAc: Hexane 1:1). 2,3-Dimethyl-5,6,7-trifluoro-2,3-naphthalene-dicarboxylate **(1)** was obtained (2.8g, 57 %). ^{1}H NMR (500 MHz, CDCl$_3$) δ 8.47 (1H, s), 8.18 (1H, s), 7. 50(1H, dt), 3.98 (3H, s), 3.97 (3H, s). ^{13}C NMR (126 MHz, CDCl$_3$) δ 167.36, 152.89, 150.76, 147.53, 145.40, 140.26, 138.22, 130.31, 129.19, 128.96, 128.78, 121.53, 109.57, 52.96. ^{19}F NMR (470 MHz, CDCl$_3$δ -129.30, 141.73, 156.30.

Calcd for [C14H9F3O4], m/z = 298.05; Found [ESI]: m/z = 321.01 [M+Na]$^+$.

2: The reagents 2,3-dimethyl-4,5,6-trifluoro-2,3-naphthalenedicarboxylate **(1)** (1.50 g, 5.0 mmol) and lithium hydroxide (480 mg, 20.1 mmol) were mixed in a THF/water solution (150mL, 2:1 vol). The resulting solution was heated to 40 °C for 5h. The solution was then acidified with hydrochloric acid and extracted by ethyl acetate. The ethyl acetate was then removed by vacuum and the crude white powder was used directly without further purification. The white powder was then dissolved in 30 mL acetic anhydride and heated at reflux for 2h. Then the excessive acetic hydride was removed under vacuum and the white residue was dried under vacuum The crude product 4,5,6-trifluoronaphtho[2,3-c]furan-1,3-dione **(2)** (1.21 g, 96%) was used directly for the next step without further purification.

3: The product 4,5,6-trifluoronaphtho[2,3-c]furan-1,3-dione **(2)** (1.21 g, 4.8 mmol, 1 equiv.) obtained from the previous step and tert-butyl acetoacetate (3.8 g, 24.0 mmol, 5 equiv.) were dissolved in 40 mL acetic anhydride and were stirred for 20 min at room temperature. Then, 10 mL triethylamine was slowly added to the solution at room temperature. After the addition, the solution

was stirred at room temperature overnight. The resulting dark solution was then poured into ice-water and filtered. The precipitate was mixed with 100mL 1M hydrochloric acid and stirred for 3h at 50 °C. The orange-yellow powder was collected by filtration and purified by column chromatography (DCM) to afford 5,6,7-trifluoro-1H-cyclopenta[b]naphthalene-1,3(2H)-dione **(3)** (910 mg, 71 %). ^{1}H NMR (400 MHz, CDCl$_3$) δ 8.76(1H, s), 8.46 (1H, s), 7.70 (1H, dt), 3.41 (2H, s). ^{13}C NMR (126 MHz, CDCl$_3$) δ 196.37, 153.47, 151.41, 148.70, 146.64, 140.94, 139.31, 138.34, 131.87, 124.99, 123.42, 117.46, 111.05, 46.46. ^{19}F NMR (376 MHz, CDCl$_3$) δ -126.39, 139.59, 153.35.

Calcd for [C13H5F3O2], m/z = 250.02; Found [ESI]: m/z = 248.81 [M-H]$^-$

3F-LIC, isomeric mixture: Compound **3** (400 mg, 1.6 mmol, 1 equiv) was dissolved in 10 mL of ethanol. Then malononitrile (1.05 g, 16 mmol, 10 equiv) was added to the solution and the solution was kept at room temperature for 20 min. Sodium acetate (660 mg, 8.0 mmol, 5 equiv) was then added in two portions, and the solution was stirred at room temperature overnight. The resulting deep red solution was poured into water, acidified with concentrated hydrochloric acid, and filtered to collect the precipitate. The precipitate was purified by column chromatography (DCM) to afford 2-(5/6,6/7,7/8-trifluoro-3-oxo-2,3-dihydro-1H-cyclopenta[b]naphthalen-1-ylidene)malononitrile **(3F-LIC, mix)** as a mixture of two isomers. (235 mg, 49 %). ^{1}H NMR (500 MHz, CDCl$_3$) δ 9.40-9.13 (1H, s), 8.72-8.44 (1H, s), 7.76 (1H, m), 3.82 (2H, s). ^{13}C NMR (126 MHz, CDCl$_3$) δ 194.44, 194.11, 165.35, 165.10, 154.26, 153.88, 152.19, 151.82, 148.64, 148.20, 146.50, 146.09, 141.61, 139.38, 137.67, 136.71, 135.77, 131.82, 131.05, 126.80, 124.94, 124.17, 120.46, 118.96, 112.25, 111.23, 80.24, 44.33. ^{19}F NMR (470 MHz, CDCl$_3$) δ -124.34, -124.77, -138.15, -139.28, -151.37, -151.78.

Calcd for [C16H5F3N2O], m/z = 298.04; Found [ESI]: m/z = 296.84 [M-H]$^-$

Scheme S2. Synthesis of CF3-LIC, mixture.
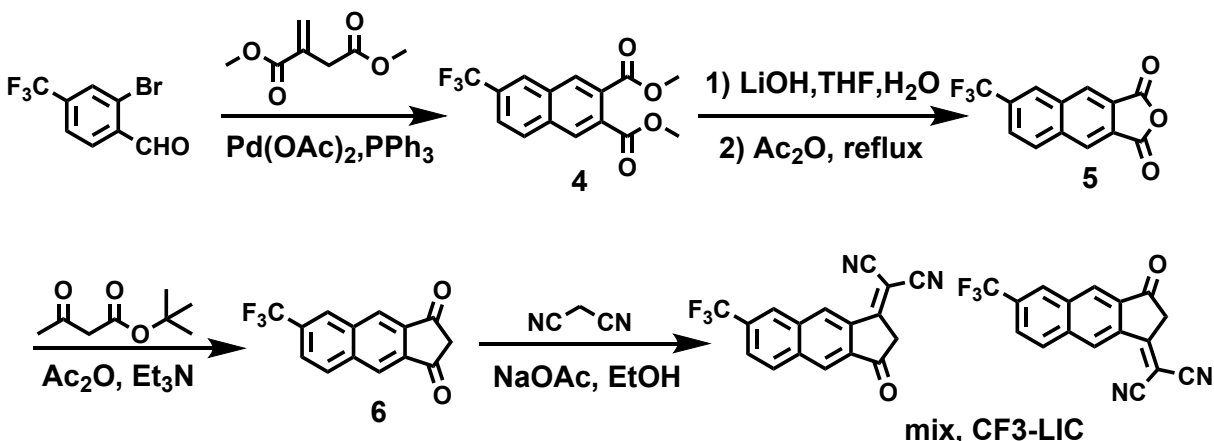
4: The reagents 4-trifluormethyl-2-bromobenzaldehyde (5.0g, 19.7 mmol, 1 equiv) and dimethyl itaconate (3.8 g, 23.7 mmol, 1.2 equiv) and sodium acetate (4.9 g, 59 mmol, 3 equiv) were mixed in 150 mL THF. The resulting solution was degassed by N_2 bubbling for 20 min. The Pd(OAc)$_2$ (222 mg, 0.99 mmol, 0.05 equiv) and PPh$_3$ (518 mg, 1.98 mmol, 0.1 equiv) was then added to the degassed the solution. The mixture was heated to 120 °C for 24h. The solution was then filtered to remove the precipitate, and the filtrate solvent was removed by evaporation. The residue was purified by column chromatography (EtOAc: Hexane 1:1). 2,3-Dimethyl-6-trifluorometyl-2,3-naphthalenedicarboxylate **(4)** was obtained (3.3g, 54 %). ^{1}H NMR (500 MHz, CDCl$_3$) δ 8.37(1H, s), 8.30 (1H, s), 8.24 (1H, s), 8.06 (1H, d), 7.81 (1H, d), 3.98 (6H, s). ^{13}C NMR (126 MHz, CDCl$_3$) δ 167.71, 167.43, 134.64, 132.29, 131.00, 130.90, 130.83, 130.75, 130.49, 130.23, 129.97, 129.85, 129.83, 129.75, 129.73, 129.70, 129.05, 128.23, 127.06, 126.40, 126.37, 126.33, 126.29, 126.26, 124.89, 124.33, 124.19, 122.72, 120.55, 53.24, 53.03, 53.01, 52.81, 52.79, 52.58. ^{19}F NMR (470 MHz, CDCl$_3$) δ -62.72.

Calcd for [C15H11F3O4], m/z = 312.06; Found [ESI]: m/z = 335.06 [M+Na]$^+$.

5: The reagents 2,3-dimethyl-6-trifluorometyl-2,3-naphthalenedicarboxylate **(4)** (3.3 g, 10.6 mmol, 1 equiv.) and lithium hydroxide (1.0 mg, 41.6 mmol, 4 equiv) were mixed in THF/water solution (150mL, 2:1 vol). The resulting solution was heated to 40 °C for 5h. The solution was then acidified with hydrochronic acid and extracted by ethyl acetate. The ethyl acetate was then removed by vacuum and the crude white powder was used directly without further purification. The white powder was then dissolved in 30 mL acetic anhydride and heat to reflux for 2h. Then the excessive acetic hydride was then removed by vacuum and the white residue was dried over vacuum The crude product of 6-(trifluoromethyl)naphtho[2,3-c]furan-1,3-dione **(5)** (2.8 g, quantitative) was used directly for the next step without further purification.

6: The product 6-trifluoromethylnaphtho[2,3-c]furan-1,3-dione **(5)** (2.5 g, 9.6 mmol) obtained from the previous step and tert-butyl acetoacetate (7.6 g, 48.0 mmol) were dissolved in 80 mL acetic

anhydride and were stirred for 20min at room temperature. Then, 20 mL triethylamine was slowly added to the solution at room temperature. After the addition, the solution was stirred at room temperature overnight. The resulting dark solution was poured into ice-water and filtered. The precipitate was mixed with 1M hydrochloric acid 100mL and stirred for 3h at 50 °C. Then the orange-yellow powder was filtered and purified by column chromatography (DCM) to afford 6-(trifluoromethyl)-1H-cyclopenta[b]naphthalene-1,3(2H)-dione **(6)** (1.2 g, 50 %). ^{1}H NMR (400 MHz, CDCl$_3$) δ 8.76(1H, s), 8.46 (1H, s), 7.70 (1H, dt), 3.41 (2H, s). ^{13}C NMR (126 MHz, CDCl$_3$) δ 196.37, 153.47, 151.41, 148.70, 146.64, 140.94, 139.31, 138.34, 131.87, 124.99, 123.42, 117.46, 111.05, 46.46. ^{19}F NMR (376 MHz, CDCl$_3$) δ -126.39, 139.59, 153.35.

Calcd for [C13H5F3O2], m/z = 264.04; Found [ESI]: m/z = 262.83 [M-H]$^-$

CF3-LIC isomeric mixture: Compound (**6**) (1.0 g, 3.8 mmol, 1 equiv.) was dissolved in 20 mL of ethanol. Then malononitrile (0.75 g, 11.4 mmol. 3 equiv) was added to the solution and the solution was kept at room temperature for 20 min. Sodium acetate (466 mg, 5.7 mmol, 1.5 equiv) was then added in two portions. The solution was stirred at room temperature overnight. The resulting deep red solution was poured to water, acidified by hydrochloric acid and filtered to collect the precipitate. The precipitate was purified by column chromatography (DCM) to afford 2-(3-oxo-6/7-(trifluoromethyl)-2,3-dihydro-1H-cyclopenta[b]naphthalen-1-ylidene)malononitrile as a mixture of two isomers. (**CF3-LIC, mix,** 235 mg, 49 %). ^{1}H NMR (500 MHz, CDCl$_3$) δ 9.30-9.25 (1H, s), 8.59-8.55 (1H, s), 8.46- 8.40 (1H, s), 8.28- 8.26 (1H, d), 7.95-7.93 (1H, m), 3.90 (2H, s). ^{13}C NMR (126 MHz, CDCl$_3$) δ 194.79, 194.61, 165.74, 165.62, 138.15, 137.45, 137.34, 137.18, 136.72, 136.52, 135.27, 134.64, 132.66, 132.44, 132.39, 132.17, 132.13, 131.91, 131.87, 131.75, 131.70, 128.81, 128.20, 128.17, 128.13, 128.09, 128.04, 128.01, 127.97, 127.75, 126.70, 126.63, 126.24, 126.22, 125.96, 125.94, 125.92, 125.89, 125.66, 124.46, 112.35, 112.33, 111.99, 111.97, 80.18, 79.97, 44.45. ^{19}F NMR (376 MHz, CDCl$_3$) δ -63.07, -63.08.

Calcd for [C16H5F3N2O], m/z = 312.05; Found [ESI]: m/z = 310.86 [M-H]$^-$

Scheme S3. Synthesis of **BTF** by Knoevenagel condensation.
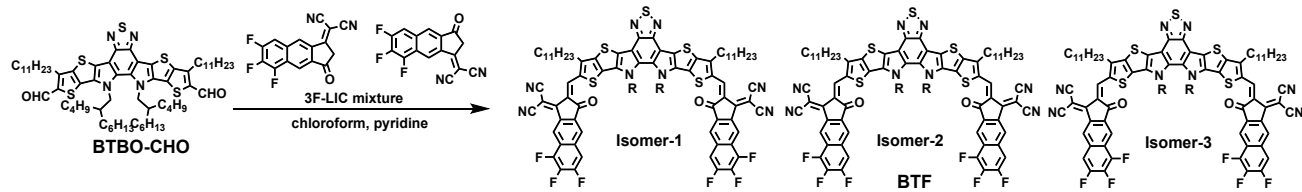
The BTBO-CHO (100 mg, 0.087 mmol, 1 equiv) and 3F-LIC mixture (105 mg, 0.35 mmol, 4 equiv) were mixed in 10 mL chloroform. Then 0.3 mL pyridine was slowly added to the mixture. The resulting solution was stirred at 60 °C overnight. Then the solution was precipitated in methanol and filtered to collect the precipitate. The precipitate was then purified by column chromatography using chloroform as eluent (85 mg, 58 %, mixture of 3 isomers, isomer-1: isomer-2: isomer-3 ≈ 1:2:1 estimated by H-NMR) ^{1}H NMR (500 MHz, CDCl$_3$) δ 9.43-9.15 (1H, s), 9.30 (1H, s) ,8.62-8.32 (1H, s), 7.68 (1H, m), 4.80 (2H, d), 3.28 (2H, t), 2.15 (1H, d), 1.91(2H, p), 1.42-0.67 (43H, m, alkyl-proton). ^{19}F NMR (470 MHz, CDCl$_3$) δ -127.40, -127.55, -139.01, -140.83, -154.18, -154.29.

Calcd for [C98H104F6O2N8S5], m/z = 1698.6790 Found: m/z[HR-APPI]: = 1699.6863 [M+H]$^+$

Scheme S4. Synthesis of **BTFM** by Knoevenagel condensation.
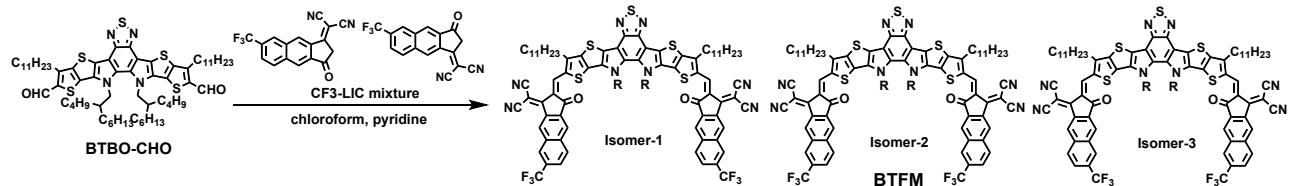
The BTBO-CHO (100 mg, 0.087 mmol, 1 equiv) and (CF3-LIC, mix) (110 mg, 0.35 mmol, 4 equiv) were mixed in 10 mL chloroform. Then 0.2 mL pyridine was slowly added to the mixture. The resulting solution was stirring at 60 °C overnight. Then the solution was precipitated in methanol and filtered to collect the precipitate. The precipitate was then purified by column chromatography using (DCM:hexane = 3:1) as eluent (70 mg, 46 %, mixture of 3 isomers, isomer-1: isomer-2: isomer-3 ≈ 1:2:1 estimated by H-NMR) ^{1}H NMR (500 MHz, CDCl$_3$) δ 9.32-9.28 (1H, s), 9.31(1H, s), 8.48-8.44 (1H, s), 8.41-8.36 (1H, s), 8.22 (1H, m), 7.88-7.87(1H, s), 4.81(2H, d), 3.29(2H, t), 2.16(1H, d), 1.91(2H, p), 1.39-0.64(43H, m, alkyl-proton). ^{19}F NMR (470 MHz, CDCl$_3$) δ -62.78, -62.82.

Calcd for [C98H104F6O2N8S5], m/z = 1726.7103 Found: m/z[HR-APPI]: = 1727.7176 [M+H]$^+$

3. Mass Spectra and NMR Spectra
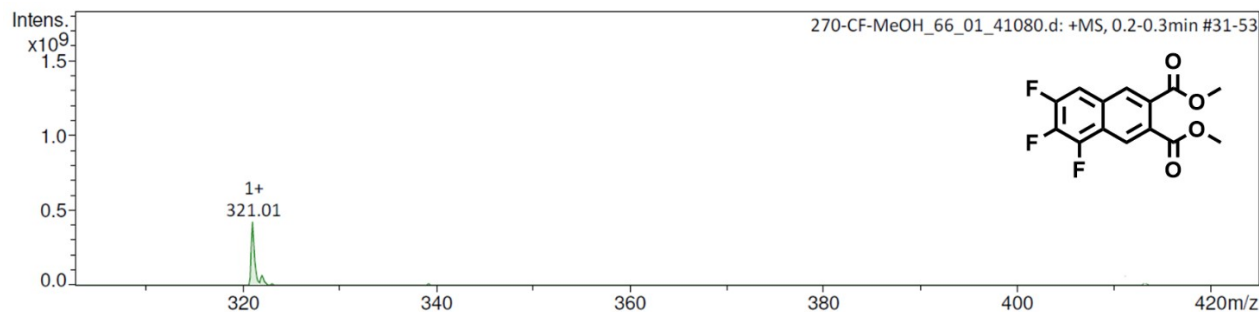
Figure S1. Mass spectrum of **1,** 2,3-Dimethyl-5,6,7-trifluoro-2,3-naphthalenedicarboxylate.
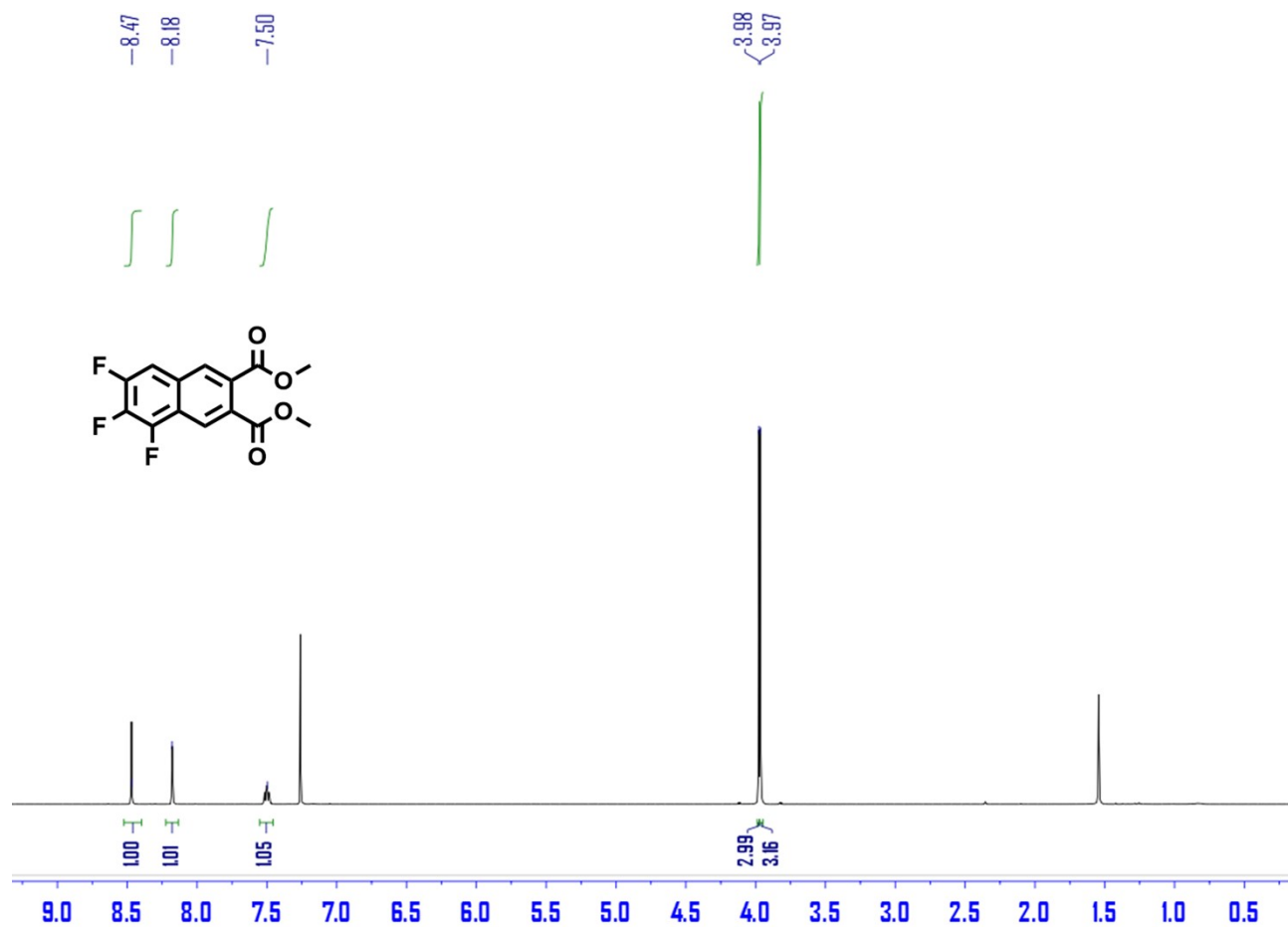
Figure S2. ^{1}H spectrum of **1,** 2,3-Dimethyl-5,6,7-trifluoro-2,3-naphthalenedicarboxylate in CDCl$_3$.
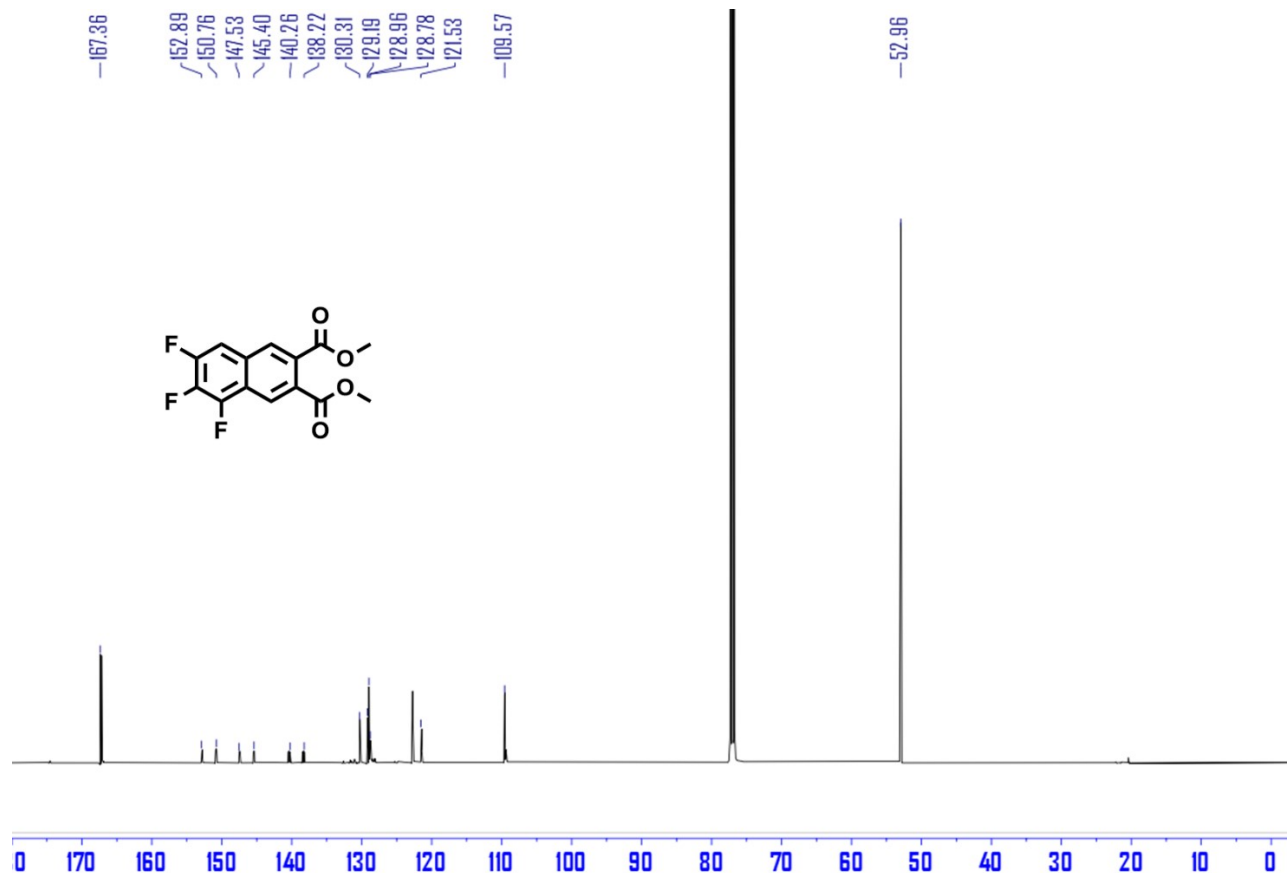
Figure S3. ^{13}C spectrum of **1,** 2,3-Dimethyl-5,6,7-trifluoro-2,3-naphthalenedicarboxylate in CDCl$_3$.
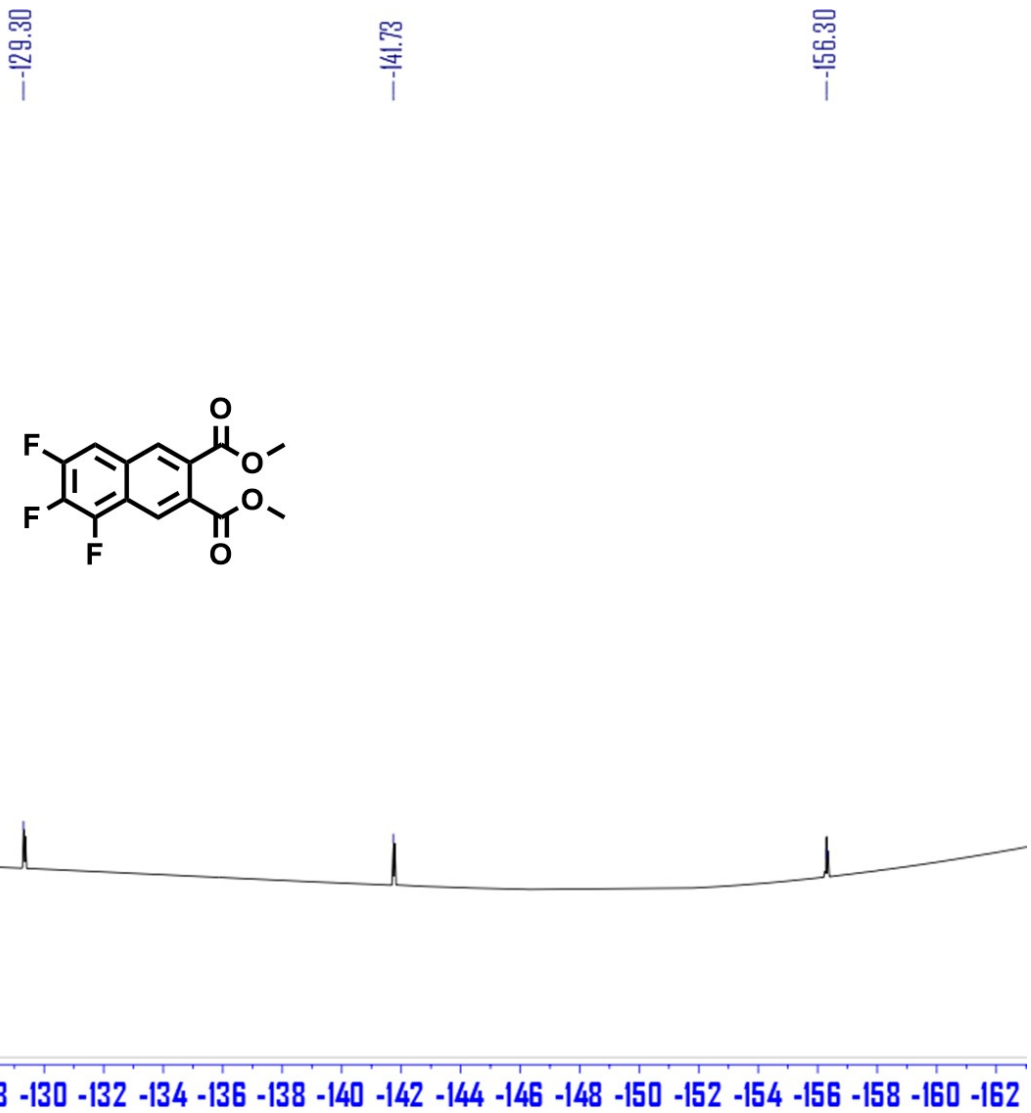
Figure S4. [19]F spectrum of **1,** 2,3-Dimethyl-5,6,7-trifluoro-2,3-naphthalenedicarboxylate in CDCl$_3$.
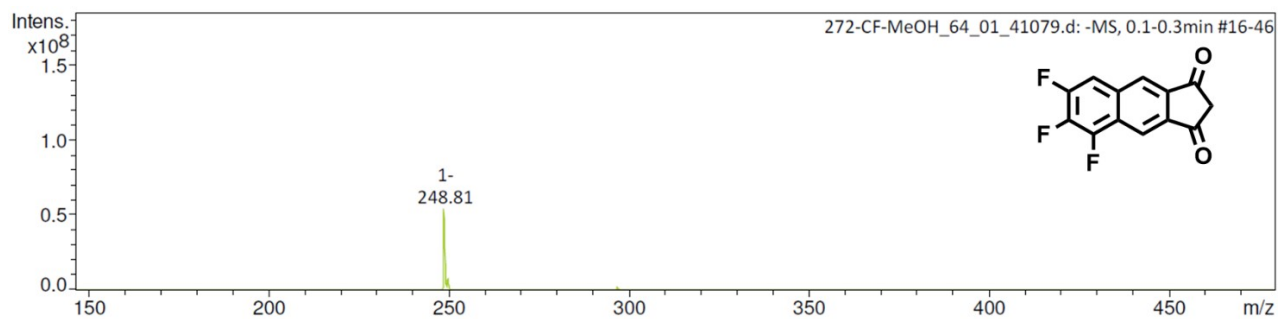
Figure S5. Mass spectrum of **3,** 5,6,7-trifluoro-1H-cyclopenta[b]naphthalene-1,3(2H)-dione
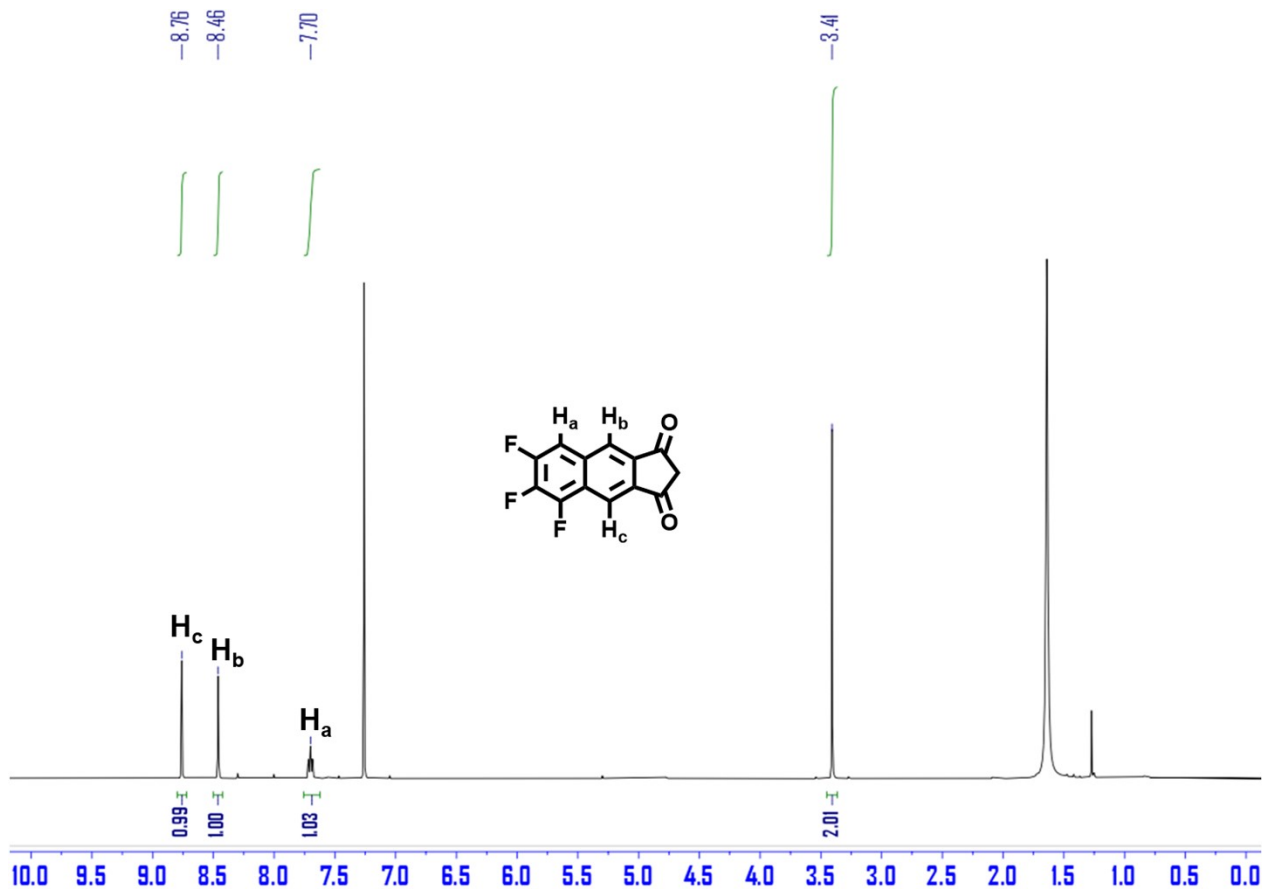
Figure S6. ^{1}H spectrum of **3,** 5,6,7-trifluoro-1H-cyclopenta[b]naphthalene-1,3(2H)-dione in CDCl$_3$.
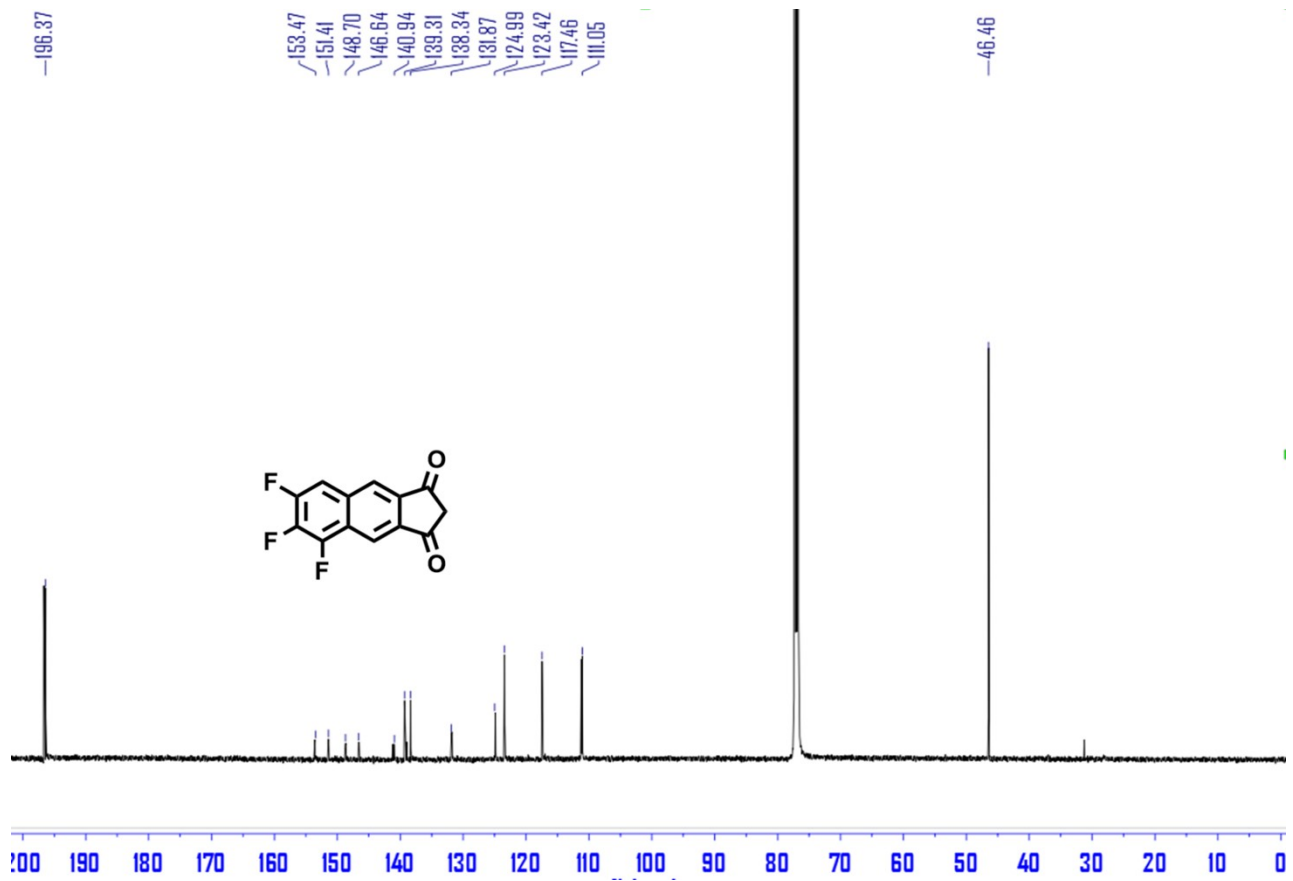
Figure S7. ^{13}C spectrum of **3,** 5,6,7-trifluoro-1H-cyclopenta[b]naphthalene-1,3(2H)-dione in CDCl$_3$.
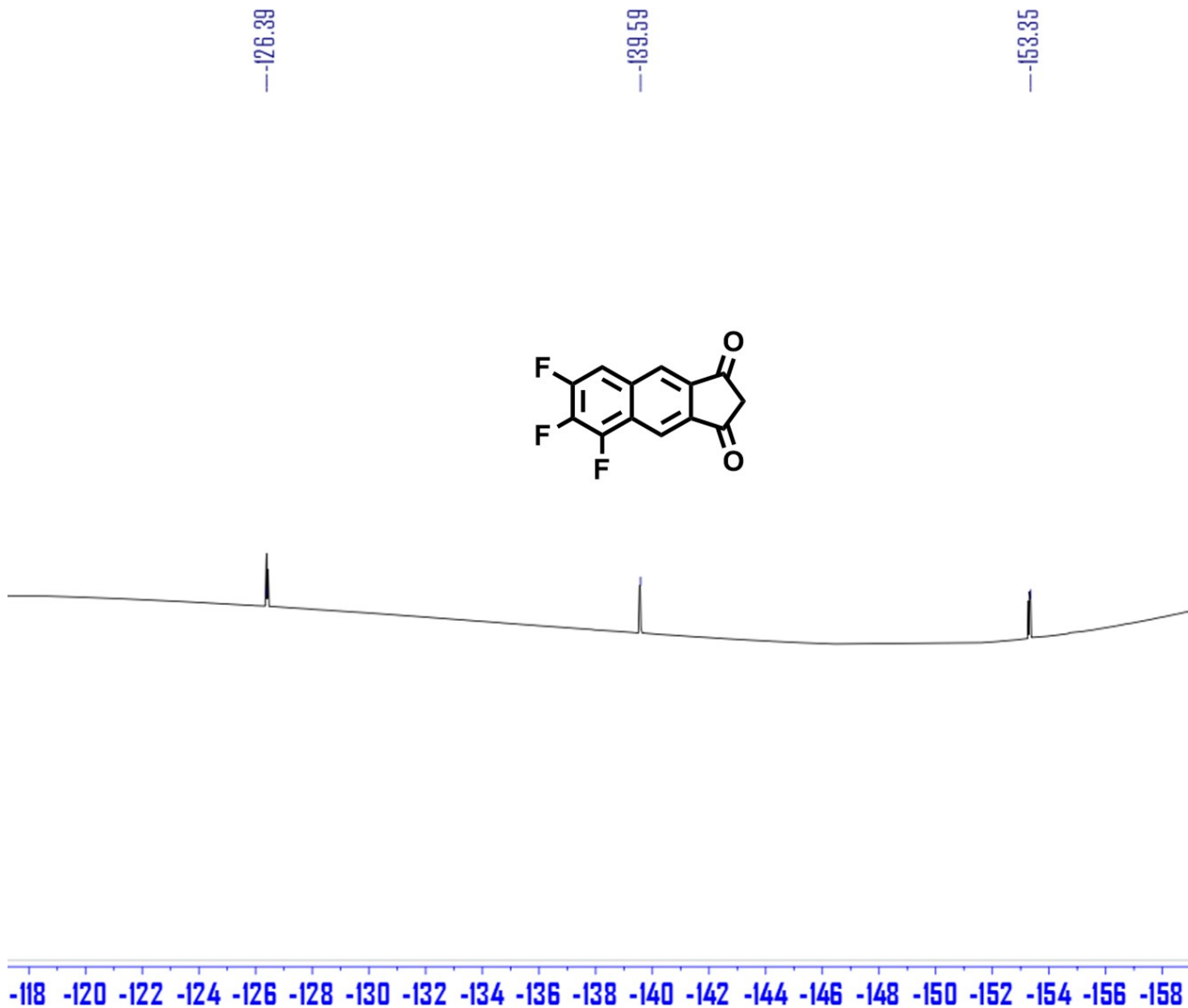
Figure S8. [19]F spectrum of **3,** 5,6,7-trifluoro-1H-cyclopenta[b]naphthalene-1,3(2H)-dione in CDCl$_3$.
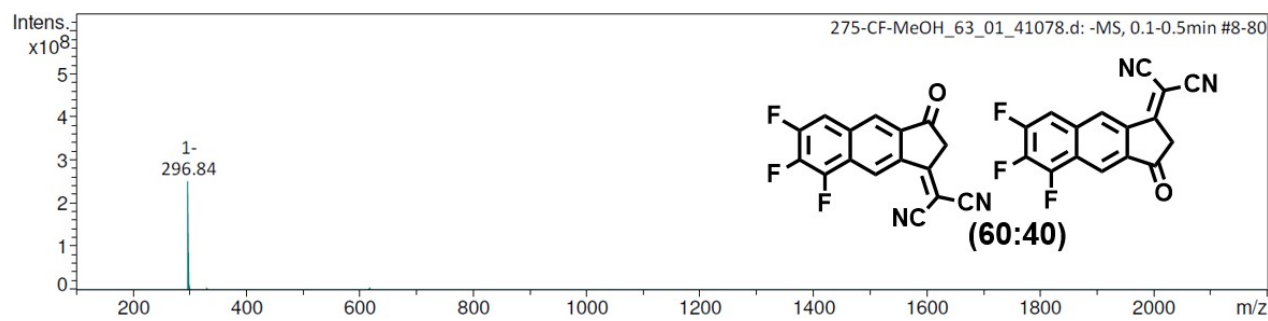
Figure S9. Mass spectrum of 3F-LIC mixture.
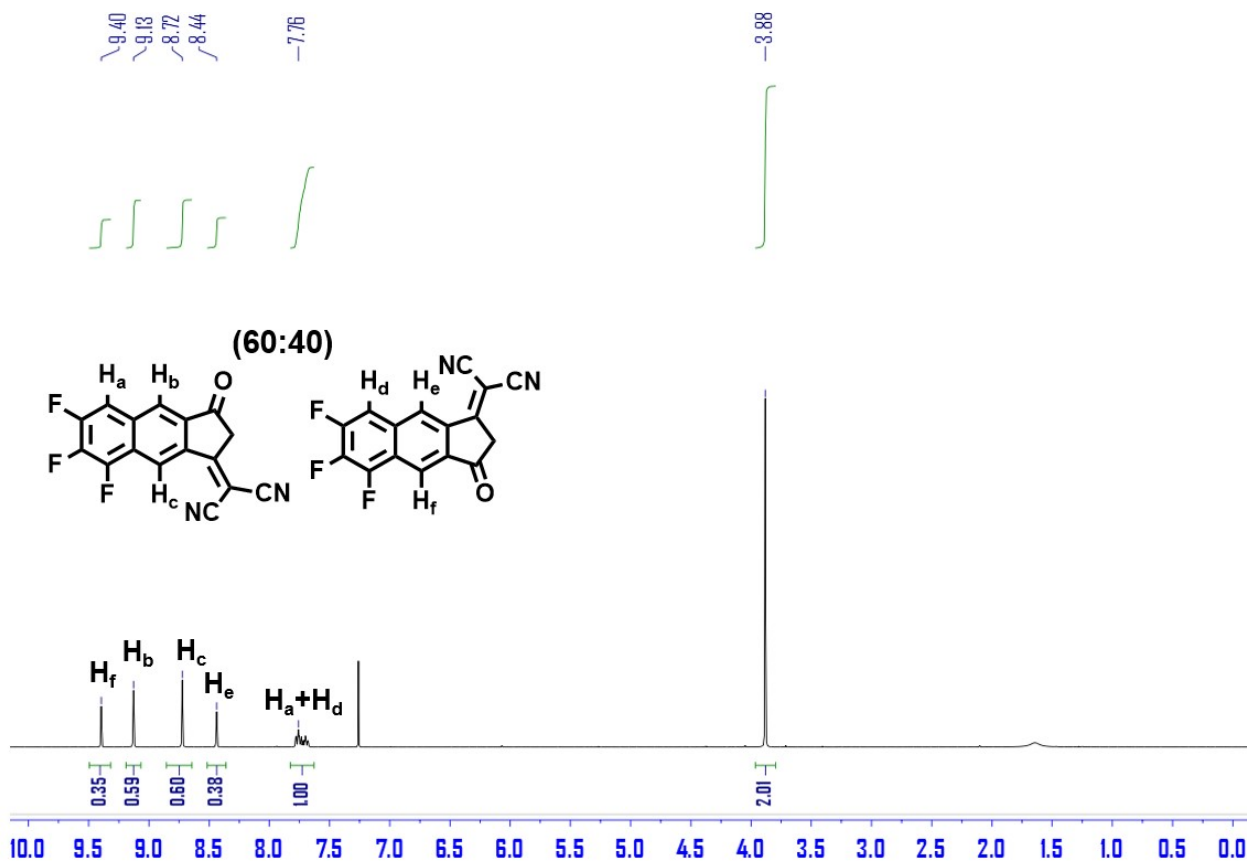
Figure S10. ¹H spectrum of 3F-LIC mixture, in CDCl₃.
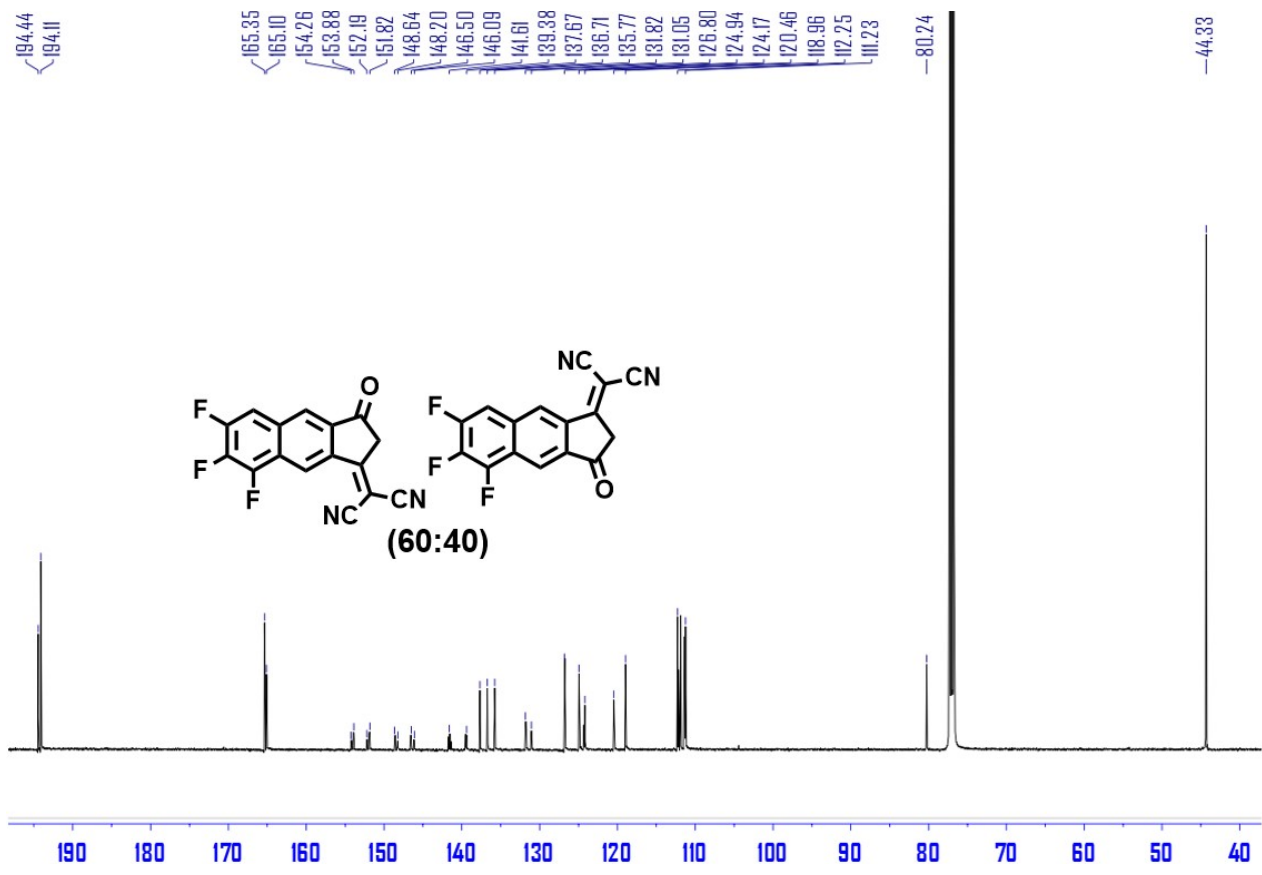
Figure S11. ^{13}C spectrum of 3F-LIC mixture, in CDCl$_3$.
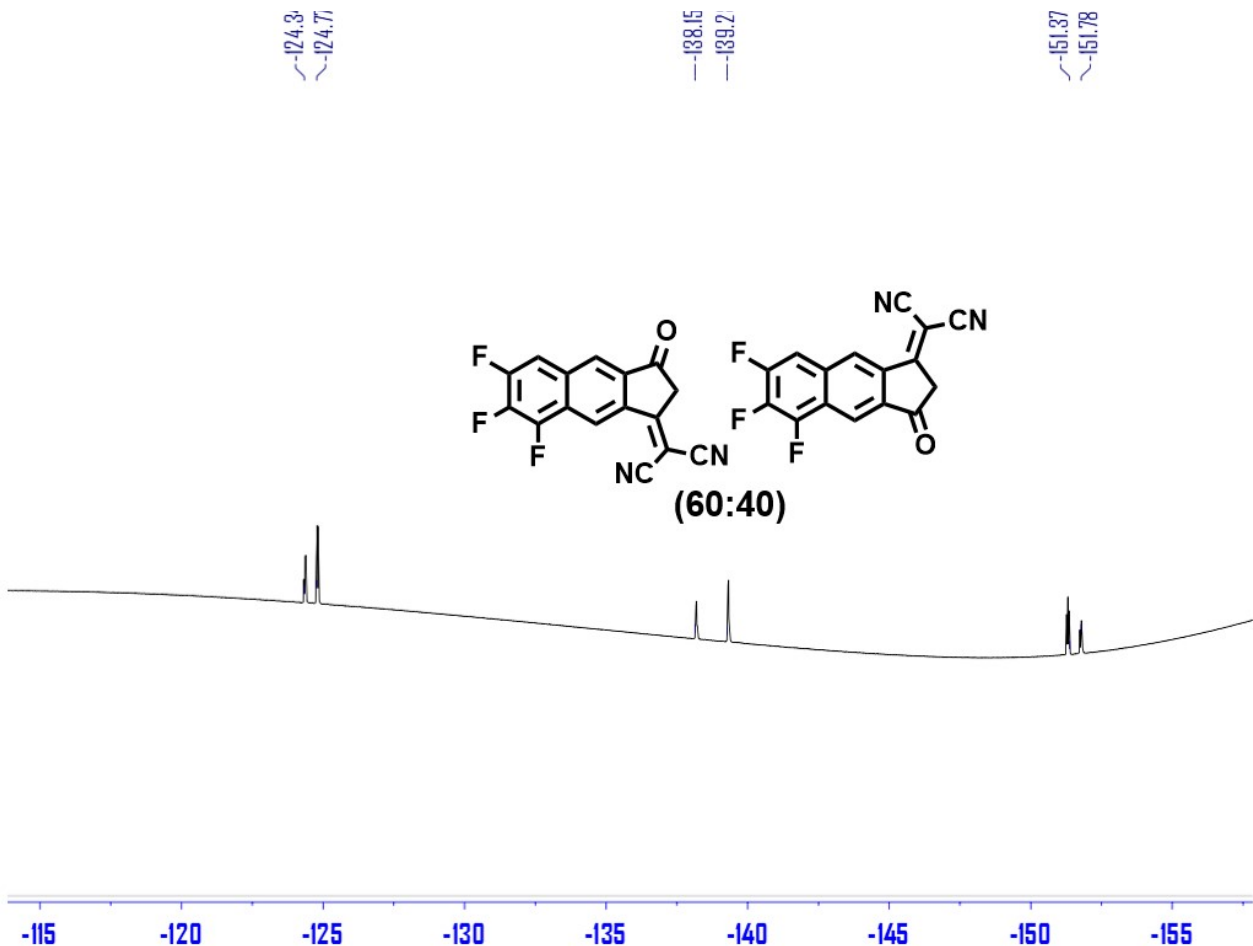
Figure S12. ^{19}F spectrum of 3F-LIC mixture, in $CDCl_3$.
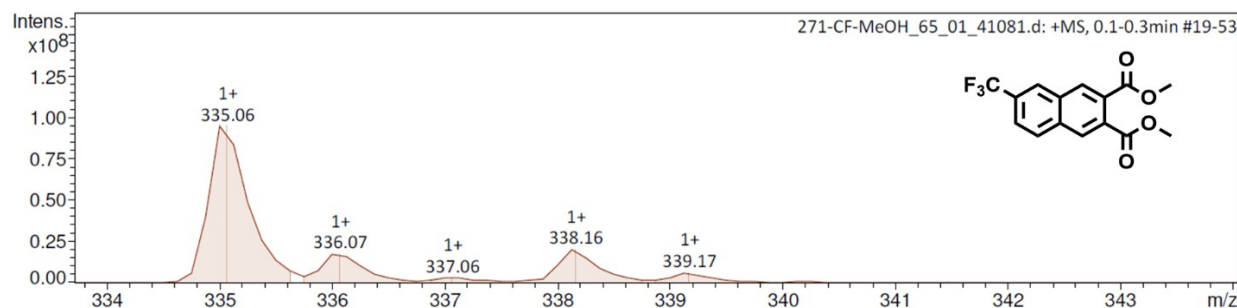
Figure S13. Mass spectrum of **4,** 2,3-Dimethyl-6-trifluorometyl-2,3-naphthalenedicarboxylate.
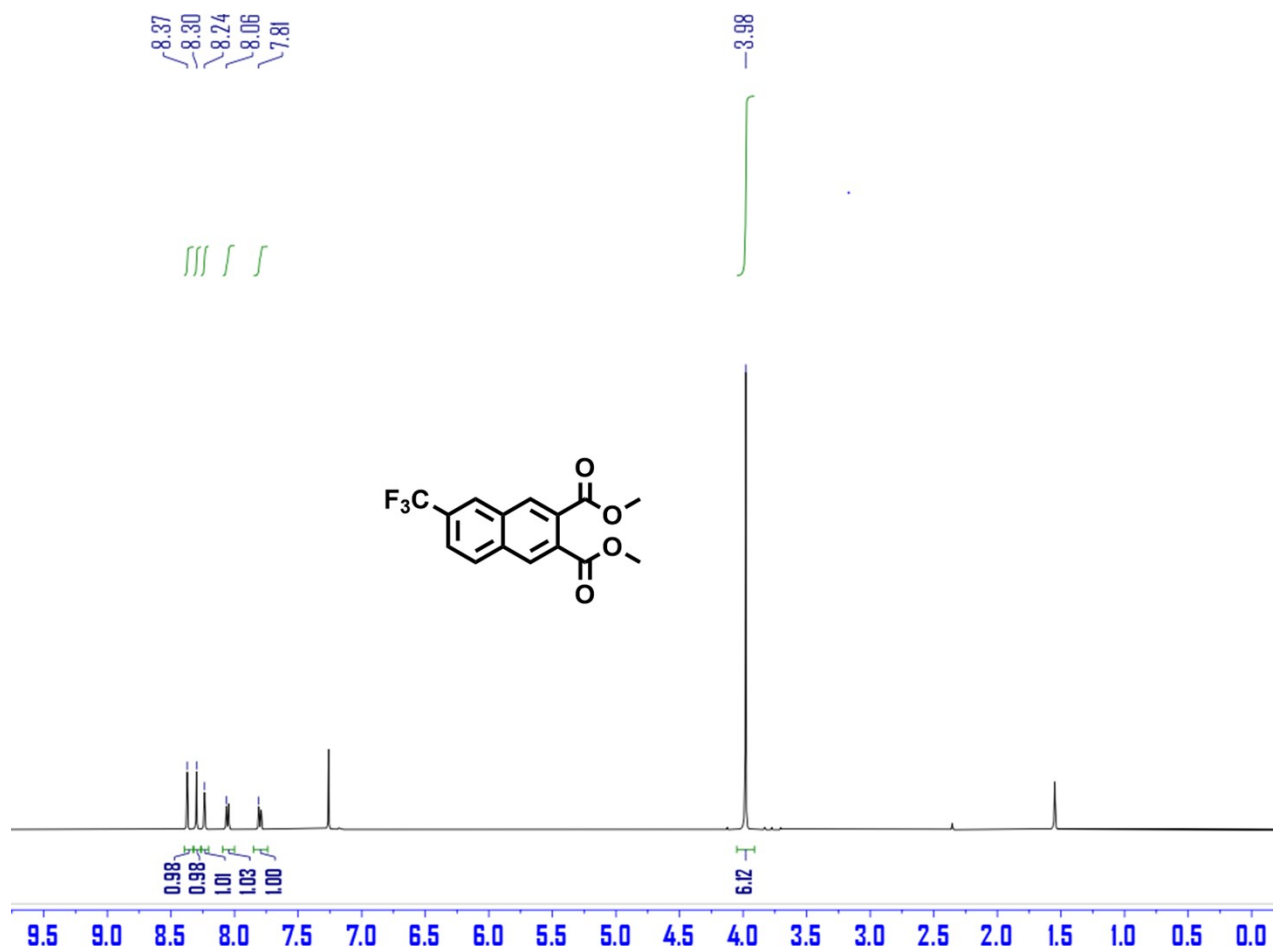

Figure S14. ¹H spectrum of **4,** 2,3-Dimethyl-6-trifluorometyl-2,3-naphthalenedicarboxylate in CDCl₃.
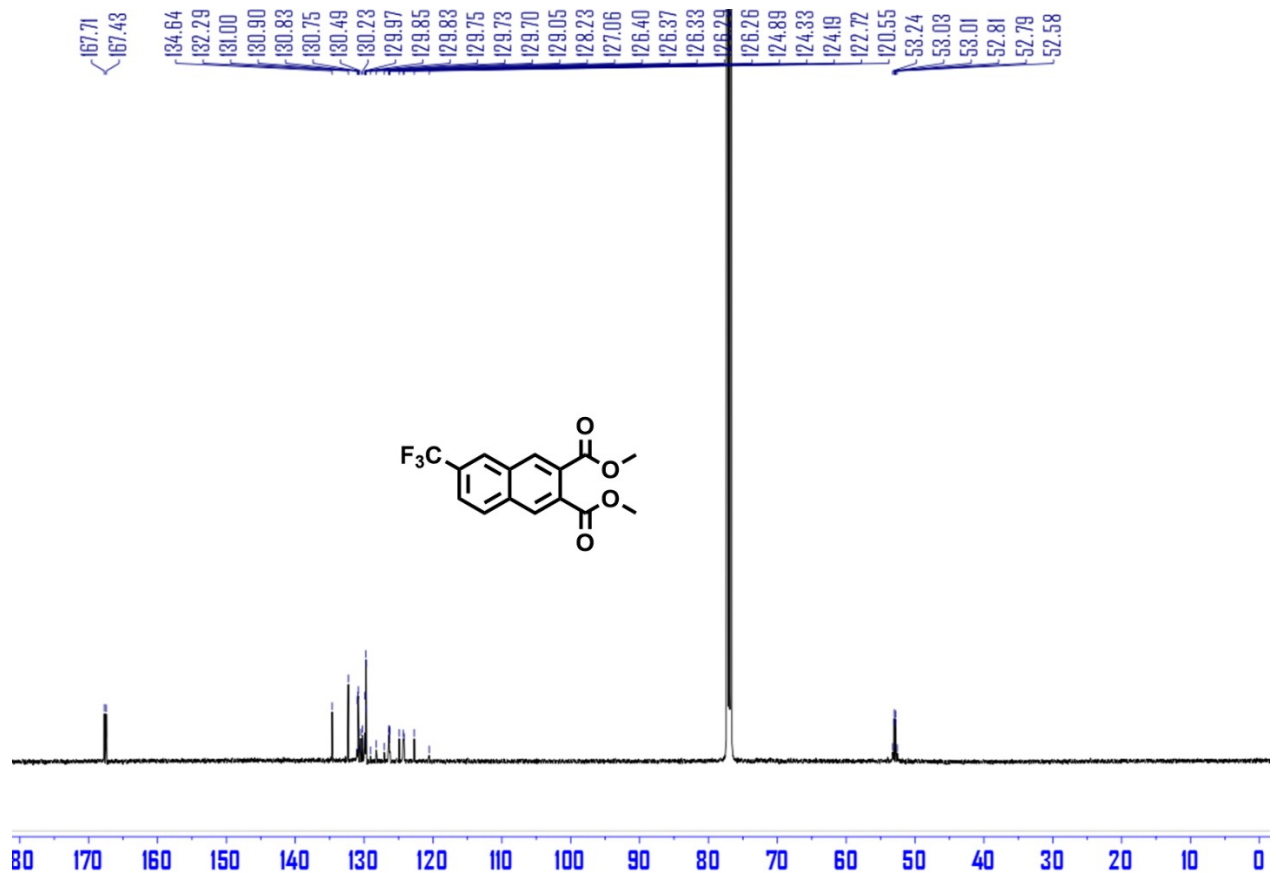
**Figure S15.** ¹³C spectrum of **4,** 2,3-Dimethyl-6-trifluorometyl-2,3-naphthalenedicarboxylate in CDCl₃.
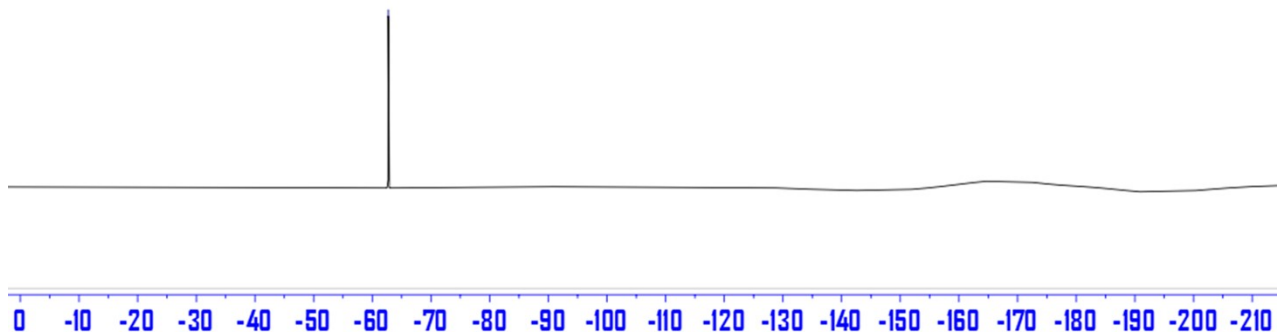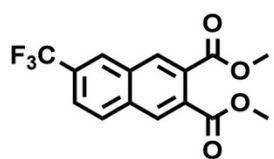
Figure S16. [19]F spectrum of **4,** 2,3-Dimethyl-6-trifluorometyl-2,3-naphthalenedicarboxylate in CDCl$_3$.
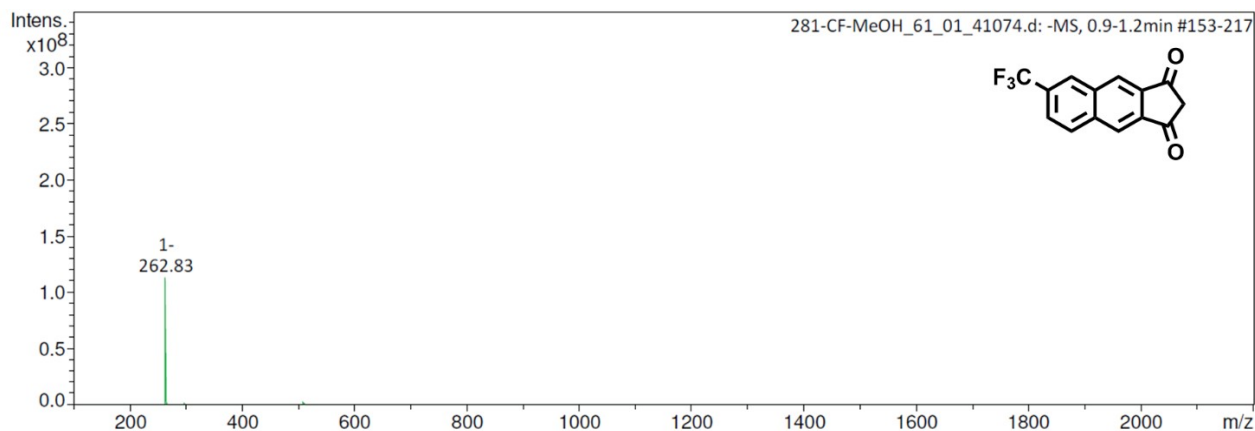
Figure S17. Mass spectrum of **6,** 2,3-Dimethyl-6-trifluorometyl-2,3-naphthalenedicarboxylate.
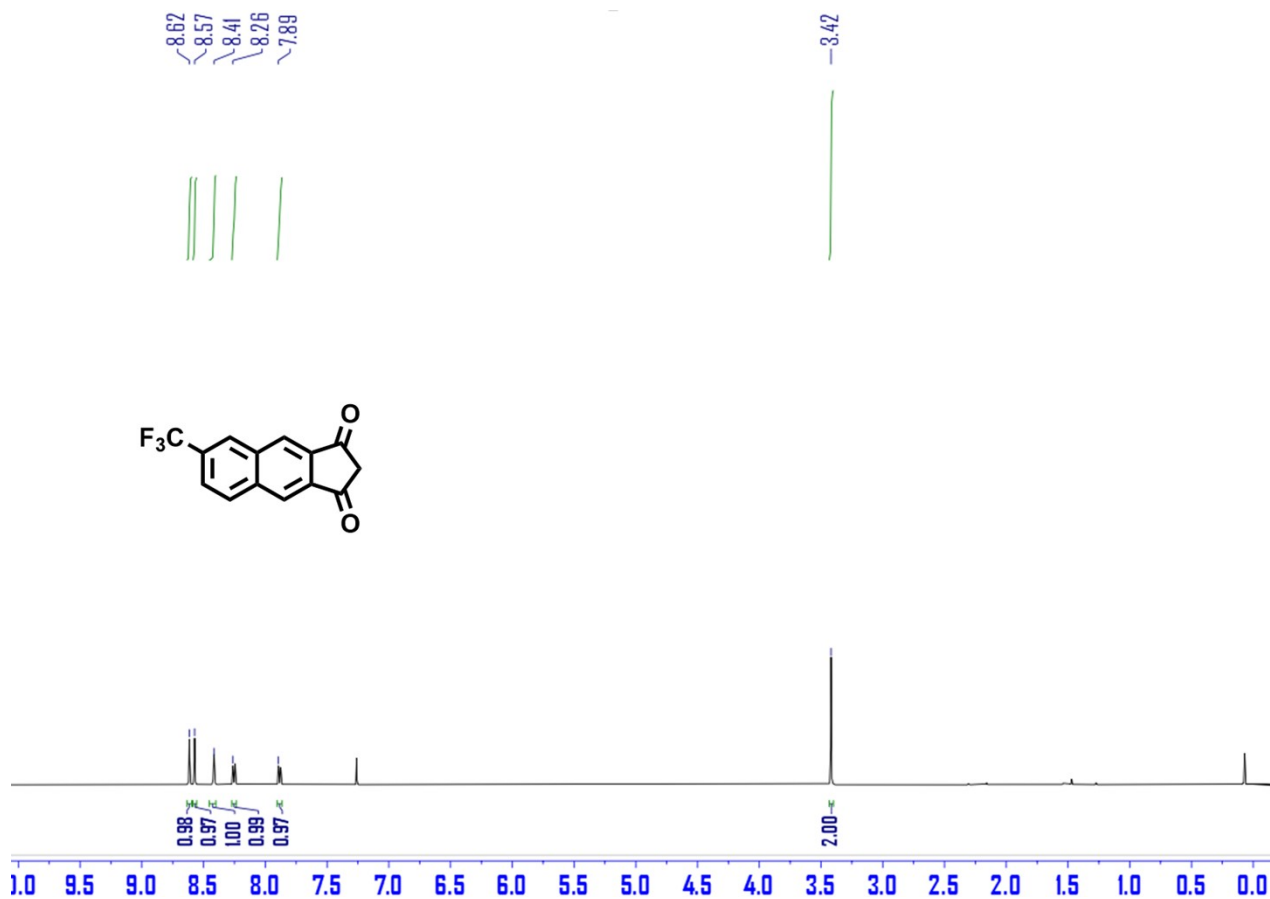
Figure S18. ¹H spectrum of **6,** 6-(trifluoromethyl)-1H-cyclopenta[b]naphthalene-1,3(2H)-dione in CDCl₃.
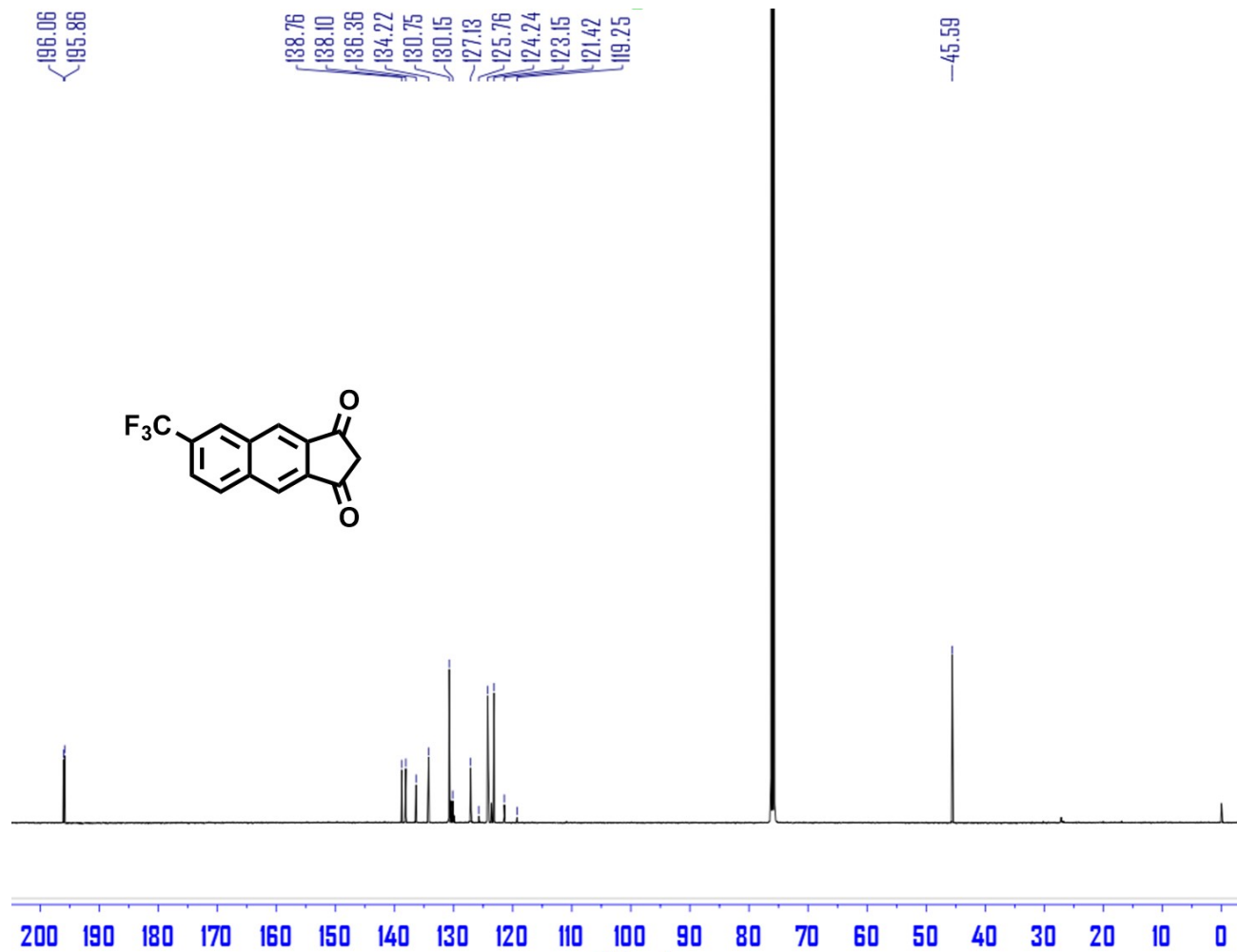
Figure S19. ^{13}C spectrum of **6,** 6-(trifluoromethyl)-1H-cyclopenta[b]naphthalene-1,3(2H)-dione in CDCl$_3$.
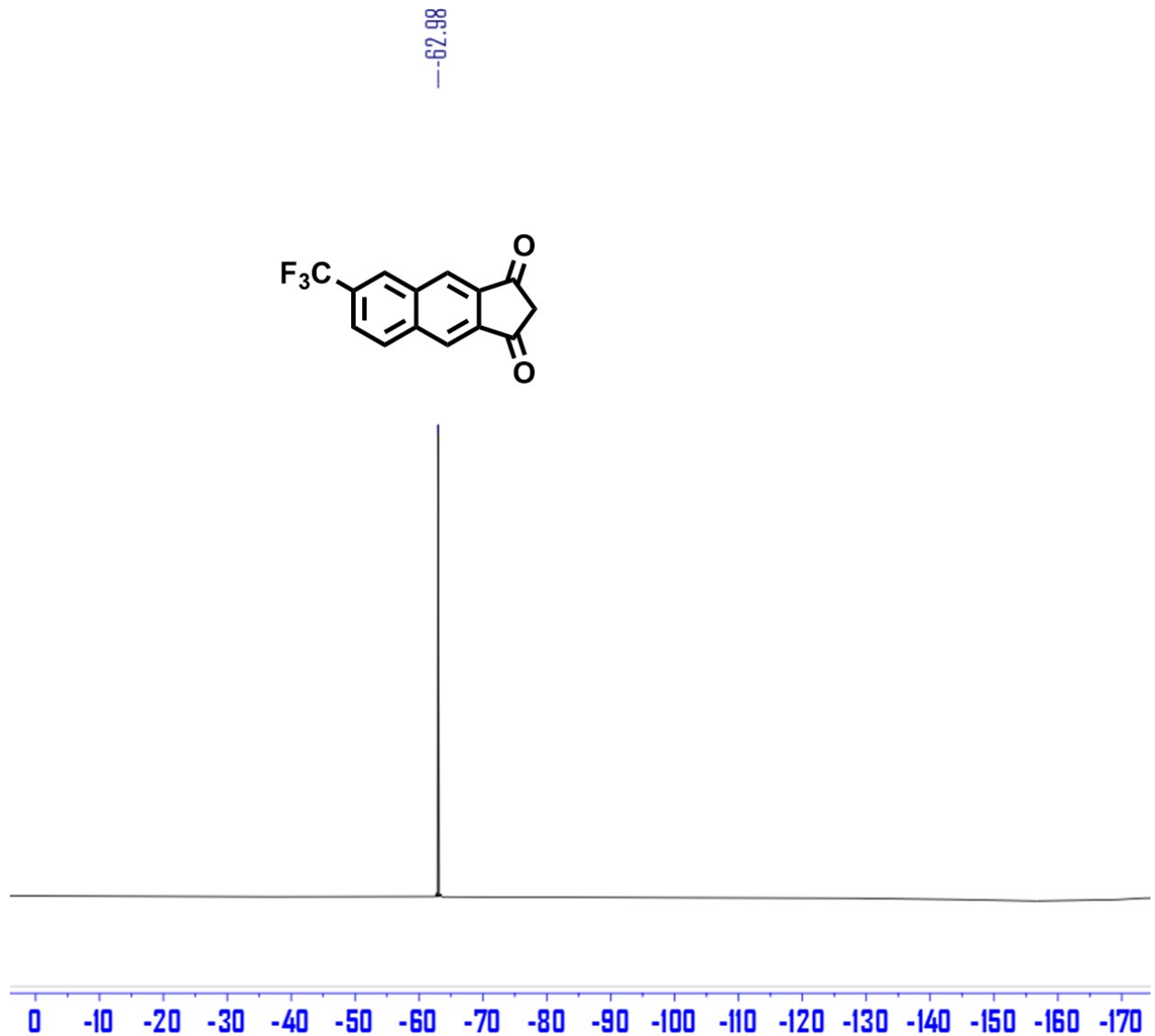
Figure S20. ^{19}F spectrum of **6,** 6-(trifluoromethyl)-1H-cyclopenta[b]naphthalene-1,3(2H)-dione in CDCl$_3$.
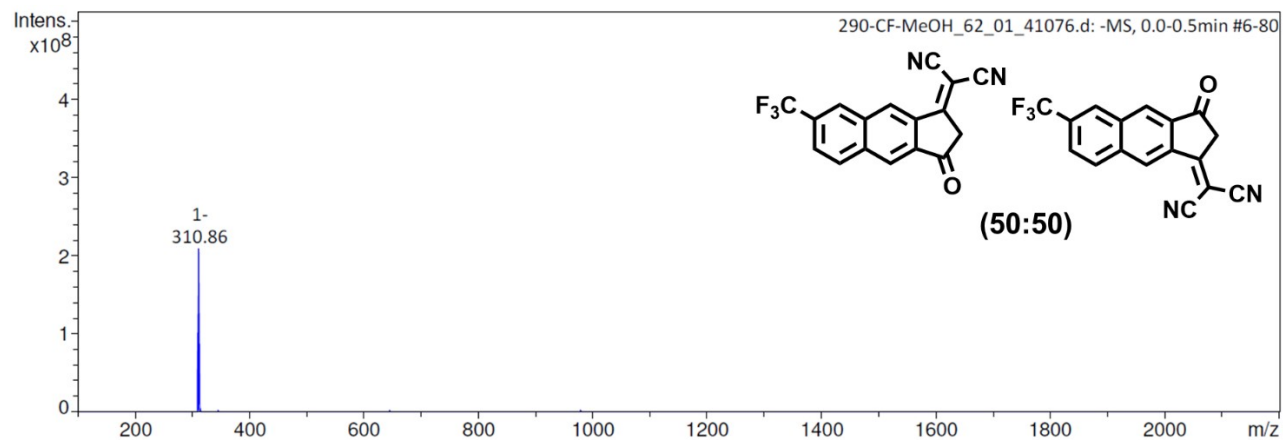
Figure S21. Mass spectrum of **CF3-LIC**, **mix**.
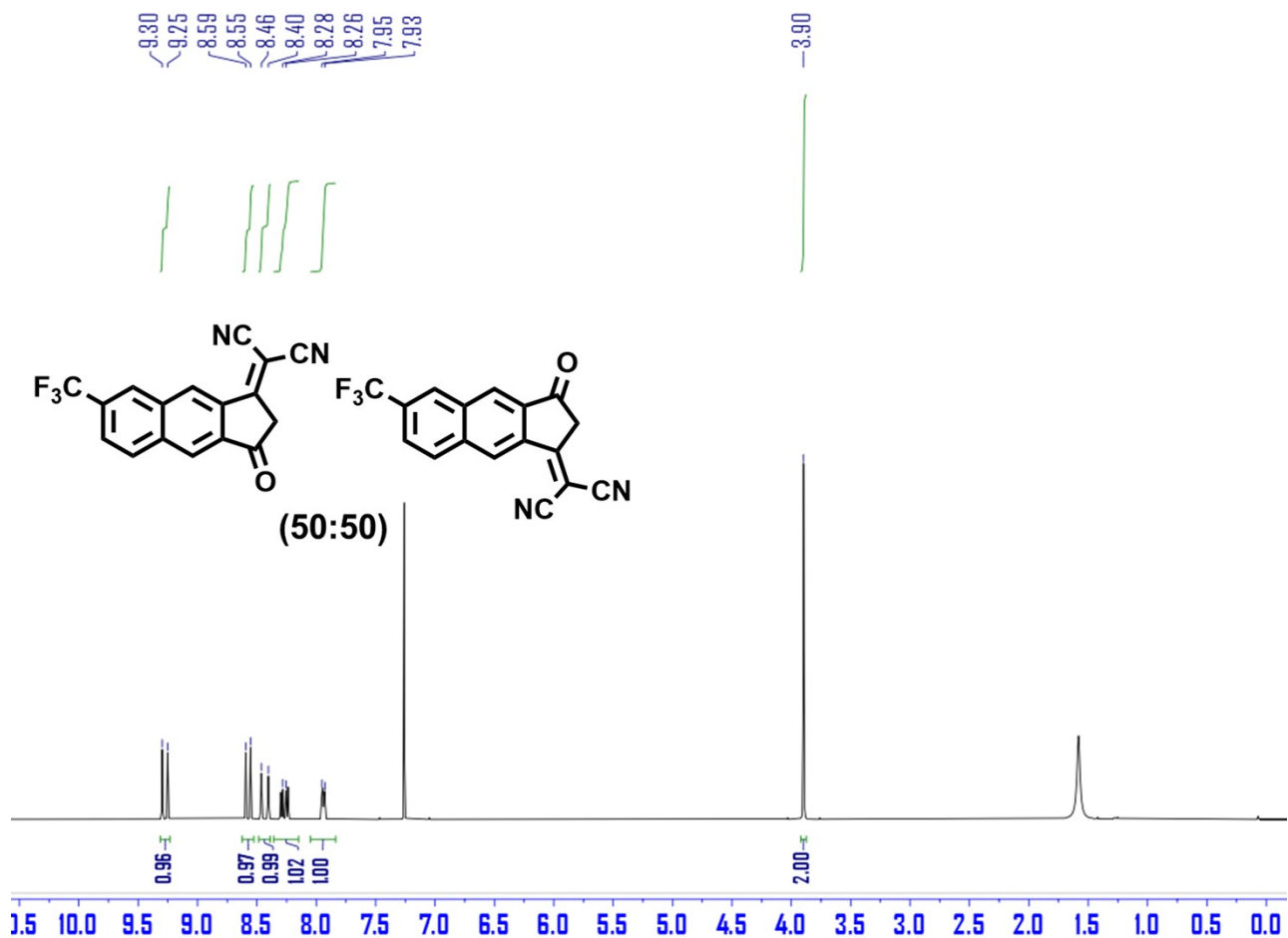
Figure S22 ^{1}H spectrum of **CF3-LIC** mixture in CDCl$_3$.
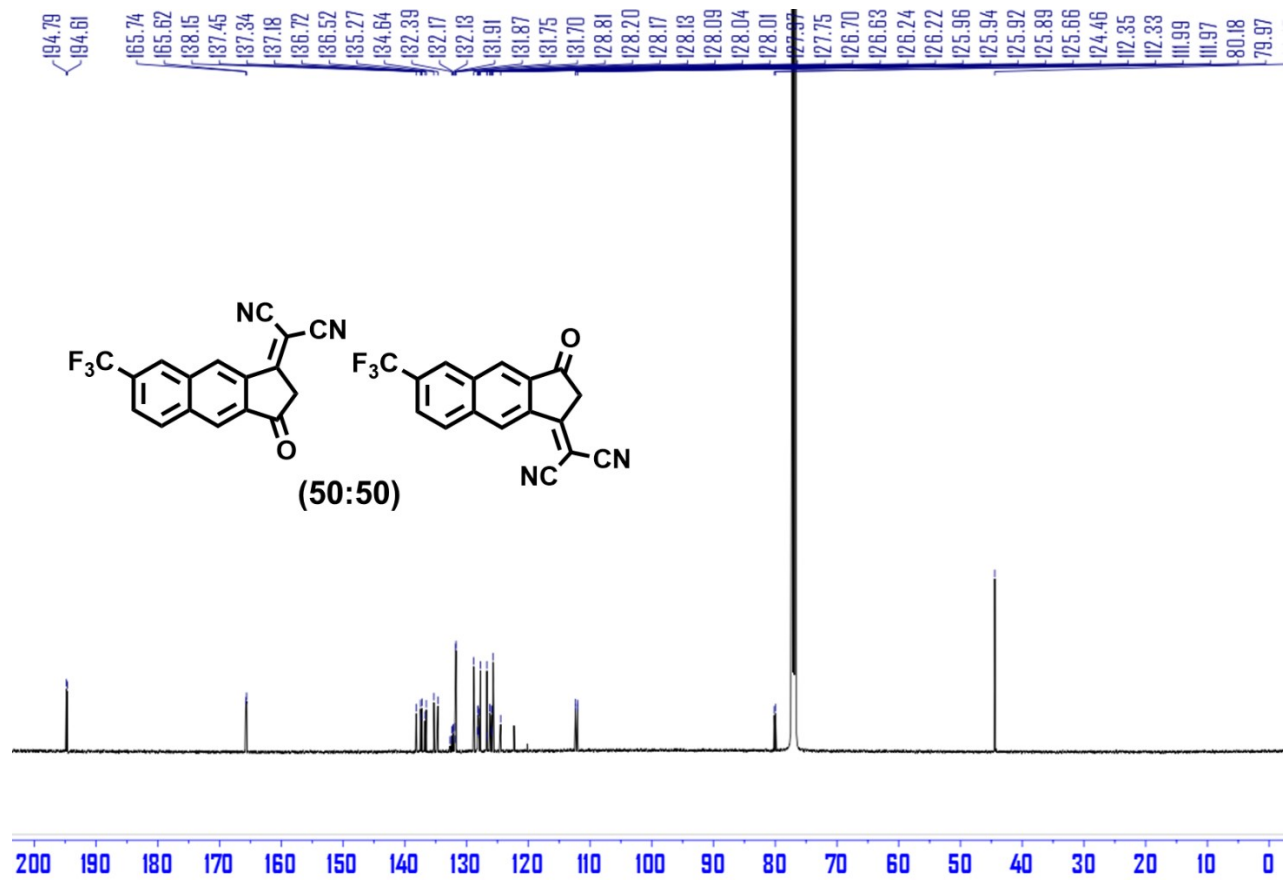
Figure S23. ^{13}C spectrum of **CF3-LIC** mixture in CDCl$_3$.
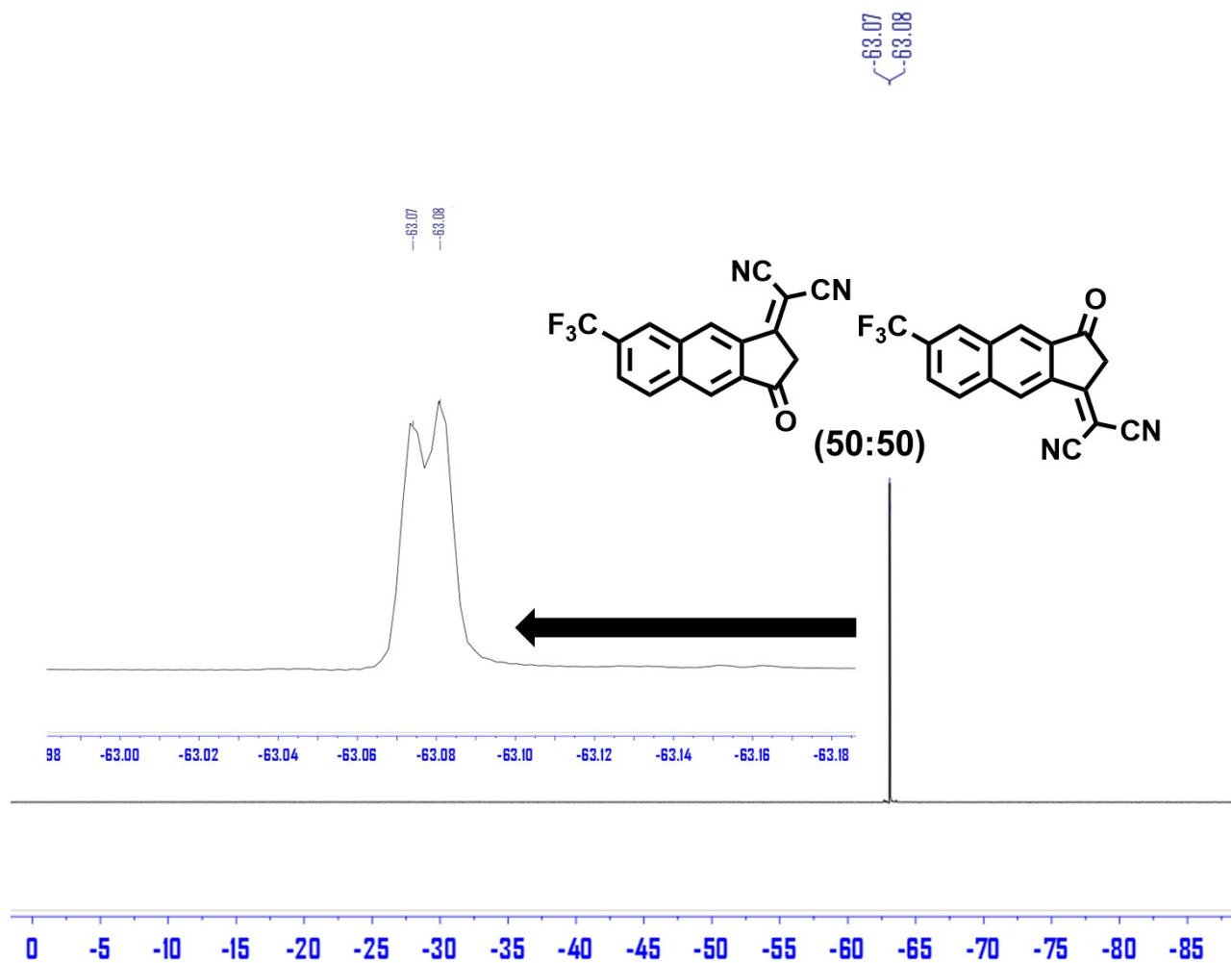
Figure S24. ^{19}F spectrum of **CF3-LIC** mixture in CDCl$_3$.
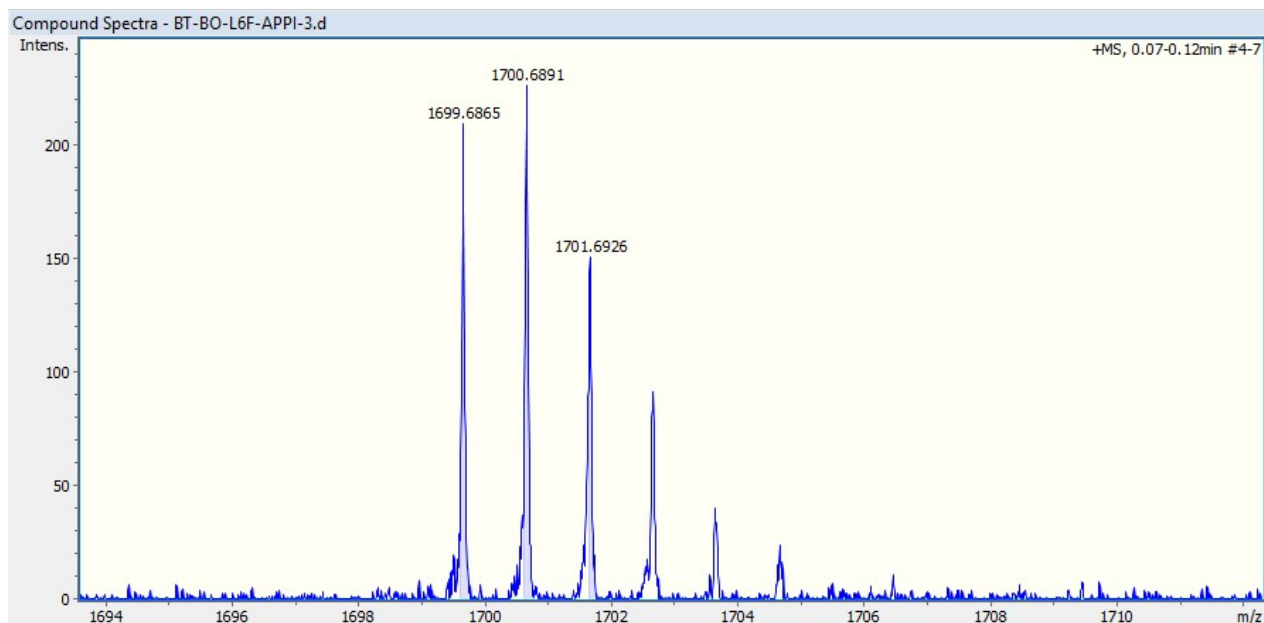
Figure S25. Mass spectrum of **BTF**.
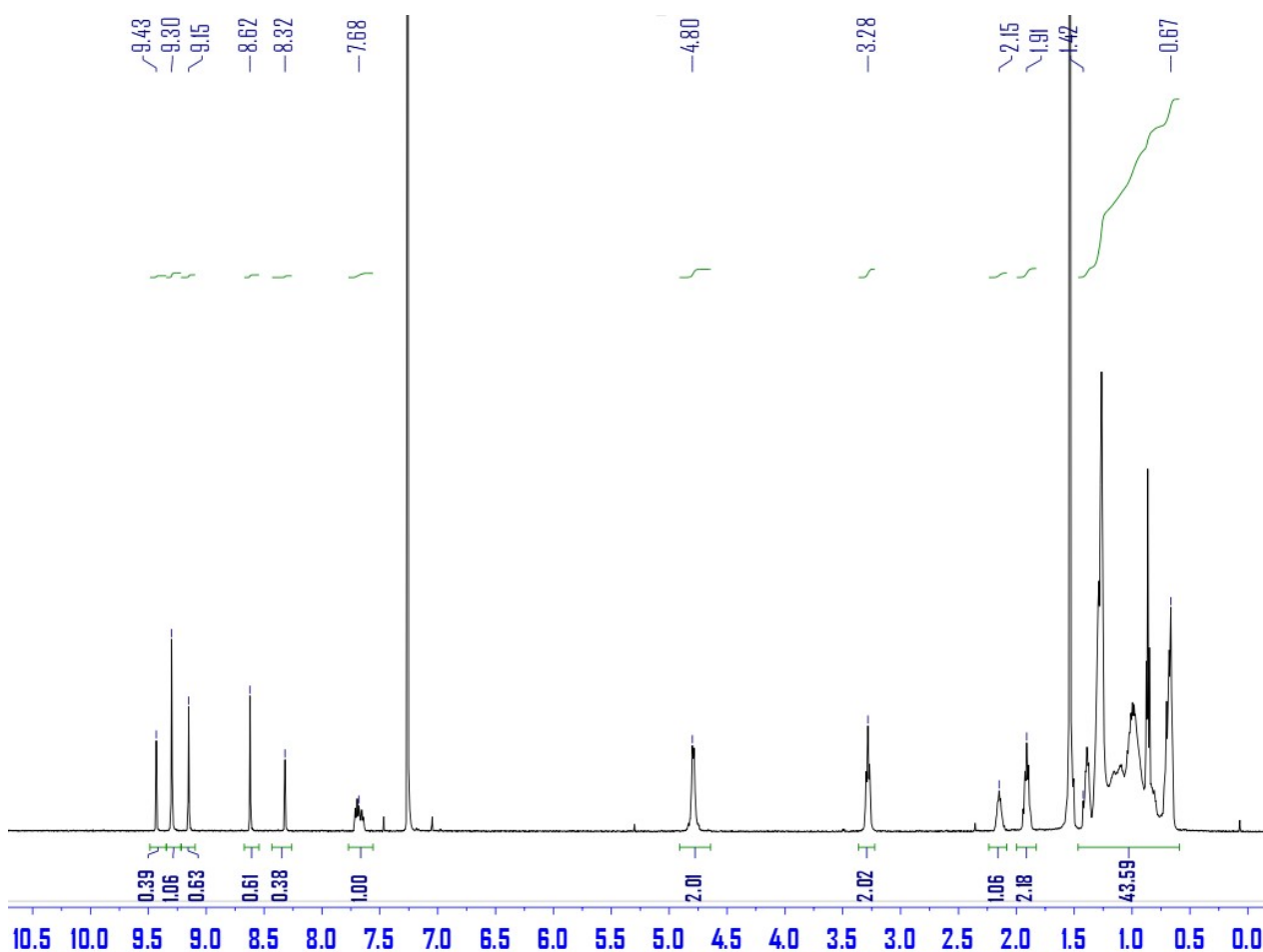
Figure S26. ¹H spectrum of **BTF** in CDCl₃.
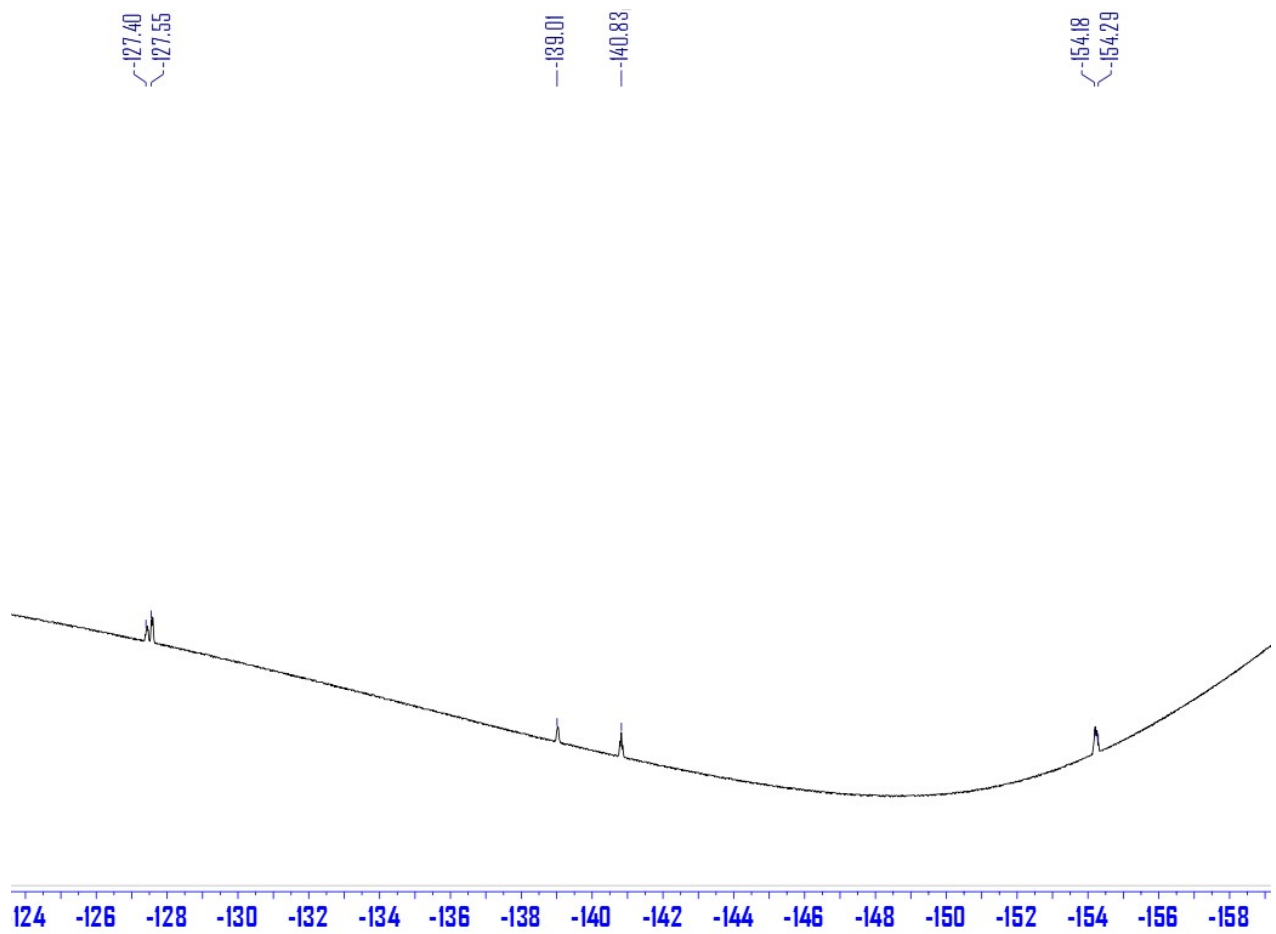
Figure S27. ^{19}F spectrum of **BTF** in CDCl$_3$.
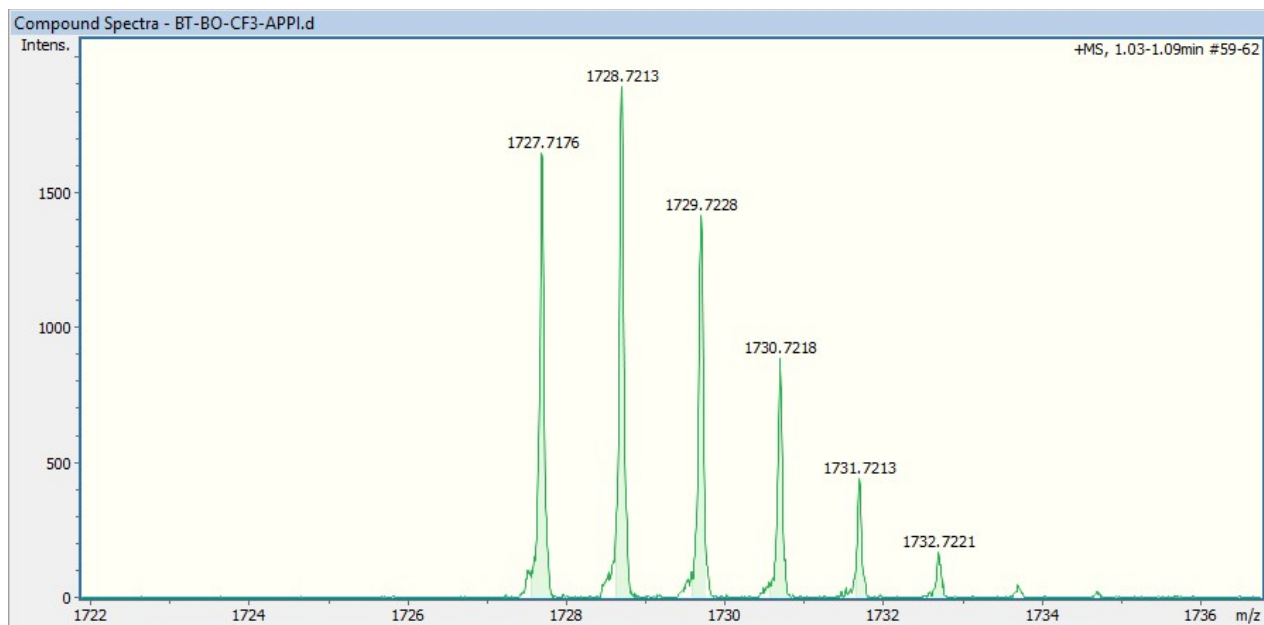
Figure S28. Mass spectrum of **BTFM**.
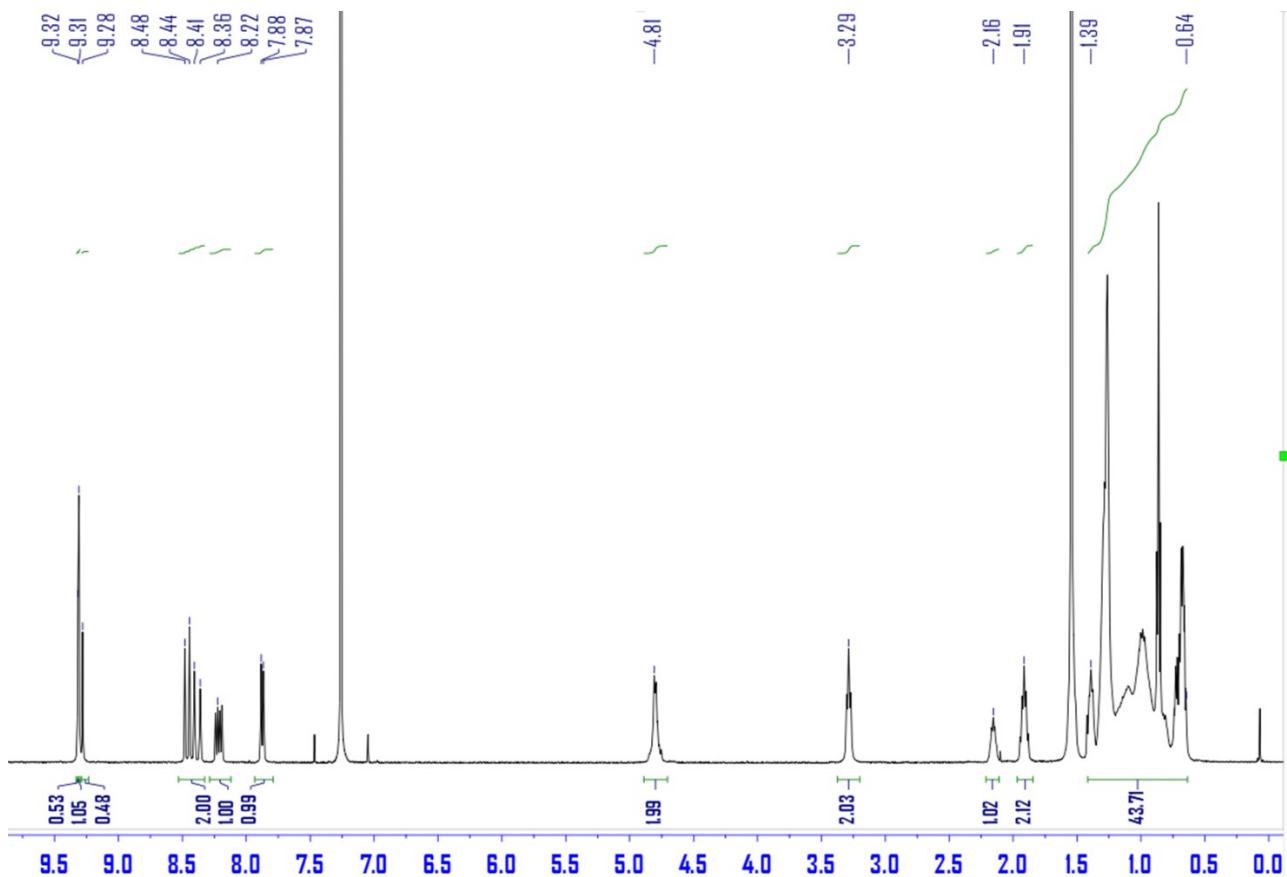
Figure S29. ^{1}H spectrum of **BTFM** in CDCl$_3$.

-62.78
-62.82
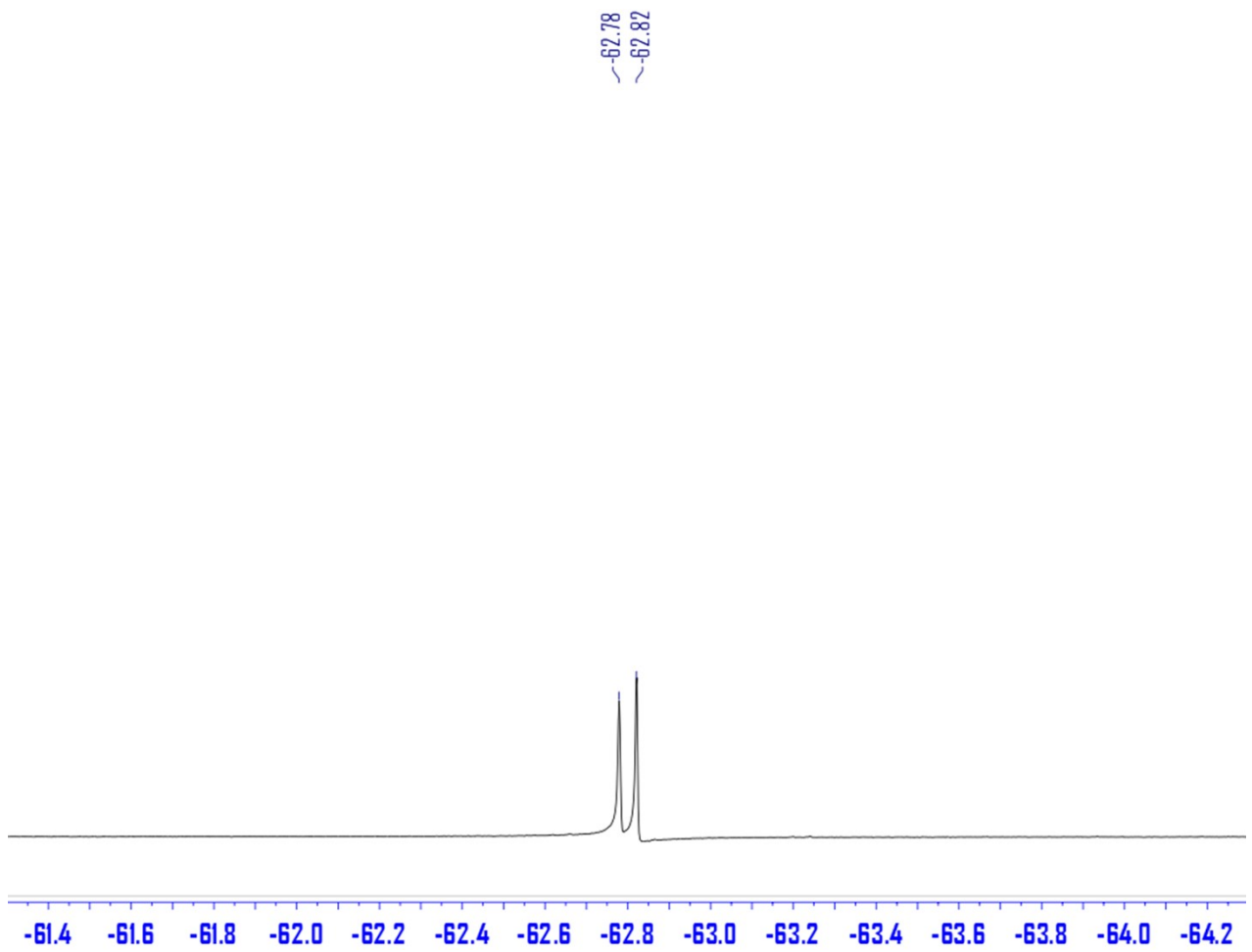
Figure S30. ^{19}F spectrum of **BTFM** in CDCl$_3$.

-61.4 -61.6 -61.8 -62.0 -62.2 -62.4 -62.6 -62.8 -63.0 -63.2 -63.4 -63.6 -63.8 -64.0 -64.2

4. Gel Permeation Chromatography (GPC)

GPC analysis was performed using a Polymer Laboratories PL-GPC 220 equipped with three PLgel 10um MIXED-B LS 300 x 7.5 mm columns and using 1,2,4-trichlorobenzene (TCB) stabilized with 0.0125 % BHT at 150 °C. Calibration was performed using polystyrene standards (860-3,752,000 g/mol). Samples were prepared by dissolving the D18-Cl polymer in stabilized TCB at 150 °C overnight to yield a solution concentration of 1.0 mg/mL, and the sample was filtered through a 0.2 μm PTFE filter prior to measurement.
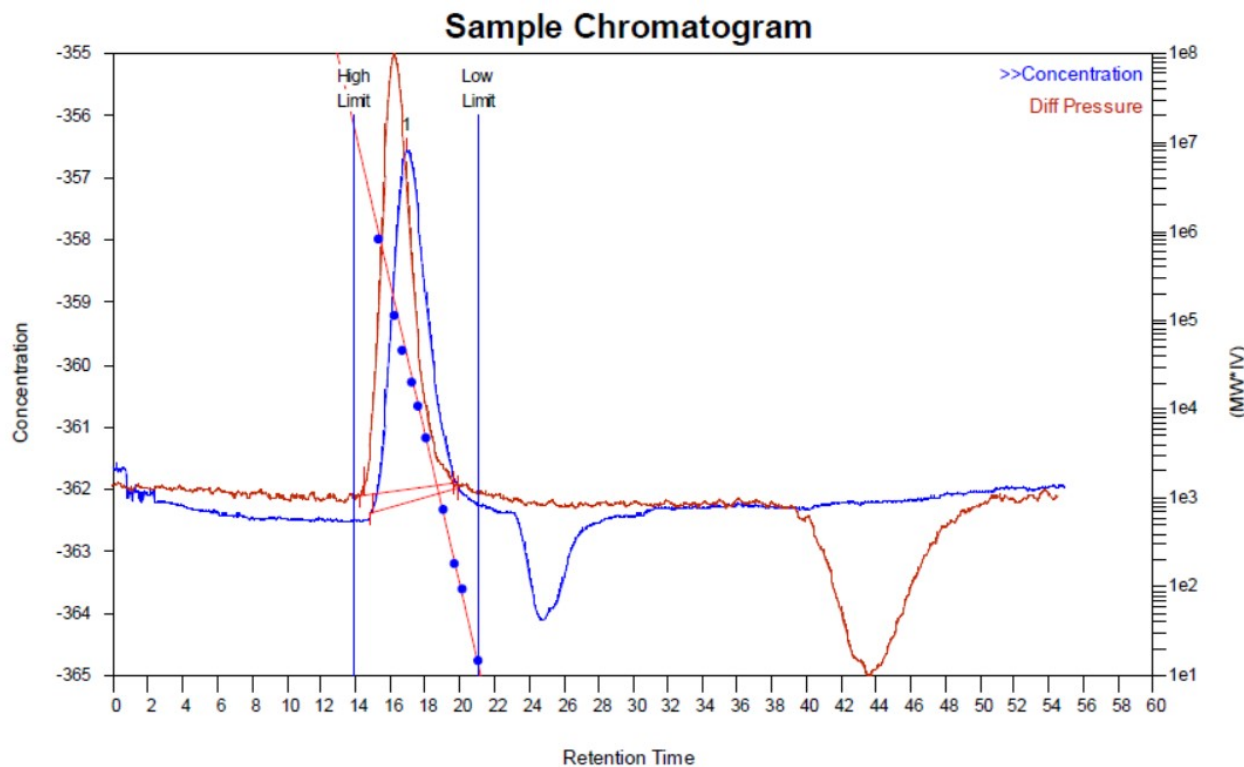
Figure S31. GPC trace of the D18-Cl.

Table S1. Molecular weight extracted from the GPC trace.

M_P	M_N	M_W	M_Z	M_{Z+1}	M_V	PDI
81343	35502	97003	192204	293759	86696	2.73

Calibration Curve: $y = 18.921080 - 0.844580x^1$

5. UV-Vis Absorption

UV-vis spectra of solutions and films were recorded on a Perkin Elmer LAMBDA 1050 spectrophotometer. The **BTF**, **BTFM**, and D18-Cl solutions were prepared at 0.00500 mg/mL in chloroform and measured at room temperature. The film optical absorption spectra were recorded from films cast from chloroform solutions (5.0 mg/mL, 1000 rpm, 1rpm = 0.105 rad/s) onto glass slides
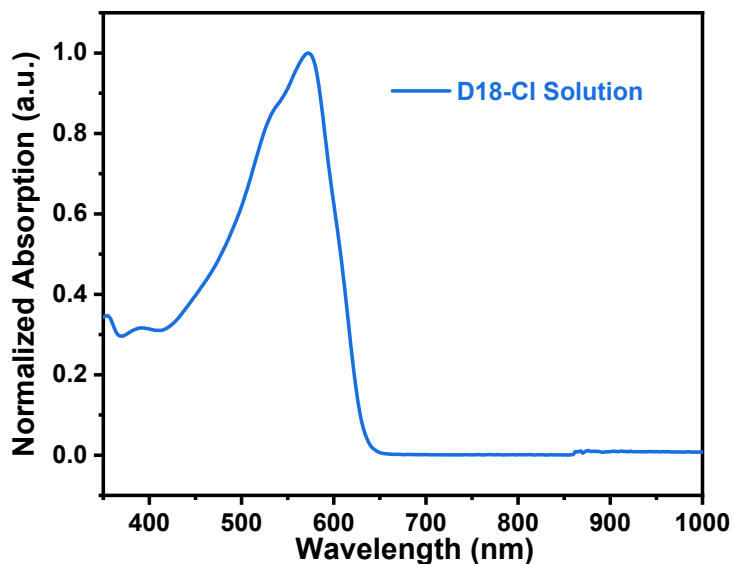
Figure S32. Solution absorption of the donor D18-Cl.

6. Cyclic Voltammetry

The CV measurements followed our previously reported procedure.[1] The electrochemical properties of the acceptor molecules were investigated as thin films in deoxygenated anhydrous acetonitrile under nitrogen at a scan rate of 100 mV/s using 0.1 M tetrakis(n-butyl)ammonium hexafluorophosphate $[(n\text{-Bu})_4N^+PF_6^-]$ as the supporting electrolyte. A Pt electrode was used for the counter electrode, a glassy carbon electrode was used as the working electrode, and Ag/Ag+(sat. NaCl) as the reference electrode. The materials of interest were drop-cast onto the Pt working electrode from 5 mg/mL CHCl$_3$ solutions. A ferrocene -ferrocenium (Fc/Fc+) redox couple was used as internal standard and was assigned absolute energy of –4.80 eV vs vacuum. The HOMO energies of the materials were determined according to the equation $E_{HOMO} = -(E_{oxonset} + 4.80)$, where $E_{oxonset}$ is the positive sweep onset of the oxidation potential relative to the measured Fc/Fc$^+$ redox couple. The LUMO energies of the acceptors were determined according to the equation $E_{LUMO} = -(E_{redonset} + 4.80)$, where $E_{redonset}$ is the positive sweep onset of reduction potential relative to the measured Fc/Fc+ redox couple.
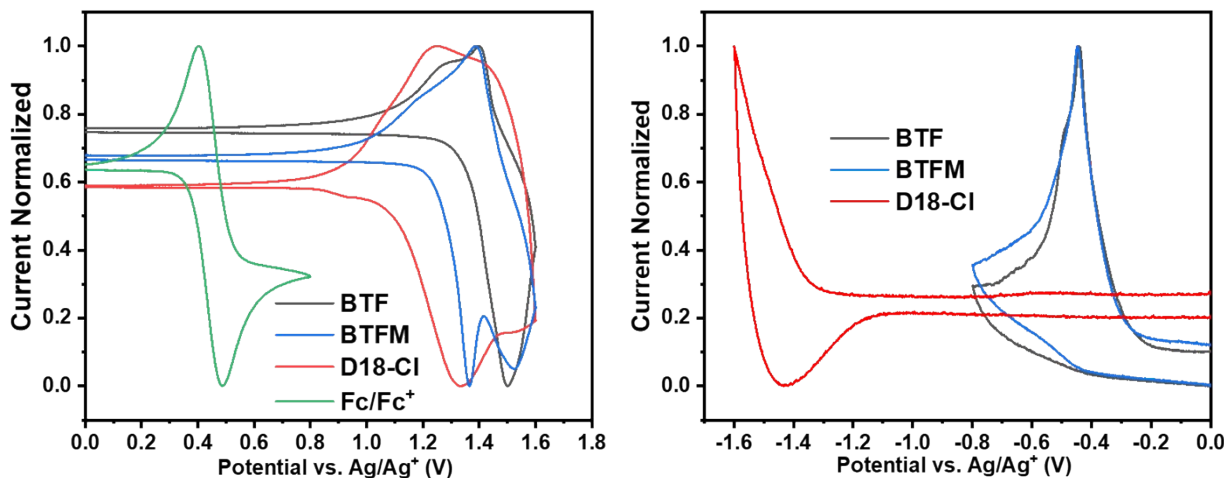
Figure S33. Cyclic voltammograms of the indicated materials: oxidation cycle. (left) and reduction cycle (right).

7. Ultraviolet Photoelectron Spectroscopy

Organic semiconductor films were spin-coated onto clean ITO/Au (50nm) substrates. ITO substrates were first washed and cleaned (see the procedure in solar cell fabrication section), and the Au layer was deposited onto ITO substrates under vacuum Then, neat acceptor and donor materials were spin-coated from 10 mg/mL chloroform solution (1000 rpm).

Ultraviolet photoelectron spectroscopy (UPS) measurements were conducted on a Thermo Scientific Escalab 250Xi ultra photoelectron spectrometer (NUANCE).
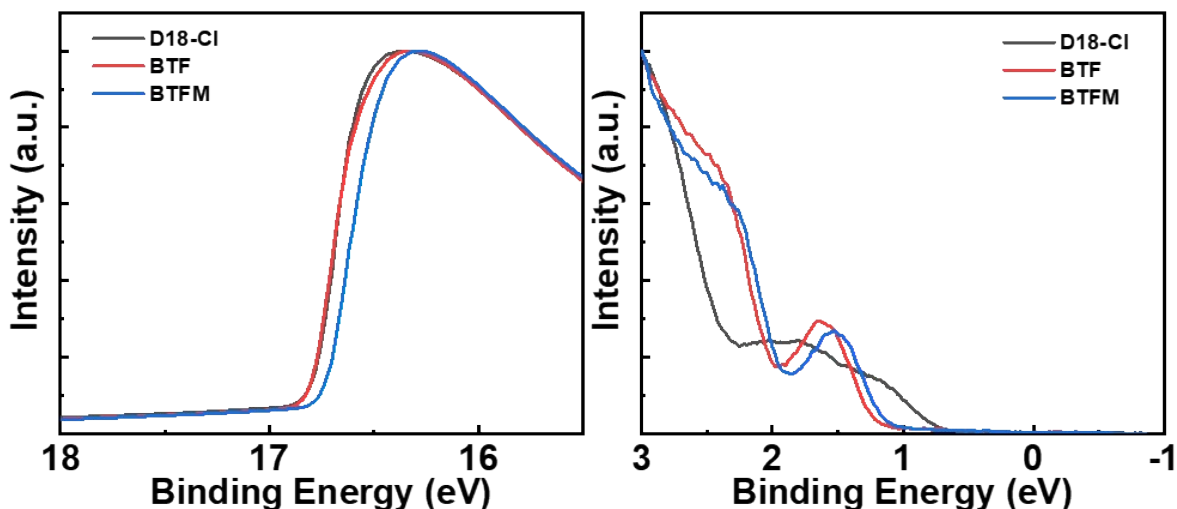
Figure S34. Cutoff and valence band regions of the UPS spectra of all the acceptors and donors. Fermi level is set at 0.0 eV.

Table S2. UPS-HOMO/LUMO level estimated from the UPS measurement.

Material	UPS-HOMO (eV)	UPS-LUMO (eV)
BTF	-5.61	-4.30
BTFM	-5.58	-4.25
D18-Cl	-5.11	-3.18

UPS-LUMO data are estimated using the following equation: UPS-LUMO = UPS-HOMO – E_g^{opt}

where the $E_g^{opt} = 1240/\lambda_{onset}^{opt}$.

8. Thermogravimetric Analysis

Thermogravimetric analysis measurements were performed on a SDT-Q600 (TA Instruments) instrument and heated at a rate of 10 °C/min under a nitrogen atmosphere. The temperature where the sample loss 5 % weight is indicated.
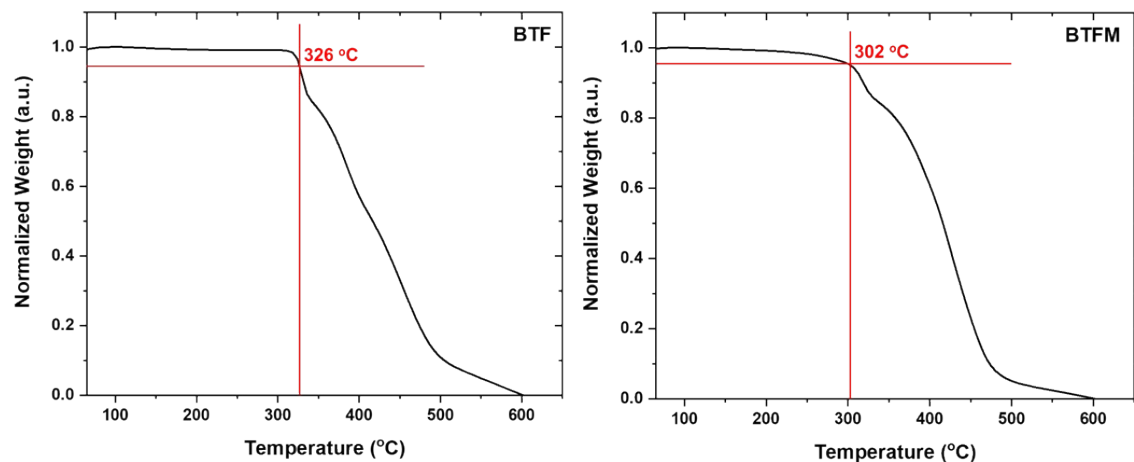
Figure S35. TGA heating traces of the BTF and BTFM.

9. Single Crystal X-Ray Structures

A suitable crystal was mounted on a glass fiber with Paratone oil on an XtaLAB Synergy R, DW system, HyPix diffractometer. The crystal was kept at 200.00(10) K during data collection. Using Olex2[2], the structure was solved with the XT structure solution program using Intrinsic Phasing and refined with the XL refinement package using Least Squares minimization.

The enhanced rigid-bond restraint (SHELX keyword RIGU) was applied globally as well as restraints on similar amplitudes separated by less than 1.7 Ang. Distance restraints were imposed on the carbon atoms on the alkyl chains.

The solvent masking procedure as implemented in Olex2 was used to remove the electronic contribution of solvent molecules from the refinement. As the exact solvent content is not known, only the atoms used in the refinement model are reported in the formula here.

Table S3. Crystal structure data and structural refinement for BTF and BTFM-1.

	BTF	BTFM-1
CCDC	**2109328**	**2109327**
Empirical formula	$C_{82}H_{90}N_8O_2S_5$	$C_{90}H_{94}N_8O_2S_5$
Formula weight	1379.931	1480.03
Temperature / K	100.0	200.01(10)
Crystal system	monoclinic	monoclinic
Space group	I2/a	C2/c
a / Å	19.1409(2)	31.3298(18)
b / Å	56.7502(7)	16.8956(7)
c / Å	24.6205(2)	32.6056(13)
$\alpha/°$	90	90
$\beta/°$	96.7880(10)	111.930(5)
$\gamma/°$	90	90
Volume / Å^3	26556.5(5)	16010.4(14)
Z	12	8
ρ_{calc} / mg mm^{-3}	1.035	1.228
μ / mm^{-1}	1.549	1.749
F(000)	8808	6288
Crystal size / mm^3	0.562 × 0.121 × 0.032	0.19 × 0.088 × 0.013
2Θ range for data collection	4.904 to 136.502°	6.05 to 88.986°
Index ranges	-17 ≤ h ≤ 22, -68 ≤ k ≤ 68, -29 ≤ l ≤ 29	-28 ≤ h ≤ 28, -15 ≤ k ≤ 15, -29 ≤ l ≤ 27
Reflections collected	179313	27053
Independent reflections	24327[R(int) = 0.0535]	6309[R(int) = 0.0728]
Data/restraints/parameters	24327/4020/1304	6309/1420/947
Goodness-of-fit on F^2	1.744	1.574
Final R indexes [I>2σ (I)]	R_1 = 0.1322, wR_2 = 0.3946	R_1 = 0.1288, wR_2 = 0.3760
Final R indexes [all data]	R_1 = 0.1472, wR_2 = 0.4169	R_1 = 0.1535, wR_2 = 0.4047
Largest diff. peak/hole / e Å^{-3}	1.321/-0.469	0.427/-0.284
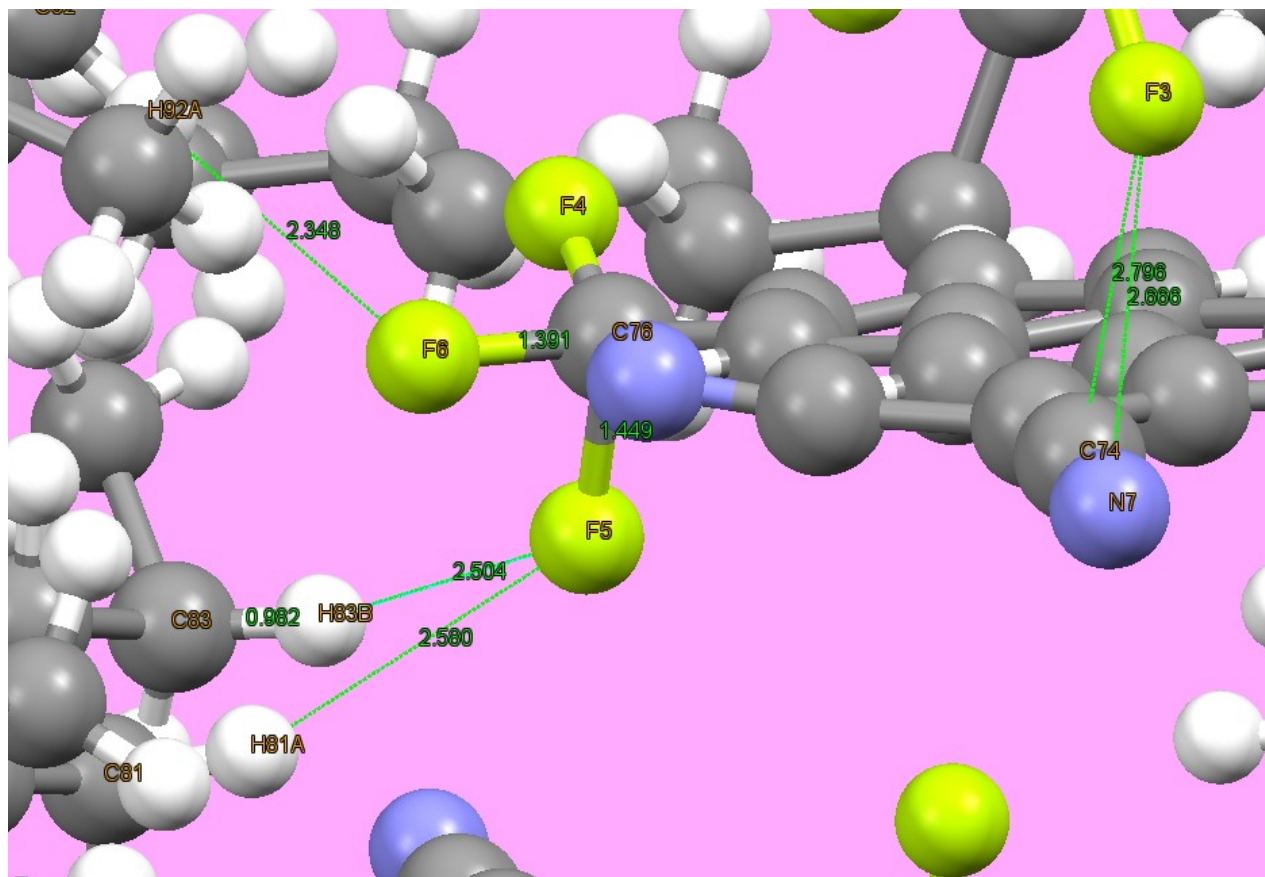
Figure S36. Cyano group – fluorine (CF_3-A)intermolecular interaction (right) and the bifurcation hydrogen bonding[3-5] between the CF_3-B and the N-alkyl chain (left) on **BTFM-1**. Note that the proton coordinates shown in the figure were calculated based on the idealized geometric positions.

Table S4. Bifurcation hydrogen bonding and fluorine-cyano interaction metrics in **BTFM-1**.

Entry	Bond (A-B)	Distance (Å)	Distance up to 3 decimal points
1	C36-F3	1.51(4)	1.514
2	C76-F4	1.27(8)	1.266
3	C76-F5	1.45(5)	1.449
4	C76-F6	1.39(5)	1.391
5	C81-H81A	0.99*	\
6	C83-H83B	0.99*	\
7	C92-H92A	0.99*	\
8	C34-N5	1.08(3)	1.082
9	C35-N6	1.135(16)	1.135
10	C74-N7	1.2(1)	1.185
11	C75-N8	1.14(7)	1.135
	Interaction (X···Y)		
12	F3···N7	2.67(8)	2.666
13	F5···H81A	2.580*	\
14	F5···H83B	2.504*	\
15	F6···H92A	2.348*	\
16	F3···C74	2.80(7)	2.796
17	N5···H89	2.474*	\

* Note that the proton coordinates in these interactions were calculated based on the idealized geometric positions.

10. Simulated Powder X-ray Diffraction Patterns
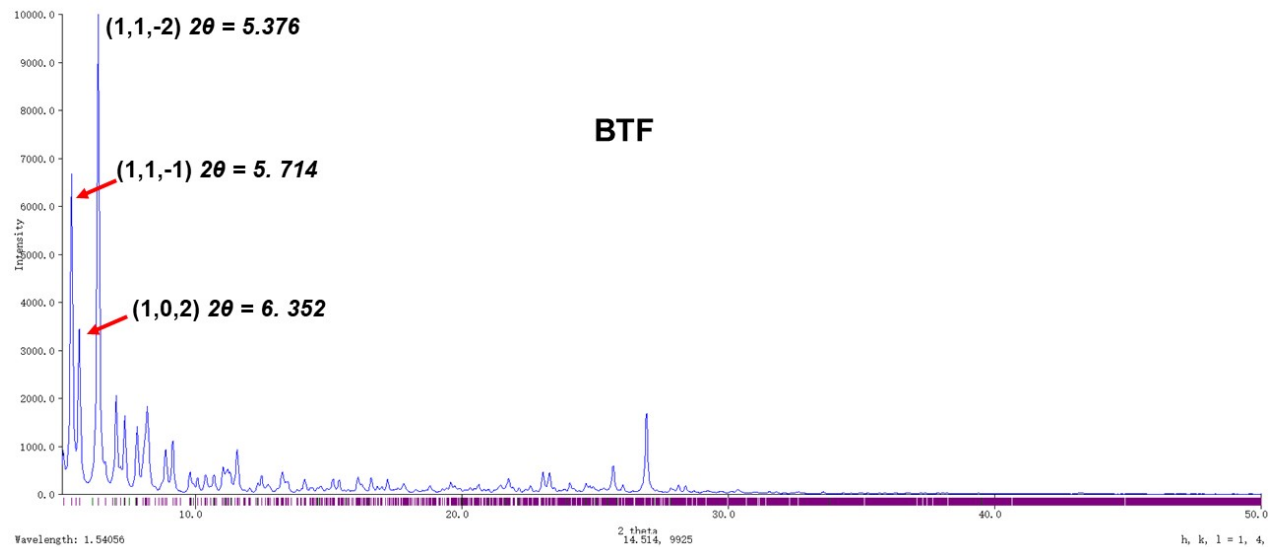
Figure S37. Simulated powder x-ray diffraction pattern generated from the **BTF** single-crystal analysis.
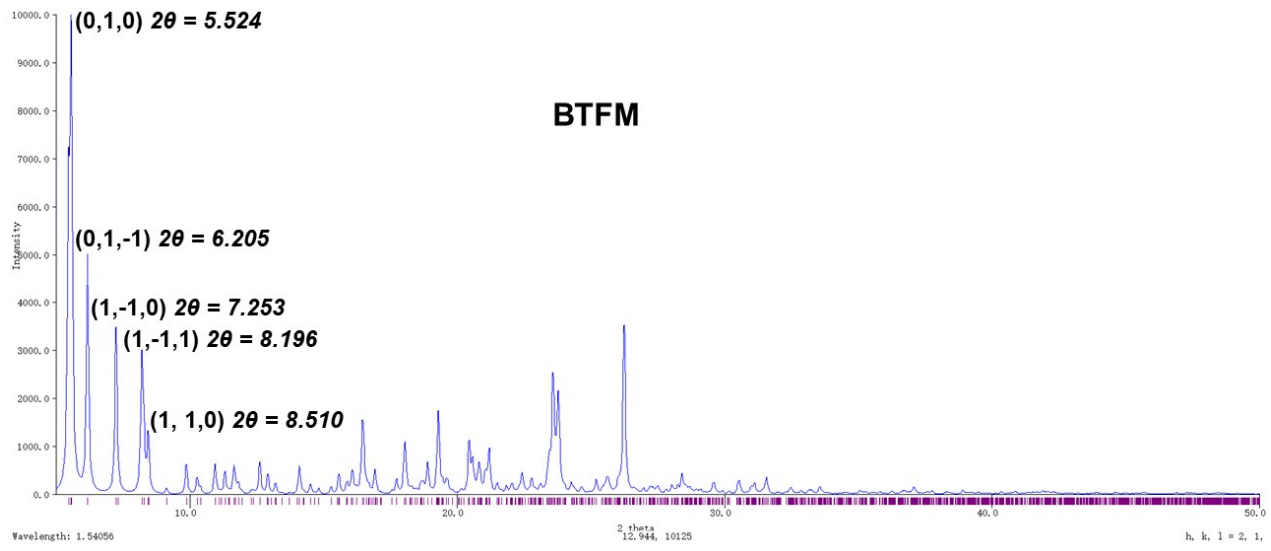
Figure S38. Simulated powder x-ray diffraction pattern generated from the **BTFM** single-crystal (isomer-I) analysis.

11. Solar cell device fabrication and characterization.

Devices with a conventional architecture (ITO /PSS:PEDOT /active layer / Electron Transportation layer (ETL)/Ag) are fabricated. Following previously reported protocols,[6] prepatterned ITO-coated glass substrates (Thin Film Devices, Inc.) with a sheet resistance of ≈15-20 Ω/sq were used as substrates. The PSS:PEDOT aqueous solution (AI 4083) was purchased from Ossila, Inc. The PSS:PEDOT aqueous solution is spin-coated on precleaned ITO glass at 5000 rpm after filtering through a 0.45-μm nylon filter and annealed for 15 min at 150°C in air. Then the device is transferred into an argon-filled glove box for the rest of the processing. After that, active layer solutions (12 mg/mL in total) were then spin-coated on top of the PSS:PEDOT layer with a spinning rate of 1500-2100 RPM (film thickness ≈200-150 nm). Then the ETL materials PDINO, PDINN, PNDIT-F3N were dissolved in methanol to a concentration of 1.0 mg/mL (for PNDIT-F3N, 0.3 % acetic acid was added) and were spin-coated on top of the active layer (spinning rate: 3000 rpm for 30s). All the substrates are loaded into a metal-evaporation chamber to perform Ag-electrode deposition (100 nm) under high vacuum(≈8 x 10^{-6} Torr). The calibrated device area is 6.25 mm^2. All the devices were then measured under a simulated AM-1.5G irradiation (100 mW cm^{-2}) illumination from the class-AAA Solar Simulator in an argon-filled glove box. The light intensity was calibrated with an NREL-certified monocrystalline Si photodiode to bring the spectral mismatch to unity. All the device parameters are reported from the champion batch of cells.

External quantum efficiency (EQE) was measured on the Newport QE-PV-SI setup. Incident light from Xe lamp (300 W) passing through a monochromator (Newport Cornerstone 260) was focused on the devices, and the current was obtained using a current pre-amplifier (Newport, 70710QE) and a lock-in amplifier (Newport, 70105 Dual channel Merlin). Before scanning EQE data, a Newport 70356 silicon diode was used as a reference.

Table S5. Photovoltaic performance parameters of **D18-Cl:BTF** blends with different D/A ratios.

Active layers (with D18-Cl)	D/A	V_{oc} (V)	J_{sc} (mA/cm^{-2})	FF (%)	PCE (%)
BTF (ETL: PDINN, with 0.5 % 1-CN as additive)	10:8	0.849	26.50	65.30	14.70 (14.46±0.20)
	10:10	0.856	26.54	70.92	16.11 (15.68±0.34)
	10:12	0.858	26.44	68.00	15.54 (15.25±0.24)
	10:14	0.859	26.12	68.97	15.48 (15.17±0.21)

Table S6. Photovoltaic performance parameters of **D18-Cl:BTFM** blends with different D/A ratios.

Active layers (with D18-Cl)	D/A	V_{oc} (V)	J_{sc} (mA/cm^{-2})	FF (%)	PCE (%)
BTFM (ETL: PDINN, o additive)	10:8	0.882	25.62	66.30	14.98 (14.75±0.42)
	10:10	0.878	26.24	64.97	14.96 (14.49±0.50)
	10:12	0.880	26.10	67.05	15.39 (15.16±0.69)
	10:14	0.881	26.14	68.71	15.88 (15.67±0.21)

Table S7. Thermal annealing impact on the photovoltaic performance parameters of the **D18-Cl:BTF** blends.

Active layers (with D18-Cl)	Temperature (ºC)	V_{oc} (V)	J_{sc} (mA/cm^{-2})	FF (%)	PCE (%)
BTF (D:A= 10:10, ETL: PDINN, no additive)	110 (3 min)	0.838	26.06	60.80	13.27 (12.90±0.26)
	As-cast	0.855	26.08	64.15	14.32 (14.08±0.24)

Table S8. Photovoltaic performance parameters of **D18-Cl:BTF** and **D18-Cl:BTFM** blends with different ratio of 1-CN additives.

Active layers (with D18-Cl)	1-CN (volume %)	V_{oc} (V)	J_{sc} (mA/cm^2)	FF (%)	PCE (%)
D18-Cl:BTF (10:10, ETL: PDINN, as-cast)	0	0.855	26.08	64.15	14.32 (14.08±0.24)
	0.5	0.856	26.54	70.90	16.11 (15.68±0.34)
	1.0	0.849	26.01	66.98	14.80 (14.22±0.34)
	2.0	0.843	25.36	71.60	15.30 (15.25±0.18)
	3.0	0.847	27.20	70.06	16.20 (15.74±0.30)
D18-Cl:BTFM (10:10, ETL: PDINN, as-cast)	0	0.878	26.24	64.97	14.96 (14.49±0.50)
	0.5	0.847	26.22	63.82	14.04 (13.79±0.16)
	1.0	0.841	25.55	64.75	14.02 (13.72±0.35)
	2.0	0.851	20.45	69.15	12.03 (11.75±0.29)
	3.0	0.861	23.92	71.29	14.63 (14.15±0.44)

Table S9. Photovoltaic performance parameters of **D18-Cl:BTF** and **D18-Cl:BTFM** blends with different ratios of DIO additive.

Active layers (with D18-Cl)	DIO (volume %)	V_{oc} (V)	J_{sc} (mA/cm^2)	FF (%)	PCE (%)
D18-Cl:BTF (D:A = 10:10, ETL: PDINN, as-cast)	0	0.855	26.08	64.15	14.62 (14.38±0.24)
	0.5	0.807	24.60	61.91	12.30 (12.14±0.16)
	1.0	0.800	24.57	61.72	12.14 (12.02±0.08)
D18-Cl:BTFM (D:A = 10:10, ETL: PDINN, as-cast)	0	0.878	26.24	64.97	14.96 (14.49±0.50)
	0.5	0.853	25.76	67.34	14.79 (14.66±0.13)
	1.0	0.826	25.29	62.42	13.04 (12.50±0.54)

Table S10. Photovoltaic performance parameters of the **D18-Cl:BTF** blend at different revolutions under the illumination of AM 1.5G,100 mW cm^{-2}.

Active layers (with D18-Cl)	RPM	V_{oc} (V)	J_{sc} (mA/cm^2)	FF (%)	PCE (%)
BTF (D:A = 10:10, ETL: PDINN, with 0.5 % 1-CN as additive)	1500	0.864	26.82	66.90	15.50 (14.58±0.58)
	1800	0.862	26.44	67.05	15.28 (14.81±0.42)
	2100	0.855	26.64	70.80	15.80 (15.49±0.29)
	2400	0.866	25.53	69.72	15.40 (14.65±0.62)

Table S11. Photovoltaic performance parameters of **D18-Cl:BTF** blends using different electron transfer layers under the illumination of AM 1.5G,100 mW cm^{-2}.

Active layers (with D18-Cl)	ETL	V_{oc} (V)	J_{sc} (mA/cm^2)	FF (%)	PCE (%)
D18-Cl:BTF (D:A= 10:10, As-cast, RPM= 2100)	PDINO	0.843	26.32	61.80	13.71 (13.07±0.30)
	PDINN	0.852	26.23	65.70	14.69 (14.19±0.36)
	PNDIT-F3N	0.867	26.18	71.71	16.27 (15.54±0.49)
	PNDIT-F3N With 0.5 % 1-CN	0.863	26.87	74.57	17.30 (16.67±0.60)
	PNDIT-F3N With 3 % 1-CN	0.866	26.28	73.06	16.62 (16.00±0.37)
BTFM (D:A= 10:14, As-cast, RPM= 2100)	PNDIT-F3N	0.875	26.72	73.12	17.10 (16.38±0.62)
	PNDIT-F3N With 0.5 % 1-CN	0.882	26.18	70.62	16.27 (15.82±0.42)
	PNDIT-F3N With 3 % 1-CN	0.872	26.45	70.24	16.20 (15.90±0.11)

12. Atomic Force Microscopy

Standard tapping-mode AFM measurements in ambient were performed on a Scanned Probe Imaging and Development (SPID) Bruker ICON using a TESPA probe. The AFM images were confirmed from different samples and scan areas. The root-mean-square roughness (Rq) values of height images were obtained from the whole scan area (3 μm × 3 μm) in the NanoScope Analysis 1.9 software.[7] All the AFM images were flattened and exported from the software.
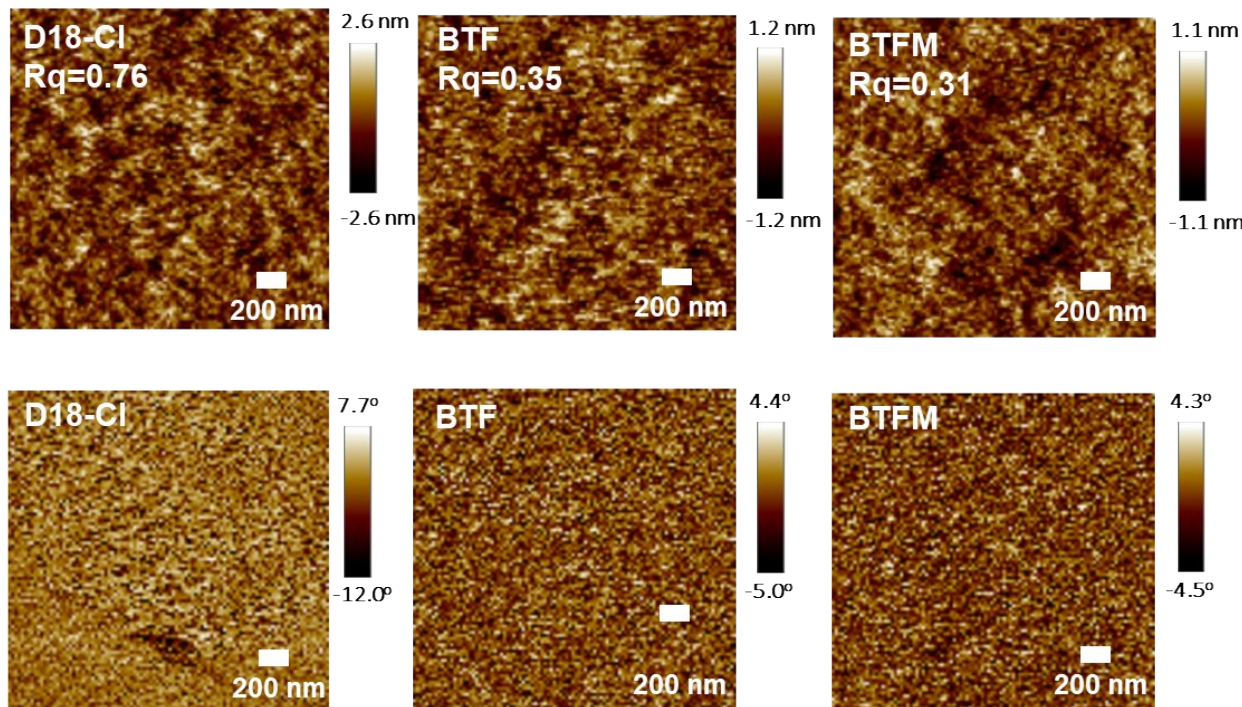
Figure S39. AFM graphic height images (top) and phase images (bottom) of the neat acceptor films and neat donor films.
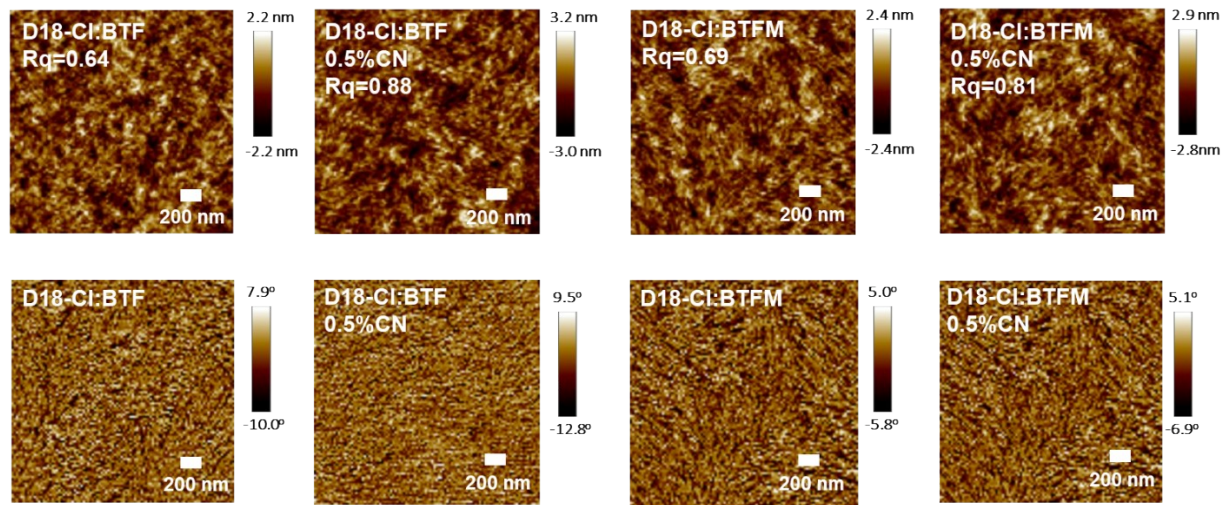
Figure S40. AFM graphic height images (top) and phase images (bottom) of the blend films.

13. Transmission Electronic Microscopy

The detailed experimental procedure followed our previous report.[6] First, a layer of poly(4-styrenesulfonic acid) (PSS, Mw $\approx$75,000, 18 % wt % in H_2O) was spin coated (rate = 3000 rpm) on top of a pre-cleaned glass slide. The obtained PSS/glass substrate thermally annealed at 150 ℃ for 20 min. Then the BHJ coating solution with the optimized device fabrication condition (D:A mass ratio = 10:10 for D19-Cl: BTF, 10:14 for D18-Cl:BTFM; total organics concentration = 10 mg/mL with or without 0.5 volume percent 1-CN) were spin coated (rate = 2100 rpm) on top on the annealed PSS/glass substrates. The obtained organics/PSS/glass substrates were then immersed into deionized water at room temperature, and after several minutes, the BHJ blend films exfoliated from the glass substrate. The floated single-layer organic blend films were transferred to transmission electron microscopy (TEM) copper grids with a lacey carbon coating (Ted Pella, Inc. PELCO No. I60). Carefully, one should make sure that the films are not folded during the transferring, and there is only one layer of the organic films transferred onto the copper grids. The films were then allowed to dry in the air before TEM measurements. TEM images were obtained on a JEOL ARM300F GrandARM TEM microscope (Northwestern University Atomic and Nanoscale Characterization Experimental Center, Electron Probe Instrumentation Center, NUANCE EPIC) TEM images were taken perpendicular to the plane of the films, and confirmed from different samples and areas, to make sure they are representative. Prior to image analysis, the signal of interest was cropped from the original EM image using FIJI.[8] Then the cropped images with a shape of 2048 × 2048 pixels were split into signal channels with a properly thickness-normalized brightness scale to ensure the brightness is uniform between the images.
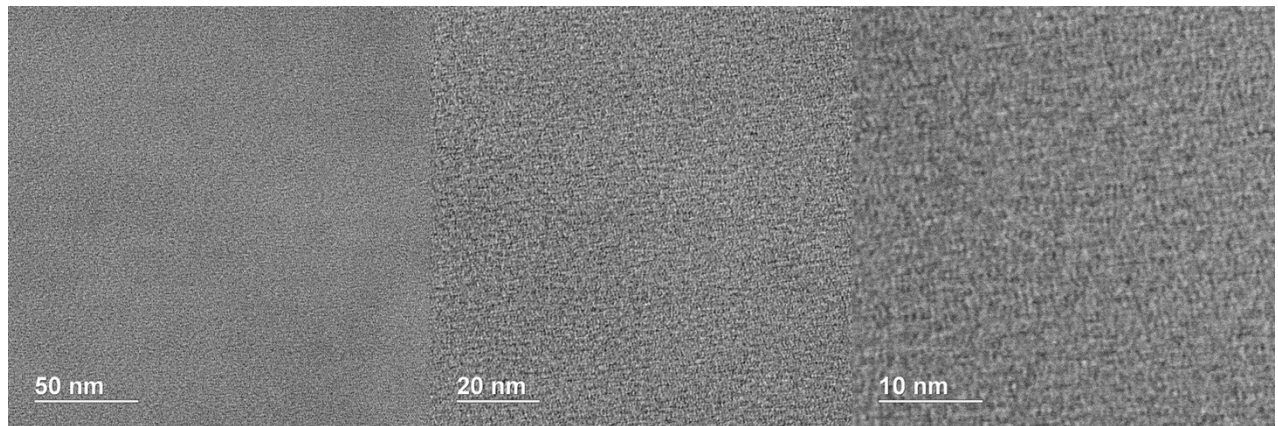
Figure S41. TEM images for the blend **D18-Cl:BTF** film without additive.
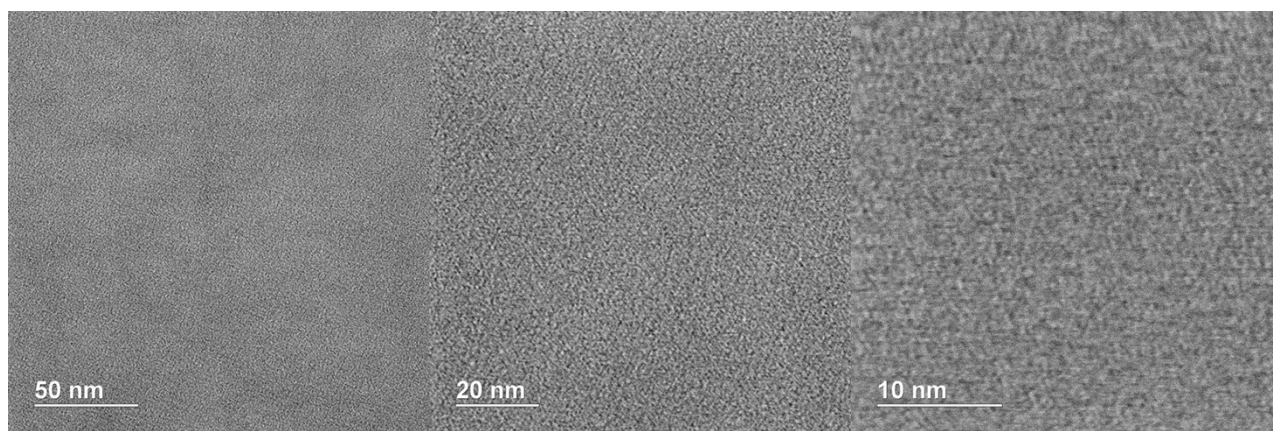
Figure S42. TEM images for the blend **D18-Cl:BTF** film with 0.5 % 1-CN as additive.
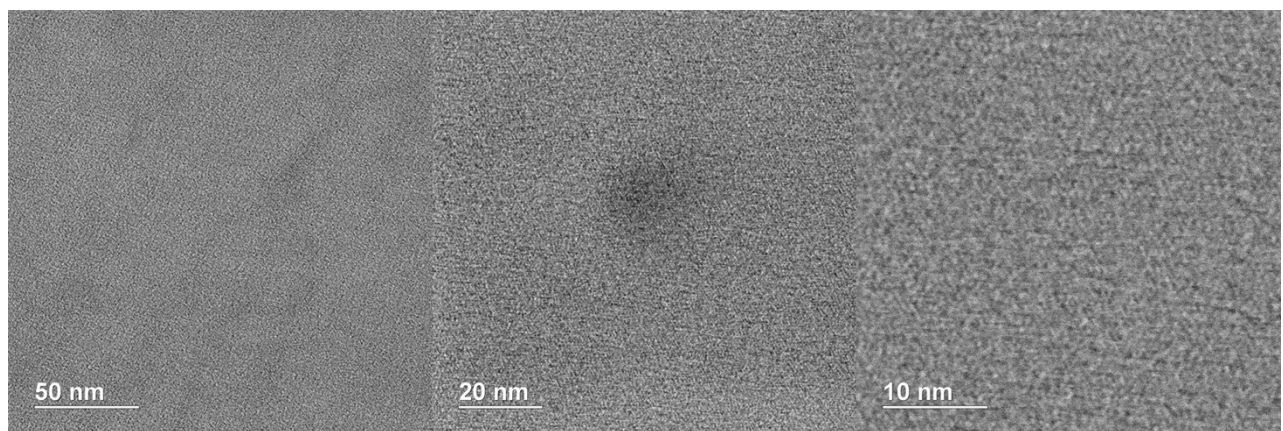
Figure S43. TEM images for the blend **D18-Cl:BTFM** film without additive.
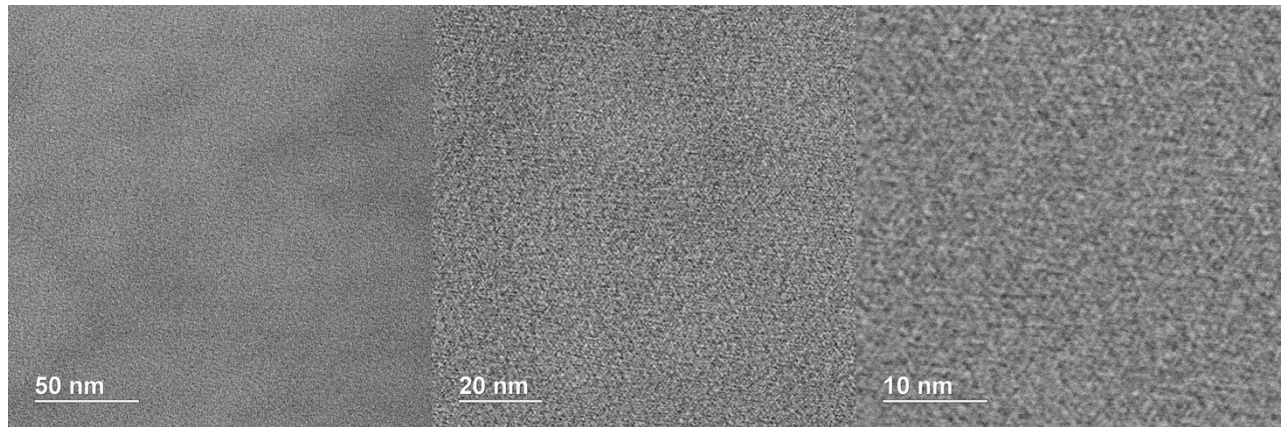
Figure S44. TEM images for the blend **D18-Cl:BTFM** film with 0.5 % 1-CN as additive.

14. Space-Charge-Limited Current Measurements

Hole and electron mobilities were measured using the space-charge-limited current (SCLC) structures which were fabricated according to the same procedure as the photovoltaic devices. The structure of ITO/MoO$_3$/Active layer/MoO$_3$/Ag was used for and hole-injection-only diode devices and the structure of ITO/ZnO/Active layer/LiF/Al was used for electron-injection-only diode devices, respectively. The SCLC mobilities were calculated by the Mott-Gurney equation:

$$J = \frac{9}{8}\varepsilon\varepsilon_0\mu\frac{V^2}{d^3}$$

where J is the current density, ε is the dielectric constant of the active layer, ε_0 is the vacuum permittivity, μ is the mobility of hole or electron and d is the thickness of the active layer, V is the internal voltage in the device, and $V = V_{appl} - V_{bi}$, where V_{appl} is the voltage applied to the device, and V_{bi} is the built-in voltage resulting from the relative work function difference between the two electrodes. Data are summarized in Table 4 of the main paper, and in Figure S45 below.
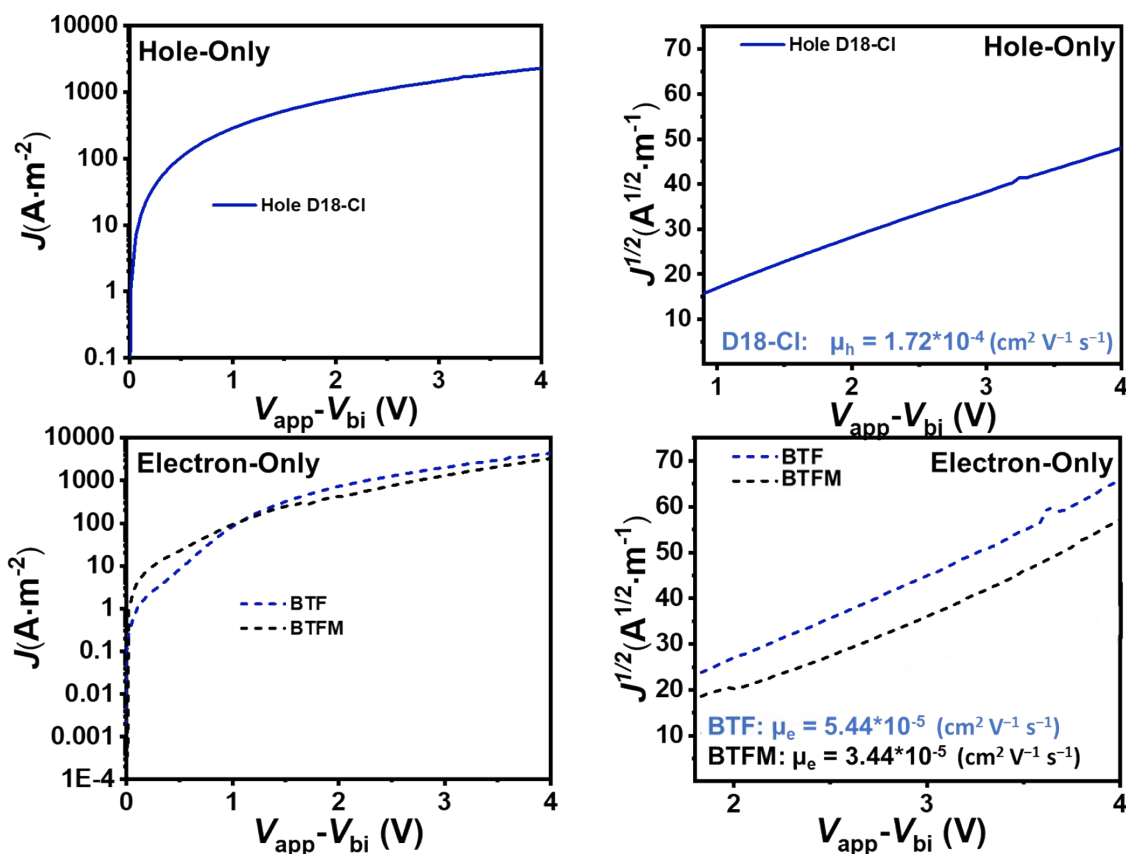
Figure S45. SCLC curves of hole-only and electron-only devices of the indicated neat films.

15. Grazing-Incidence Wide-Angle X-Ray Scattering (GIWAXS)

Neat acceptor films and blend films were spin-coated from $CHCl_3$ solutions. For neat acceptor films, the acceptor was spin coated from chloroform (5 mg/mL, 1000 rpm, 60 s), blend films were spin-coated from $CHCl_3$ (11 mg/mL, 1000 rpm, 60 s, D:A = 1:1 for fluorinated acceptor, D:A = 1:1.2 for non-fluorinated acceptor), and the donor was spin-coated from chloroform (5 mg/mL, 1000 rpm, 90 s).

GIWAXS measurements were performed at the 11-BM Complex Materials Scattering (CMS) beamLine of the National Synchrotron Light Source II (NSLS-II) with a beam energy of 13.5 keV. The 2D scattering patterns were collected at an X-ray incidence angle of 0.14° with a Pilatus 1M detector with a pixel size of 172 μm and placed about 250 mm from the sample. The 2-D data were analyzed using Nika software based on Igor Pro.[9] Sector averaged 1D scattering profiles were obtained from 15° cake sectors. Pole figures were constructed from the 2D GIWAXS images corrected for the missing wedge by integrating the intensities at each detector azimuth within the q-range of the first order lamellar diffraction peaks of the polymer and acceptor. A linear background defined by the intensities at the two ends of the integrated q-range was subtracted. The relative degree of crystallinity (rDoC) was calculated by integrating the intensities over the crystallographic orientation sphere: rDoC = $\dfrac{\int_0^{\pi/2} I(\chi)\sin\chi\, d\chi}{}$ and normalized to illuminated volume (sample width and film thickness).
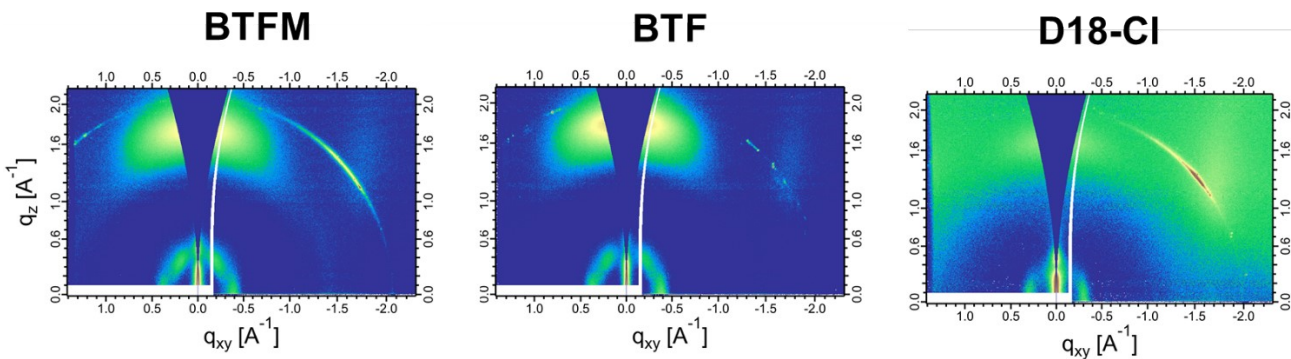
Figure S46. 2-D GIWAXS data from the neat films.

Table S12. In-Plane locations of low-q peaks, and corresponding d-spacings and coherence lengths for the pristine and blend samples.

Film	loc (Å⁻¹)	d-spacing (Å)	FWHM (Å⁻¹)	CL (nm)
BTFM	0.38	16.5	0.13	4.8
BTF	0.38	16.5	0.12	5.2
D18-Cl	0.32	19.6	\	\
D18-Cl: BTFM	0.32	19.6	0.08	7.9
	0.40	15.7	0.07	9.0
D18-Cl: BTFM with 3 % 1-CN	0.32	19.6	0.03	20.9
	0.38	16.5	0.03	20.9
D18-Cl: BTF	0.32	19.6	0.07	9.0
	0.39	16.1	0.05	12.6
D18-Cl: BTF with 3 % 1-CN	0.32	19.6	0.03	20.9
	0.38	16.5	0.11	5.7

Table S13. Out-of-Plane locations of the π stacking peak in q-space, and the corresponding d-spacings and coherence lengths for the pristine and blend samples.

Film	OOP (h00) loc (Å⁻¹)	OOP (h00) d-spacing (Å)	OOP (h00) FWHM (Å⁻¹)	OOP (h00) CL (nm)
BTFM	1.71	3.7	0.28	2.2
BTF	1.77	3.5	0.25	2.5
D18-Cl	1.64	3.8	\	\
D18-Cl: BTFM	1.64	3.8	0.26	2.4
	1.74	3.6	0.26	2.4
D18-Cl: BTFM with 3 % 1-CN	1.68	3.7	0.14	4.5
	1.8	3.5	0.09	7.0
D18-Cl: BTF	1.73	3.6	0.26	2.4
D18-Cl: BTF with 3 % 1-CN	1.68	3.7	0.13	4.8
	1.78	3.5	0.18	3.5
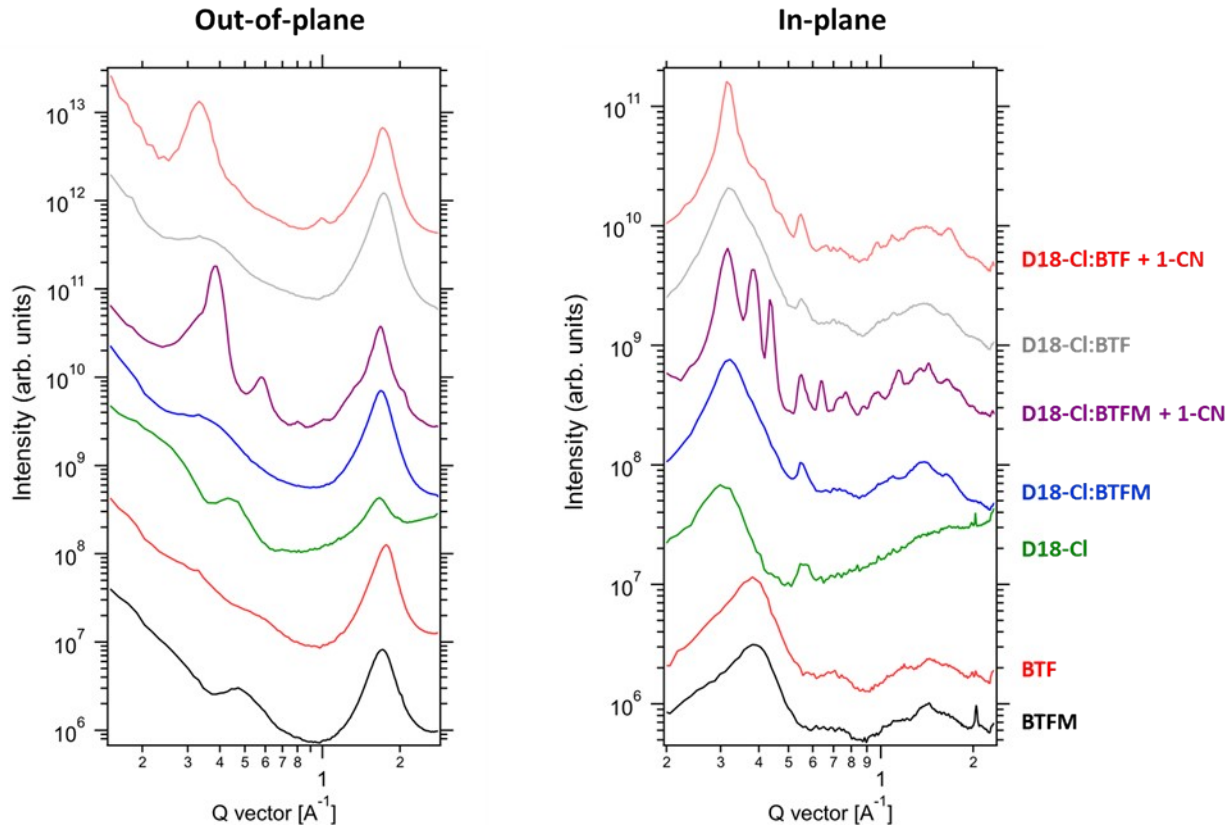
Figure S47. Sector-averaged line profiles obtained from 15° out-of-plane and in-plane cake sectors in the 2-D GIWAXS data from neat and blend films. Profiles have been shifted vertically for clarity.
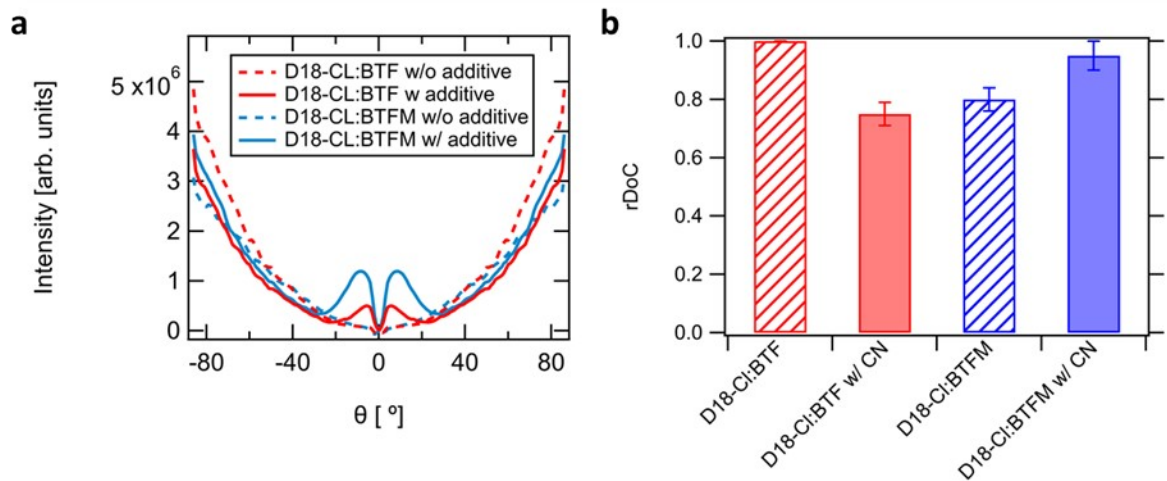
Figure S48. (a) Pole figures calculated from low peaks over the q-range 0.3 Å⁻¹ to 0.5 Å⁻¹. (b) Plot of relative degree of crystallinity of the blend films obtained by integrating the pole figures.

16. Resonant Soft X-ray Scattering

The experimental procedure follows our previous reported protocol.[10] This resonant scattering technique exploits the optical contrast between the polymer and the NFAs molecules near the carbon 1s absorption edge. The scattering contrast for a 2-component system is directly proportional to $\Delta\delta_{12}^2 + \Delta\beta_{12}^2$, where the complex refractive index $n = 1 - \delta + i\beta$. The real part of the complex refractive index $(1 - \delta)$ is related to dispersion and the imaginary part (β) is related to absorption. The scattering arises from composition correlations weighted by scattering contrast and respective volume fractions of these correlations. The scattering profile is the Fourier transform of the scattering density in a sample with the dominant peak representing the domain spacing or the median size scale. The azimuthally averaged scattering profiles for all the samples measured at X-ray energy of 283.5 eV where the donor-acceptor (D/A) material contrast is expected to be higher is shown in Figure S49. The energy dependence of the integrated scattering intensity (ISI) reveals the physical origin underlying the contrast that produces the scattering. The relative phase purity variations for the respective samples were calculated as normalized $\sqrt{(ISI)}$ over the measured q-range at X-ray energies in the range 283 to 284 eV that emphasize the composition variations in the BHJ blends.

RSoXS measurements were performed in transmission geometry at the SST-1 Beamline at NSLS-II.[11] BHJ active layers were cast on 2 cm × 2 cm Si/PEDOT:PSS substrate. Blends were prepared using the same conditions as OPV devices. RSoXS samples of the BHJ films were prepared by a wet floatation method. The films were scored with a scalpel and then introduced to a bath of deionized water. The bottom-most sacrificial organic layer (PSS) was dissolved leaving the BHJ active layer floating on the water surface. The floating films were then transferred onto a 100 nm Si3N4 window (Norcada) for RSoXS measurements. The 2D data were collected using an in-vacuum [base pressure $\sim 10^{-10}$ kPa (10^{-9} mBar)] CCD detector (greateyes GmbH, 4096 × 4096 pixels). 1D scattering profiles were obtained from the 2D scattering patterns using a custom Nika analysis package and normalized for the incident X-ray flux. As the integrated scattering intensity is affected by the distance traversed through the sample by the X-rays the RSoXS scattering intensities were normalized for absorption and film thickness. Film thicknesses were measured using an ellipsometer (M2000-XI, J. A. Woollam) prior to transfer.
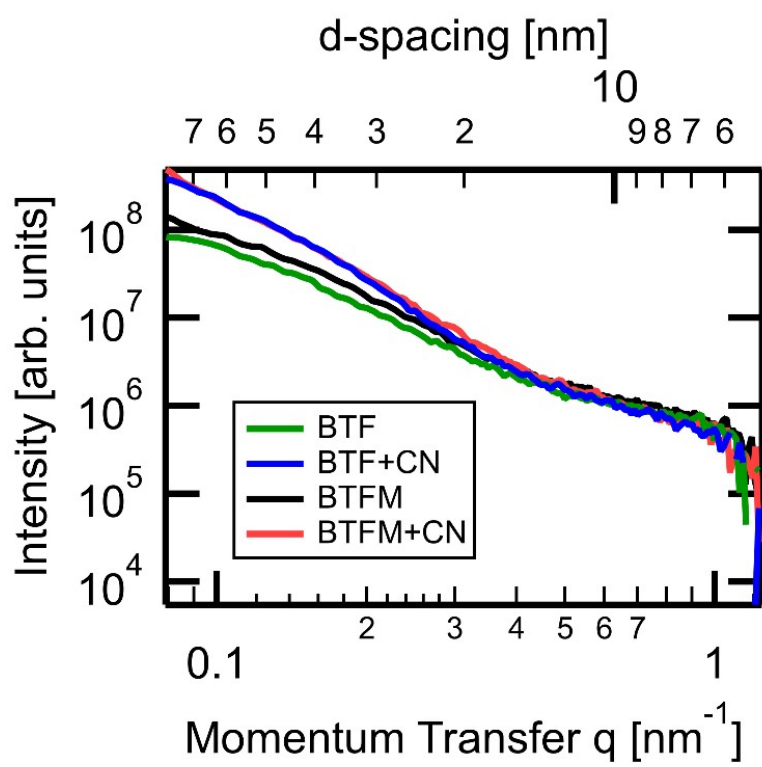
Figure S49. Azimuthally averaged 1-d RSoXS profiles acquired at X-ray energy of 283.5 eV.

17. Femtosecond Transient Absorption Spectroscopy

The femtosecond (fsTA) and nanosecond (nsTA) transient absorption measurements are performed as described previously.[12] Briefly, ≈50 % of the output of a 1 kHz, 1W, 100 fs Ti:sapphire laser system at 827 nm (Tsunami oscillator/Spitfire amplifier, Spectra-Physics) is used to pump a non-collinear optical parametric amplifier (TOPAS-Prime, Light-Conversion LLC) tuned to 830 nm. The 830 nm pump is depolarized to suppress effects due to orientation-dependent dynamics. The probe in fsTA is generated using ≈10 % of the remaining output by driving continuum generation in a sapphire plate (430-850 nm) or a proprietary crystal from Ultrafast Systems (850-1600 nm). The probe in nsTA is generated in a separately delayed broadband laser system (EOS, Ultrafast Systems). The pump and probe are spatially overlapped at the sample. The transmitted probe is detected on a commercial spectrometer (Helios-EOS, Ultrafast Systems), where the Helios spectrometer is used for pump-probe delays up to 7.4 ns and the EOS spectrometer is used for pump-probe delays from 0.6 ns to 340 μs.

The donor-acceptor blend films and the neat acceptor films are measured at room temperature under a vacuum of 10^{-3} Torr to minimize potential sample degradation due to air exposure. Excitation energies of 0.4 μJ/pulse and 1 μJ/pulse are used for the fsTA and nsTA experiments, respectively. Prior to kinetic analysis, the fsTA and nsTA data are scatter-subtracted and chirp-corrected, and the visible and NIR data are spectrally merged (Surface Xplorer 4, Ultrafast Systems). In fsTA spectra, data near 835 nm are omitted due to pump scatter and residual light used to generate the white light probe. In nsTA spectra, data near 835 nm and 1060 nm are omitted due to pump scatter and saturation of light used to generate the white light probe, respectively.

The kinetic analysis is based on a global fit to selected single-wavelength kinetics and is implemented in MATLAB. The time resolution is ≈300 fs (full width at half maximum); the assumption of a uniform instrument response across the frequency domain and a fixed time-zero (t_0) is implicit in global analysis. The kinetic data from multiple wavelengths are fit using global analysis. Each wavelength is given an initial amplitude that is representative of the spectral intensity at time t_0. The rate constants and t_0 are shared between the various kinetic data and are varied globally across the kinetic data to fit the specified models.

To fit the fsTA data, a non-linear, sequential kinetic model with four species is used in which the last term is quadratic to account for bimolecular recombination:

$$dA/dt = -k_1[A]$$
$$dB/dt = k_1[A] - k_2[B]$$
$$dC/dt = k_2[B] - k_3[C]$$
$$dD/dt = k_3[C] - k_4[D]^2$$

Equation S1

To fit the nsTA data, a non-linear, sequential kinetic model with two species is used in which the last term is quadratic to account for bimolecular recombination:

$$dA/dt = -k_1[A]$$
$$dB/dt = k_1[A] - k_2[B]^2$$

Equation S2

The MATLAB program simultaneously fits the transient absorption as a function of time at selected wavelengths for each data set by numerically solving the system of differential equations (i.e., Eqn. S1 or S2) using the Runge-Kutta algorithm. The solutions are convoluted with a Gaussian instrument response function with a width of ≈300 fs and a least-squares fitting algorithm using the Simplex method is used to find the fitting parameters that match the kinetic data.

The fitting parameters are then inserted into the differential equations, which are solved for the populations of the various states within the model (i.e., A(t), B(t), C(t), and D(t)). Finally, the matrix containing all of the raw data is deconvoluted with the populations as functions of time to produce the evolution-associated spectra. Transient absorption spectra at selected time delays, evolution-associated spectra, kinetics and corresponding fits at selected wavelengths, and model population dynamics for the fsTA (Fig. S50-S55) and nsTA (Figs. S56-S61) data as well summaries of the rate constants (Tables S14-S15) are provided, below.
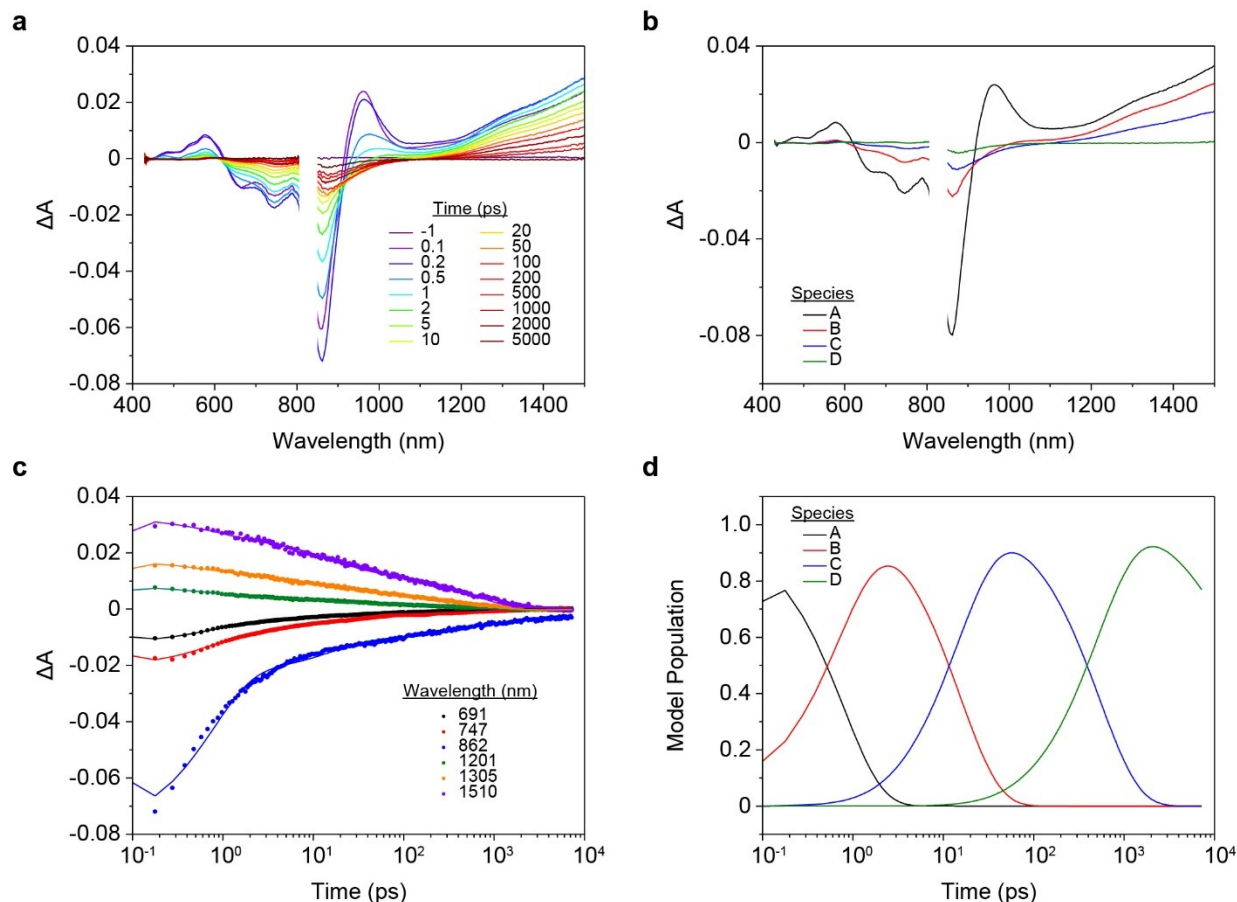
Figure S50. fsTA of neat **BTF films** excited at 830 nm. (a) Transient absorption spectra at the indicated time delays, (b) evolution-associated spectra, (c) kinetics, and corresponding fits at the indicated wavelengths, and (d) model population dynamics. Global fits in (b), (c), and (d) are conducted with the kinetic model described above and in Eqn. S1.
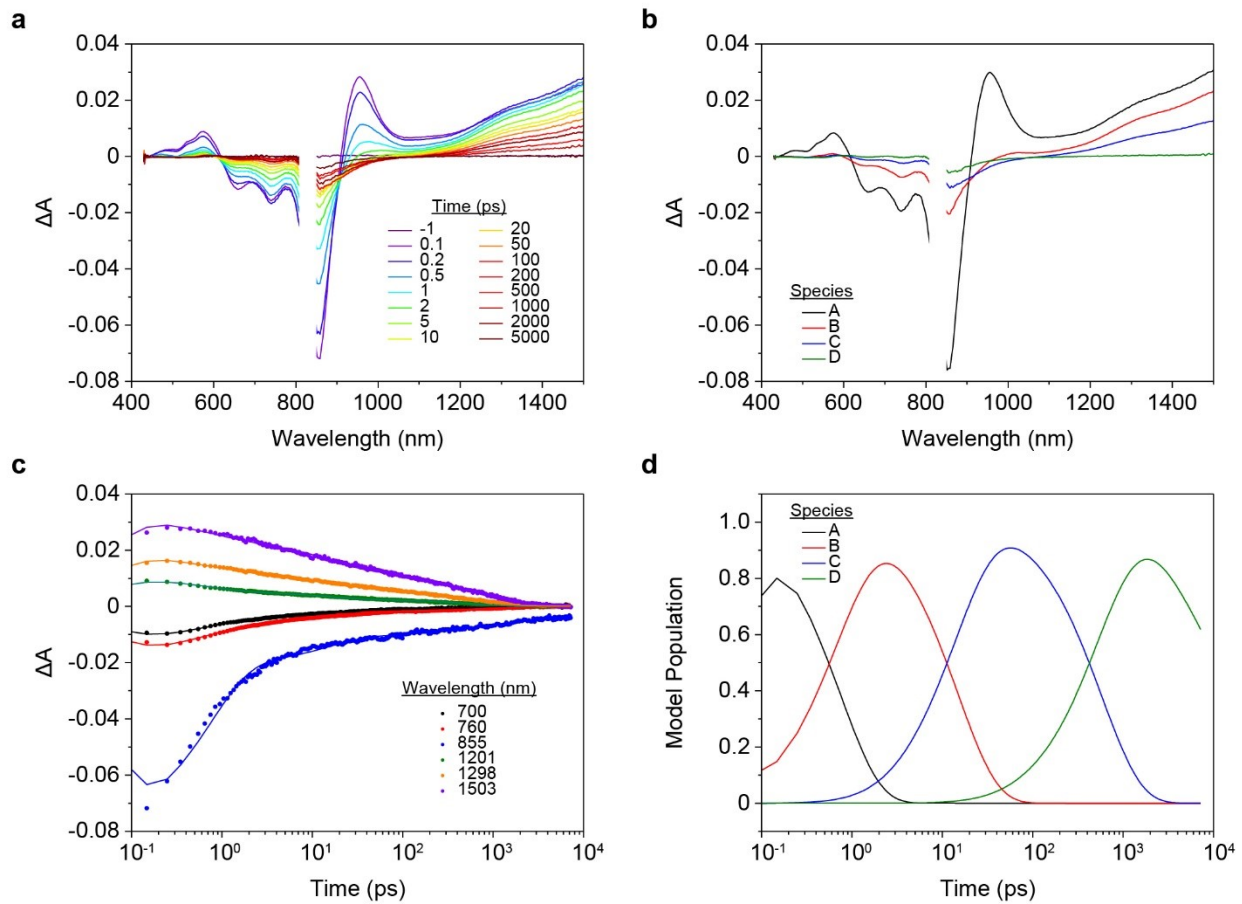
Figure S51. fsTA of neat **BTFM** films excited at 830 nm. (a) Transient absorption spectra at the indicated time delays, (b) evolution-associated spectra, (c) kinetics, and corresponding fits at the indicated wavelengths, and (d) model population dynamics. Global fits in (b), (c), and (d) are conducted with the kinetic model described above and in Eqn. S1.
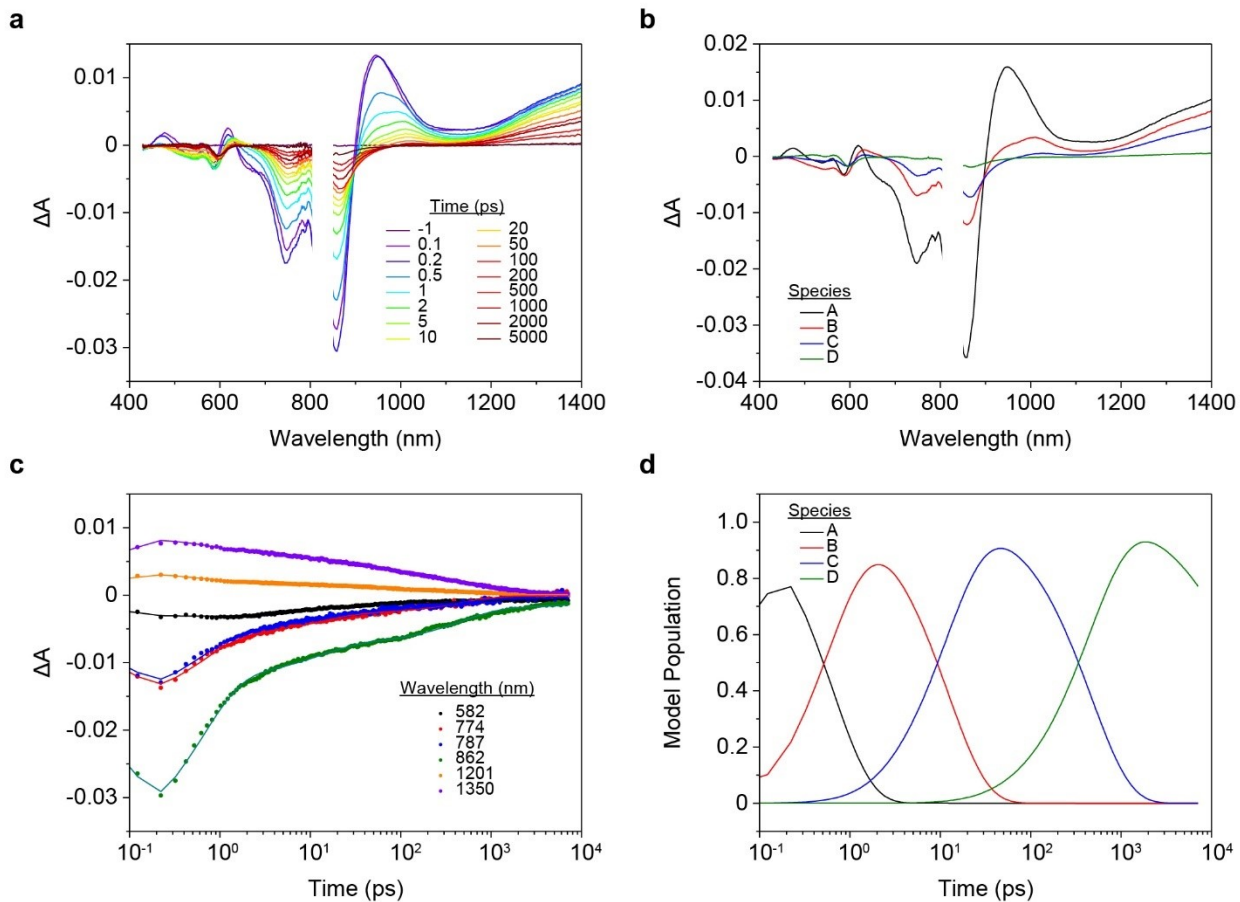
Figure S52. <u>fsTA</u> of **D18-Cl:BTF** (without 1-CN additive) blend films excited at 830 nm. (a) Transient absorption spectra at the indicated time delays, (b) evolution-associated spectra, (c) kinetics, and corresponding fits at the indicated wavelengths, and (d) model population dynamics. Global fits in (b), (c), and (d) are conducted with the kinetic model described above and in Eqn. S1.
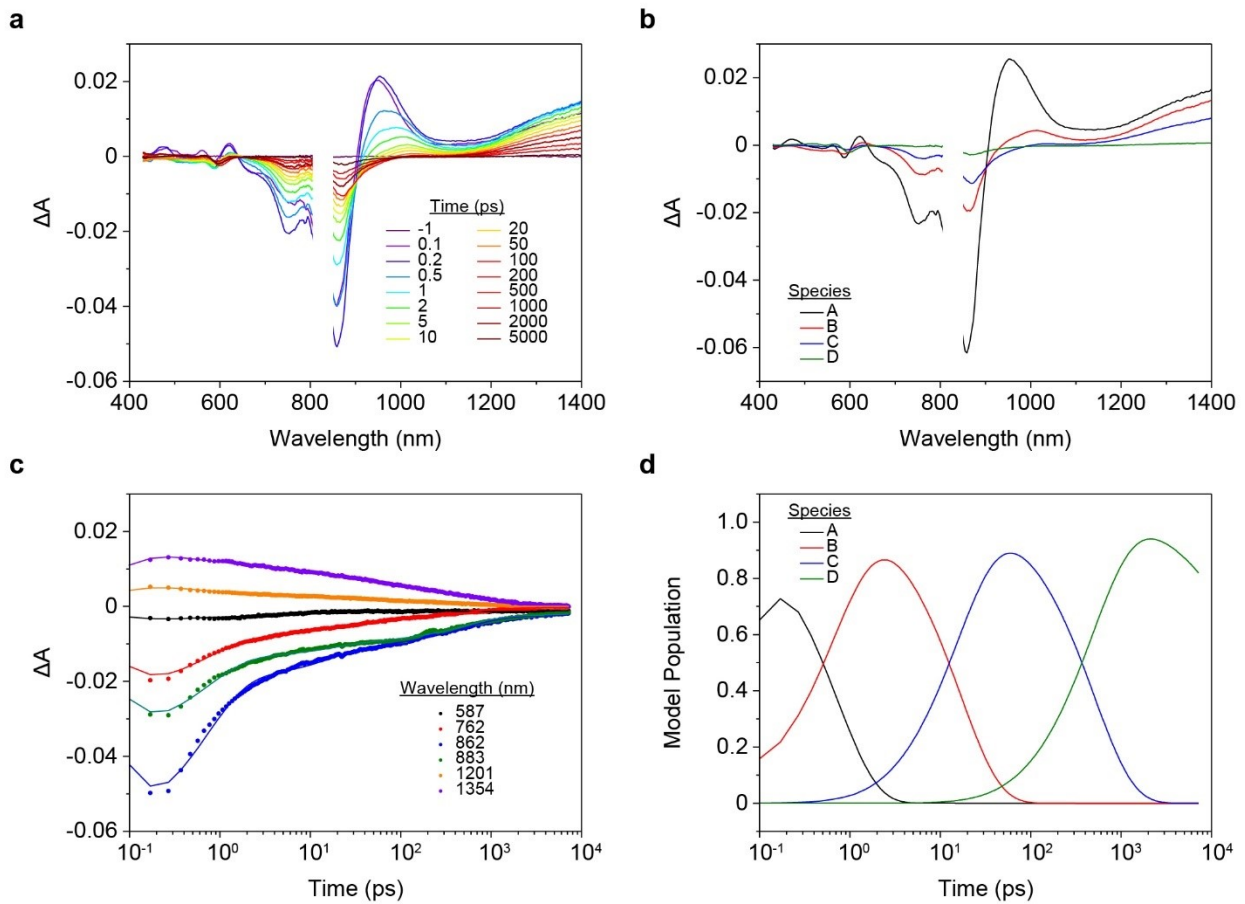
Figure S53. fsTA of **D18-Cl:BTF** (with 1-CN additive) blend films excited at 830 nm. (a) Transient absorption spectra at the indicated time delays, (b) evolution-associated spectra, (c) kinetics, and corresponding fits at the indicated wavelengths, and (d) model population dynamics. Global fits in (b), (c), and (d) are conducted with the kinetic model described above and in Eqn. S1.
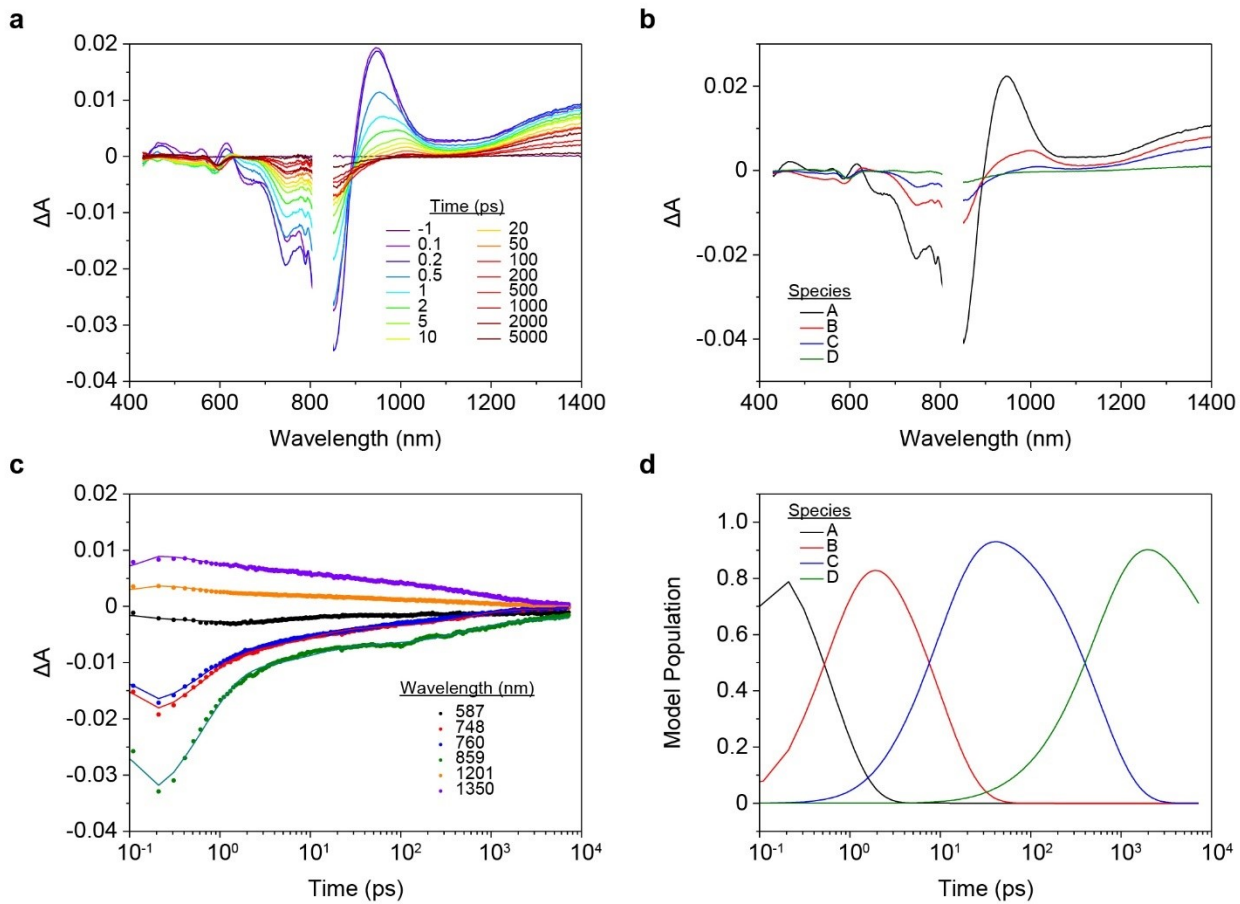
Figure S54. fsTA of **D18-Cl:BTFM** (without 1-CN additive) blend films excited at 830 nm. (a) Transient absorption spectra at the indicated time delays, (b) evolution-associated spectra, (c) kinetics, and corresponding fits at the indicated wavelengths, and (d) model population dynamics. Global fits in (b), (c), and (d) are conducted with the kinetic model described above and in Eqn. S1.
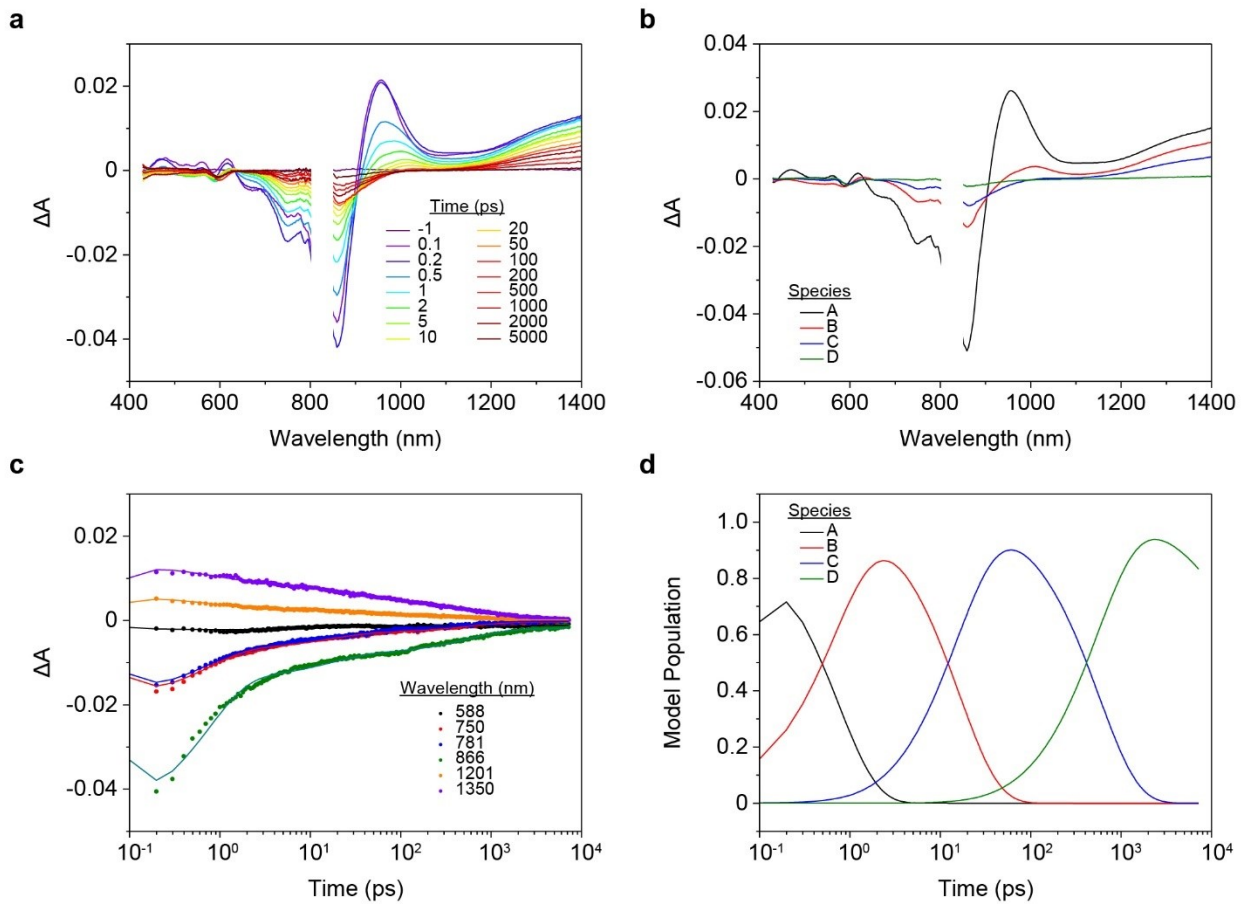
Figure S55. fsTA of **D18-Cl:BTFM** (with 1-CN additive) blend films excited at 830 nm. (a) Transient absorption spectra at the indicated time delays, (b) evolution-associated spectra, (c) kinetics, and corresponding fits at the indicated wavelengths, and (d) model population dynamics. Global fits in (b), (c), and (d) are conducted with the kinetic model described above and in Eqn. S1.
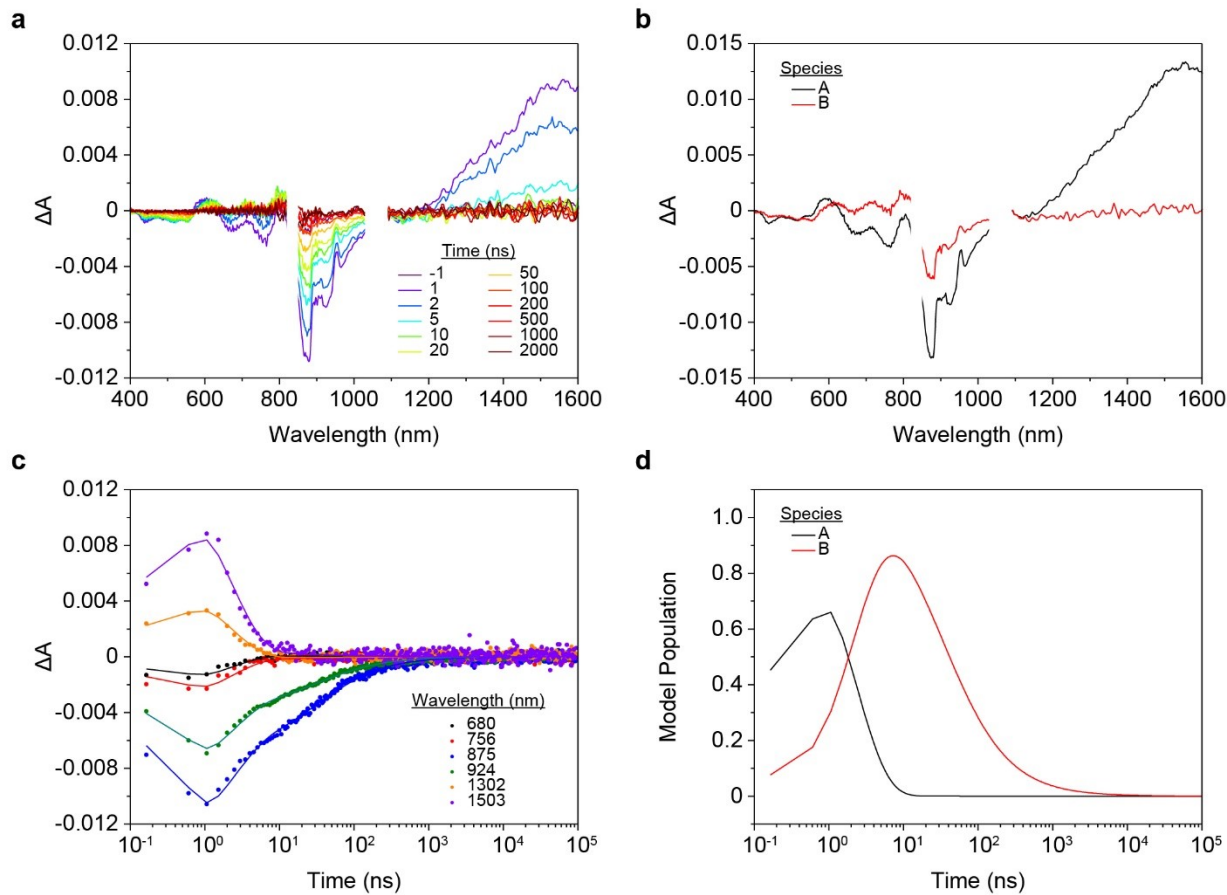
Figure S56. nsTA of neat **BTF** films excited at 830 nm. (a) Transient absorption spectra at the indicated time delays, (b) evolution-associated spectra, (c) kinetics, and corresponding fits at the indicated wavelengths, and (d) model population dynamics. Global fits in (b), (c), and (d) are conducted with the kinetic model described above and in Eqn. S2.
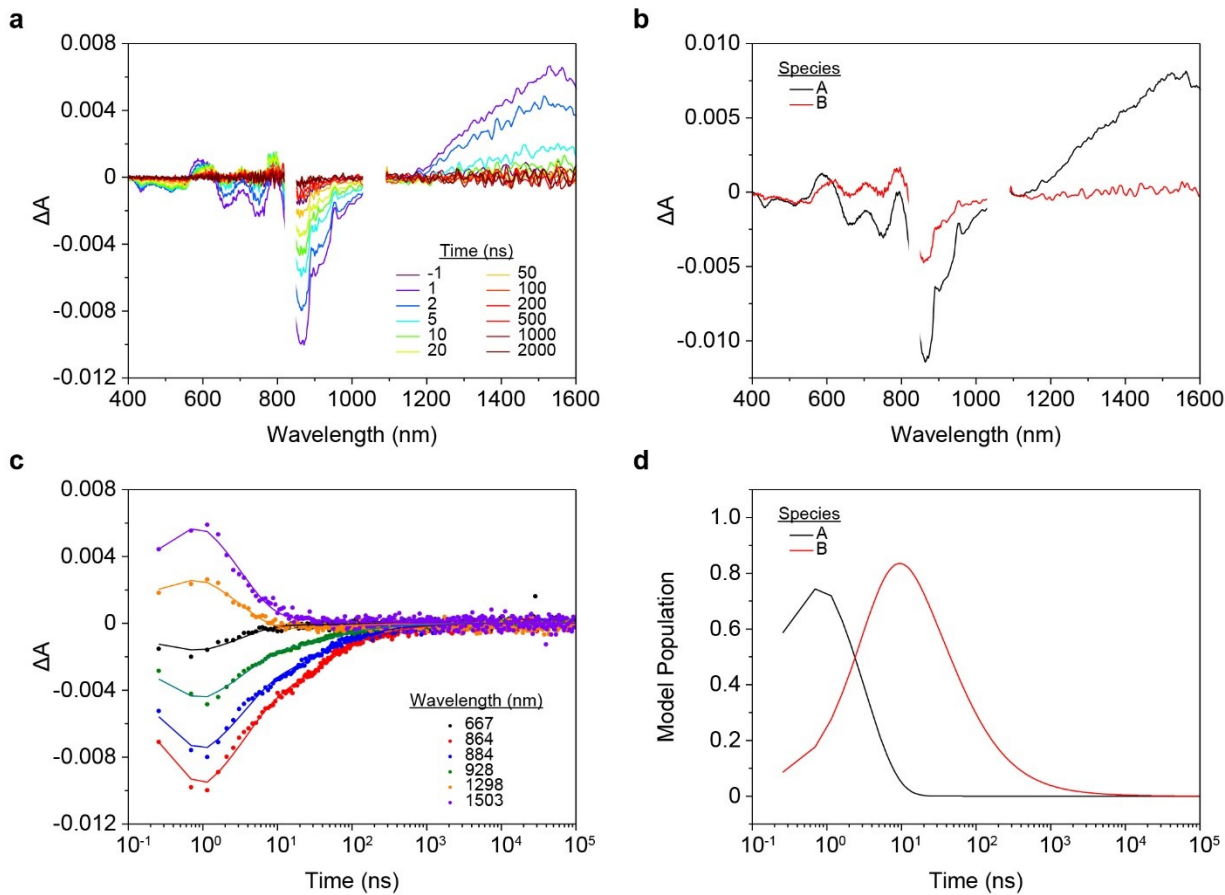
Figure S57. nsTA of neat **BTFM** films excited at 830 nm. (a) Transient absorption spectra at the indicated time delays, (b) evolution-associated spectra, (c) kinetics, and corresponding fits at the indicated wavelengths, and (d) model population dynamics. Global fits in (b), (c), and (d) are conducted with the kinetic model described above and in Eqn. S2.
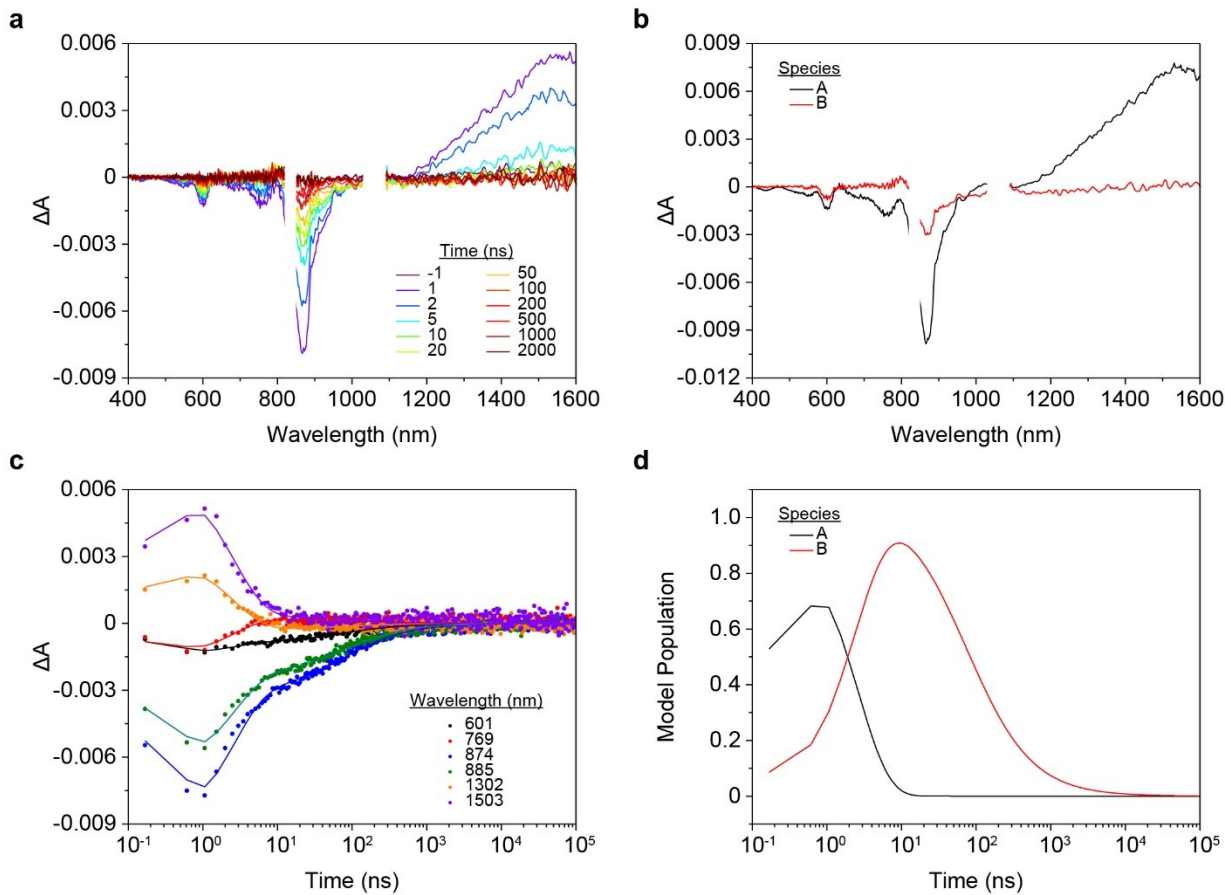
Figure S58. <u>nsTA</u> of **D18-Cl:BTF** (without 1-CN additive) blend films excited at 830 nm. (a) Transient absorption spectra at the indicated time delays, (b) evolution-associated spectra, (c) kinetics, and corresponding fits at the indicated wavelengths, and (d) model population dynamics. Global fits in (b), (c), and (d) are conducted with the kinetic model described above and in Eqn. S2.
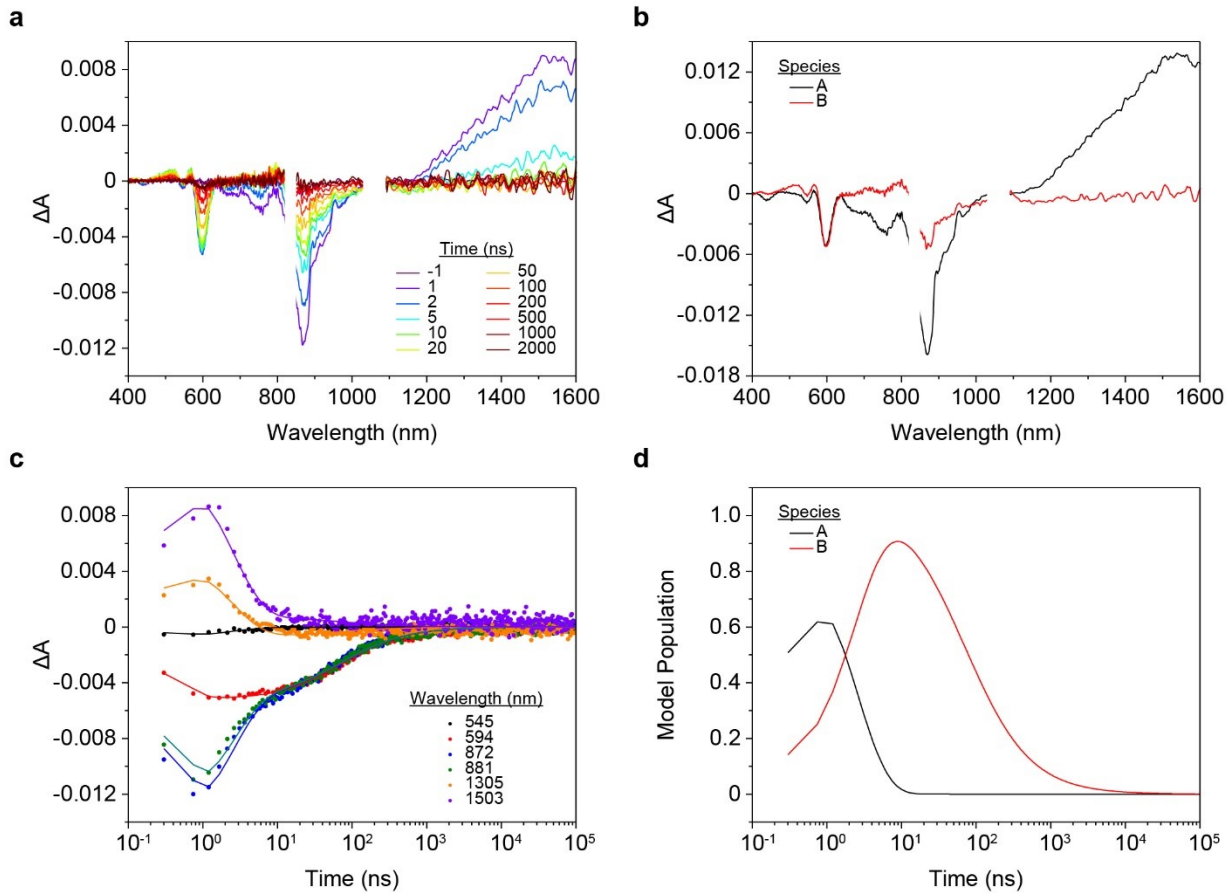
Figure S59. nsTA of **D18-Cl:BTF (with 1-CN additive) blend films** excited at 830 nm. (a) Transient absorption spectra at the indicated time delays, (b) evolution-associated spectra, (c) kinetics, and corresponding fits at the indicated wavelengths, and (d) model population dynamics. Global fits in (b), (c), and (d) are conducted with the kinetic model described above and in Eqn. S2.
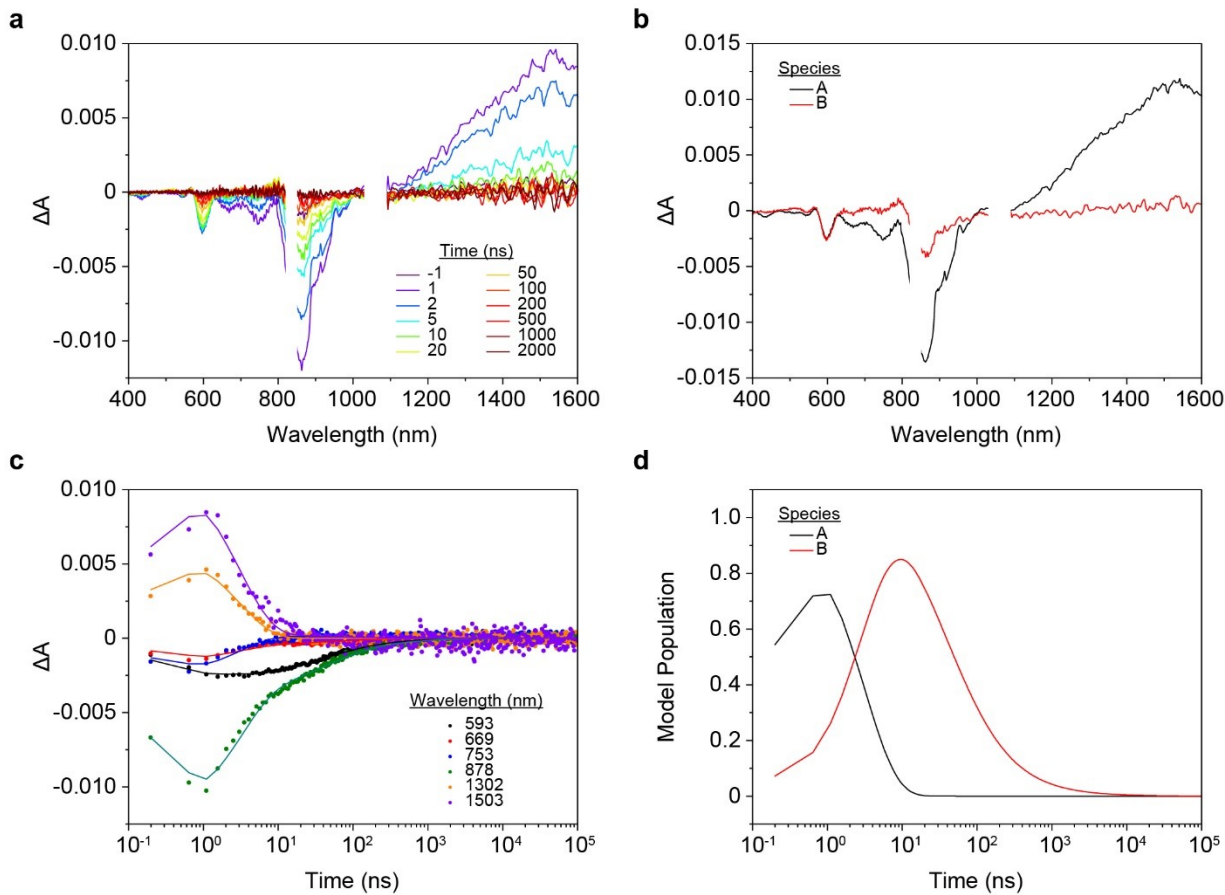
Figure S60. nsTA of **D18-Cl:BTFM** (without 1-CN additive) blend films excited at 830 nm. (a) Transient absorption spectra at the indicated time delays, (b) evolution-associated spectra, (c) kinetics, and corresponding fits at the indicated wavelengths, and (d) model population dynamics. Global fits in (b), (c), and (d) are conducted with the kinetic model described above and in Eqn. S2.
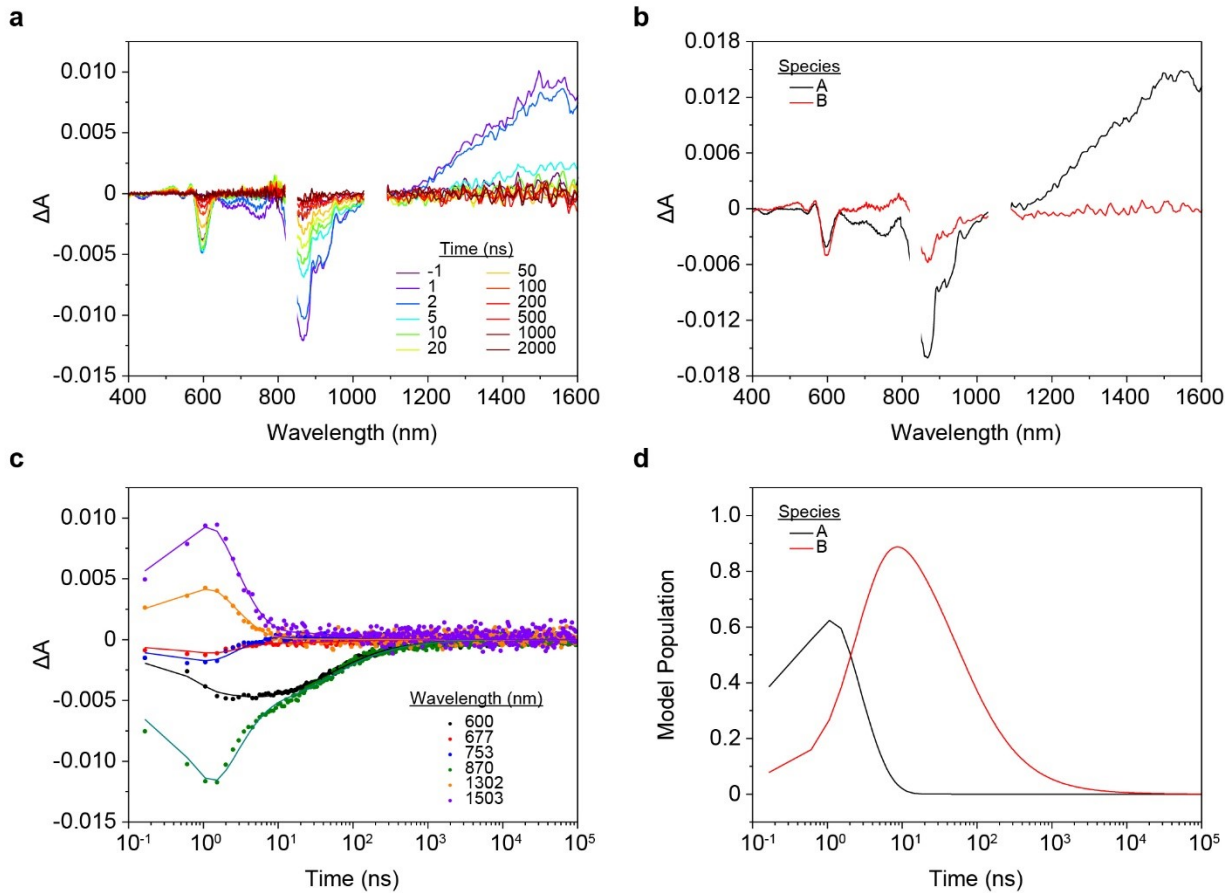
**Figure S61.** <u>nsTA</u> of **D18-Cl:BTFM** (with 1-CN additive) blend films excited at 830 nm. (a) Transient absorption spectra at the indicated time delays, (b) evolution-associated spectra, (c) kinetics, and corresponding fits at the indicated wavelengths, and (d) model population dynamics. Global fits in (b), (c), and (d) are conducted with the kinetic model described above and in Eqn. S2.

Table S14. Kinetic rate constants determined via global analysis, as described above, for the fsTA data of the films in Fig. S50–S55.

Film	Additive	k_1 (s^{-1})	k_2 (s^{-1})	k_3 (s^{-1})	k_4 (ΔA^{-1} s^{-1})
BTF	—	$(1.28 \pm 0.02) \times 10^{12}$	$(6.46 \pm 0.09) \times 10^{10}$	$(1.86 \pm 0.02) \times 10^{9}$	$< 10^8$
BTFM	—	$(1.32 \pm 0.02) \times 10^{12}$	$(6.69 \pm 0.09) \times 10^{10}$	$(1.71 \pm 0.02) \times 10^{9}$	$< 10^8$
D18-Cl:BTF	—	$(1.55 \pm 0.01) \times 10^{12}$	$(8.2 \pm 0.1) \times 10^{10}$	$(2.14 \pm 0.03) \times 10^{9}$	$< 10^8$
D18-Cl:BTF	1-CN	$(1.35 \pm 0.01) \times 10^{12}$	$(5.9 \pm 0.1) \times 10^{10}$	$(1.98 \pm 0.03) \times 10^{9}$	$< 10^8$
D18-Cl:BTFM	—	$(1.59 \pm 0.02) \times 10^{12}$	$(10.2 \pm 0.2) \times 10^{10}$	$(1.80 \pm 0.03) \times 10^{9}$	$< 10^8$
D18-Cl:BTFM	1-CN	$(1.34 \pm 0.02) \times 10^{12}$	$(6.11 \pm 0.08) \times 10^{10}$	$(1.75 \pm 0.02) \times 10^{9}$	$< 10^8$

Table S15. Kinetic rate constants determined via global analysis, as described above, for the nsTA data of the films in Fig. S56–S61.

Film	Additive	k_1 (s^{-1})	k_2 (ΔA^{-1} s^{-1})
BTF	—	$(4.4 \pm 0.1) \times 10^8$	$(2.64 \pm 0.08) \times 10^{7}$
BTFM	—	$(3.03 \pm 0.07) \times 10^{8}$	$(2.51 \pm 0.09) \times 10^{7}$
D18-Cl:BTF	—	$(3.98 \pm 0.09) \times 10^{8}$	$(1.26 \pm 0.03) \times 10^{7}$
D18-Cl:BTF	1-CN	$(4.1 \pm 0.1) \times 10^8$	$(1.33 \pm 0.03) \times 10^{7}$
D18-Cl:BTFM	—	$(3.19 \pm 0.08) \times 10^{8}$	$(2.25 \pm 0.09) \times 10^{7}$
D18-Cl:BTFM	1-CN	$(4.1 \pm 0.1) \times 10^8$	$(1.76 \pm 0.05) \times 10^{7}$

18. Computational Methods

Single molecules were taken from their respective single crystal structures and their alkyl chains were truncated down to methylene units; hydrogen atoms were then added to form methyl units in the Avogadro program (version 1.2.0)[9]. The added hydrogen atoms were energy minimized at the molecular mechanics / universal force field level MM/UFF[13], in Avogadro; this gives reasonable C H bond lengths and angles. The structures were subsequently optimized with Density Functional Theory (DFT) using KDIIS in vacuum in Orca (version 4.1.2)[14], using the Becke three-parameter Lee Yang Parr (B3LYP[15]) hybrid functional with the second generation Ahlrich's triple zeta basis set with a polarization function (Def2-TZVP[16]), and the third generation Grimme's dispersion correction plus Becke Johnson damping (D3BJ) with a tight SCF and Grid2 integration. The FMOs, I.E.s/E.A.s, and internal electron reorganization energies[17] were evaluated with a final grid of 4. To speed up the convergence and reduce the computational cost, the resolution of the identity chain-of sphere integration for the Hartree Fock exchange (RIJCOSX[18, 19]) was applied with its Def2/J basis[18, 20]. The molecular structures and orbital surfaces were visualized in the ChemCraft program (version 574b) with the isosurface value of ±0.006.

The methyl-truncated molecules were also used for the electron coupling. For each single crystal, the nuclear coordinates of these structures were labeled A, and the nearest neighbor molecules to each A structure were given the labels B, C, D…*etc*.. With structure A, the nearest neighbors form the dimer pairs for the electron coupling calculations, such as AB, AC, AD…*etc*.. The coupling was performed with the Frozen density Embedding (FDE) method[10] in the ADF program[16]. The electron reorganization energies were calculated with the four-point procedure. In addition to the Cartesian coordinates in Section 18.5, the geometries are also freely available to download from: https://doi.org/10.6084/m9.figshare.17062337.v1.

18.1 Molecular Energy Levels
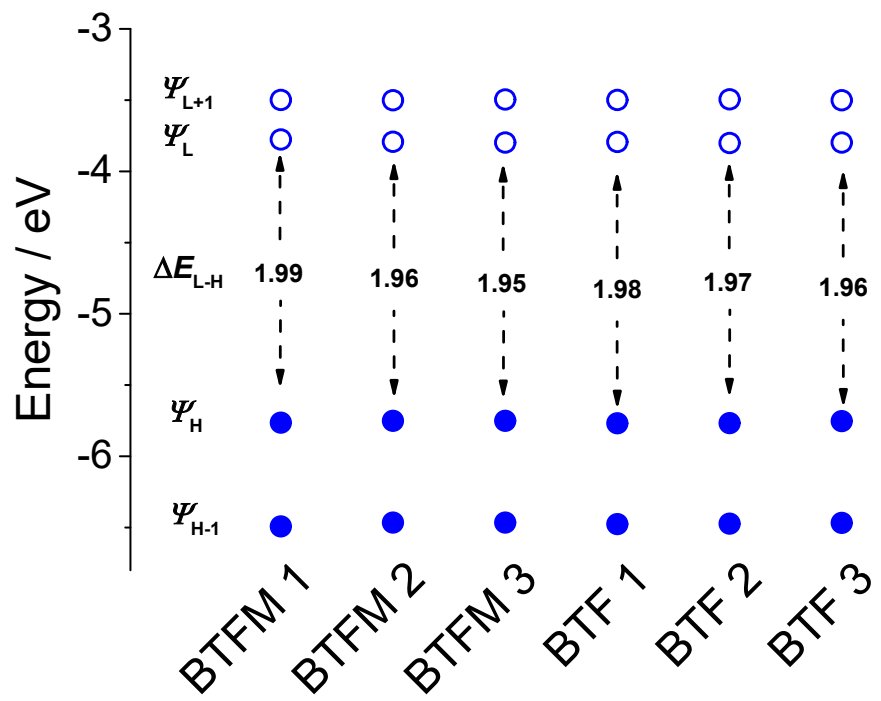
Figure S62. Relative energies and energy gaps (eV) of the frontier molecular orbitals for the **BTFM** and **BTF** structures.

18.2 Internal Reorganization Energies (IREs)

Table S16. The internal electron reorganization energies of the three isomers considered for the BTFM and BTF structures.

Entry	λ_e / eV
BTFM isomer 1	0.128
BTFM isomer 2	0.125
BTFM isomer 3	0.117
BTF isomer 1	0.130
BTF isomer 2	0.124
BTF isomer 3	0.122

18.3 Vertical Ionization and Electron Affinities

Table S17. Vertical and adiabatic ionizations and electron affinities of the three isomers considered for the **BTFM** and **BTF** structures.

Entry	IE_v / eV	IE_A / eV	EA_v / eV	EA_A / eV
BTFM isomer 1	6.558	6.452	3.030	3.211
BTFM isomer 2	7.360	7.222	3.053	3.090
BTFM isomer 3	7.363	7.180	3.067	3.130
BTF isomer 1	7.368	6.492	3.050	3.099
BTF isomer 2	7.365	6.455	3.060	3.070
BTF isomer 3	6.536	6.449	3.059	3.117

18.4 Electron couplings
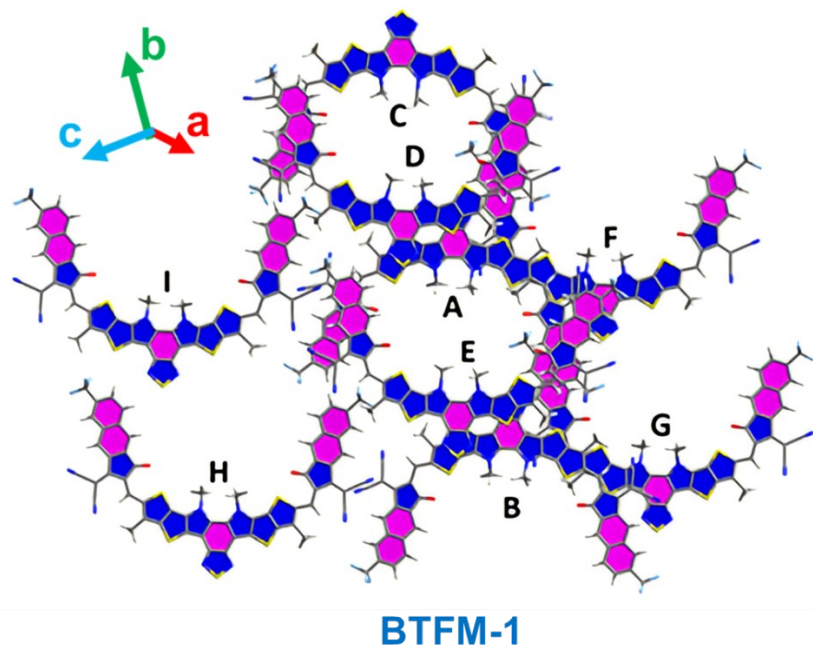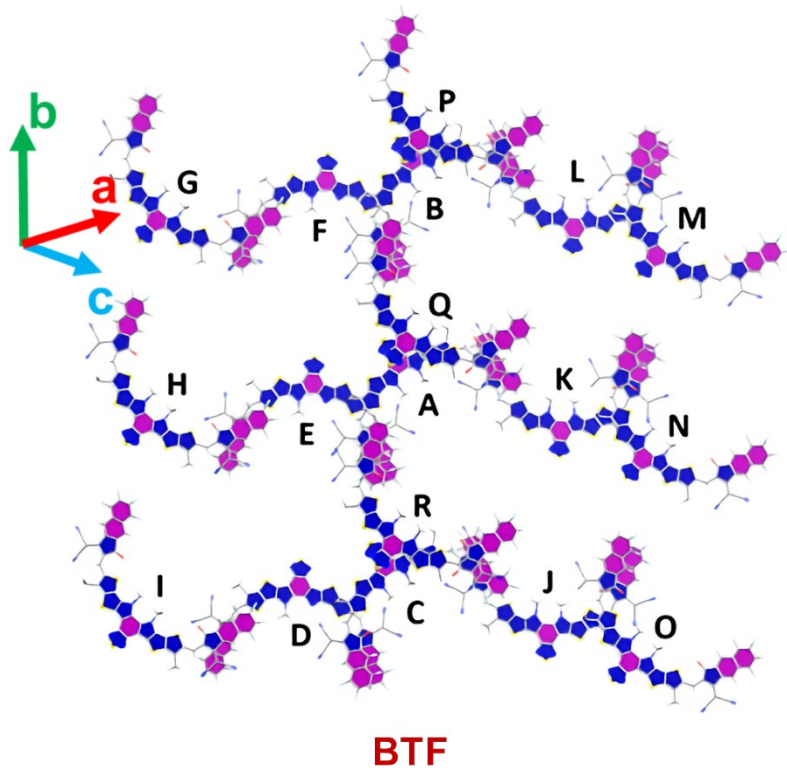
Figure S63. Nearest neighbor molecules and their alphabetical labels in the single-crystal structures of **BTF** and **BTFM-1.**

Table S18. Electronic couplings in **BTF** and **BTFM-1**; positive values are for hole and negative values for electron coupling.

Labels refer to the numbering scheme in the figures in the main text as defined in the Methods Section.

BTF	
Label	E-Coupling / meV
AB	0
AC	0
AD	0
AE	16.466
AF	0
AG	0
AH	0
AI	0
AJ	0
AK	26.166
AL	0
AM	0
AN	0
AO	0
AP	0
AQ	22.693
AR	7.761

BTFM-1	
Label	E-Coupling / meV
AB	1.482
AC	0.897
AD	2.682
AE	71.556
AF	17.109
AG	20.964
AH	0.43
AI	14.906

Ψ_H

Ψ_L
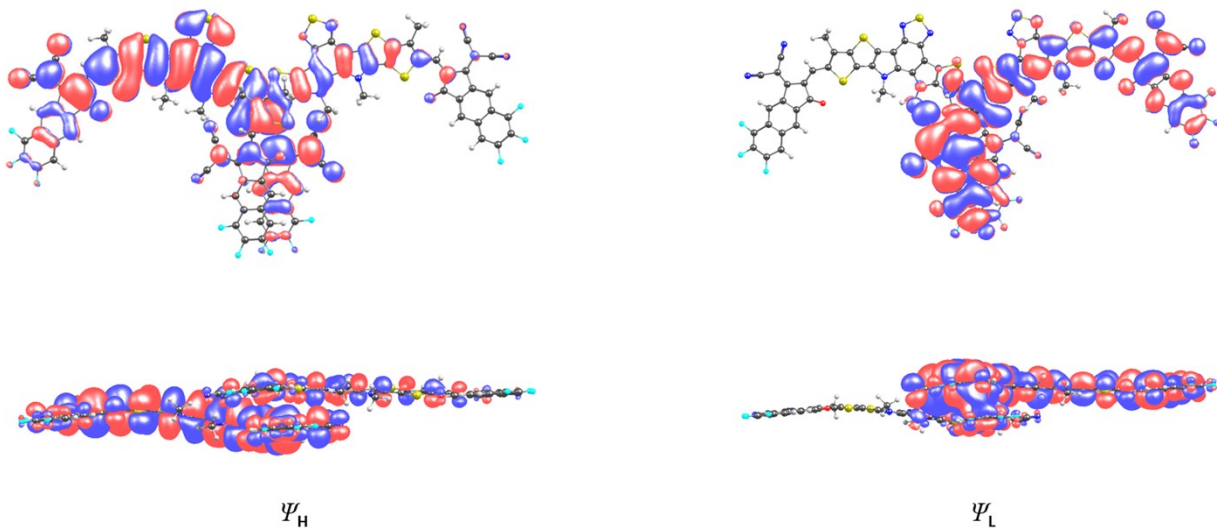
Figure S64. FMO of the dimer AE in the **BTF** single crystal.

Ψ_H

Ψ_L
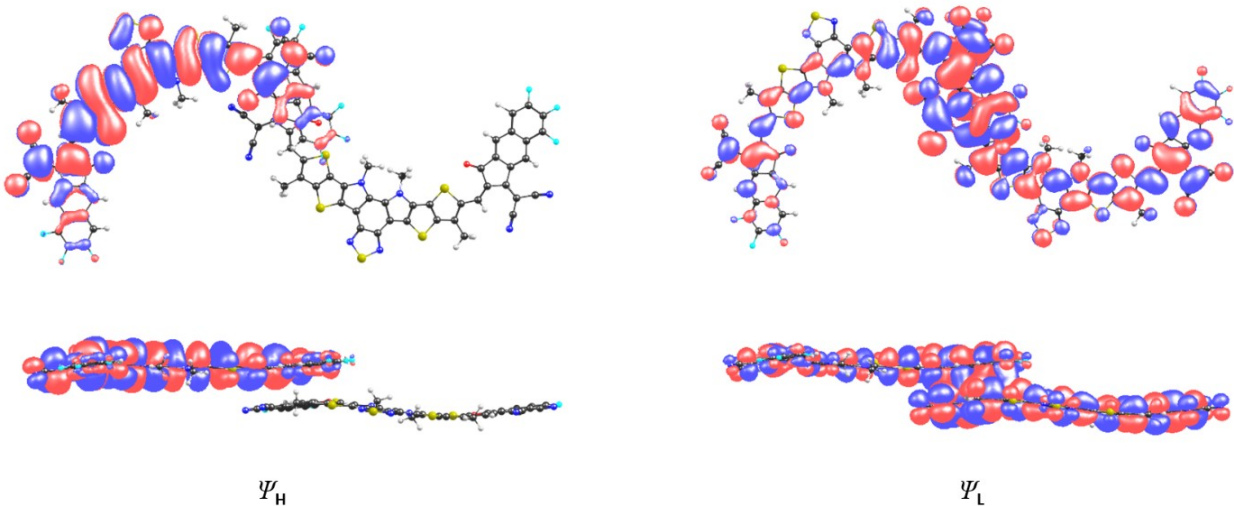
Figure S65. FMO of the dimer AK in the **BTF** single crystal.

Ψ_H

Ψ_L
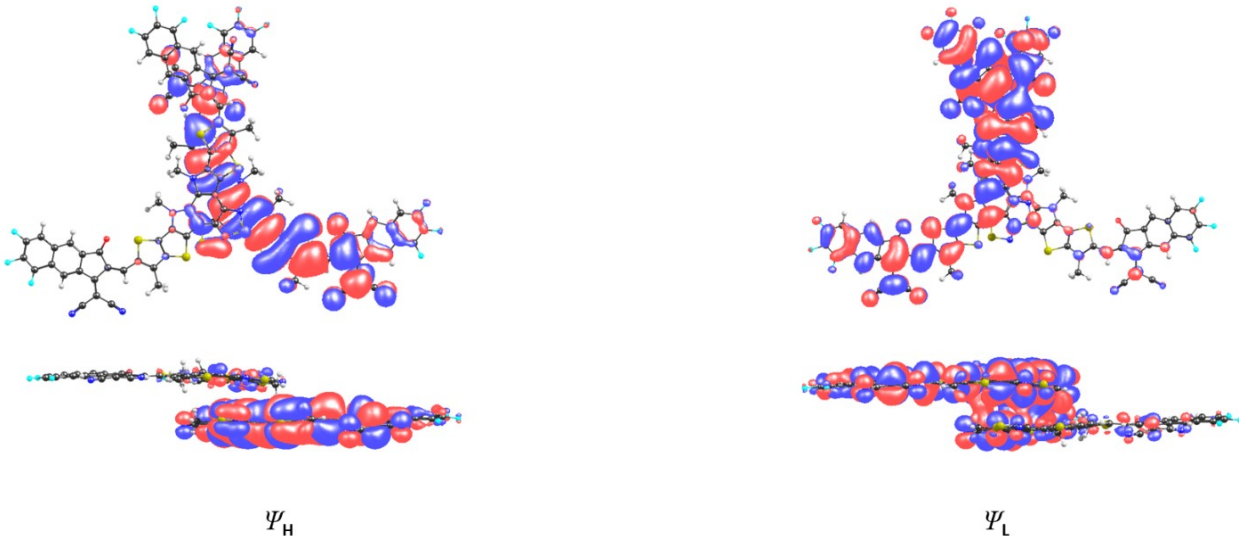
Figure S66. FMO of the dimer AQ in the **BTF** single crystal.

Ψ_H

Ψ_L
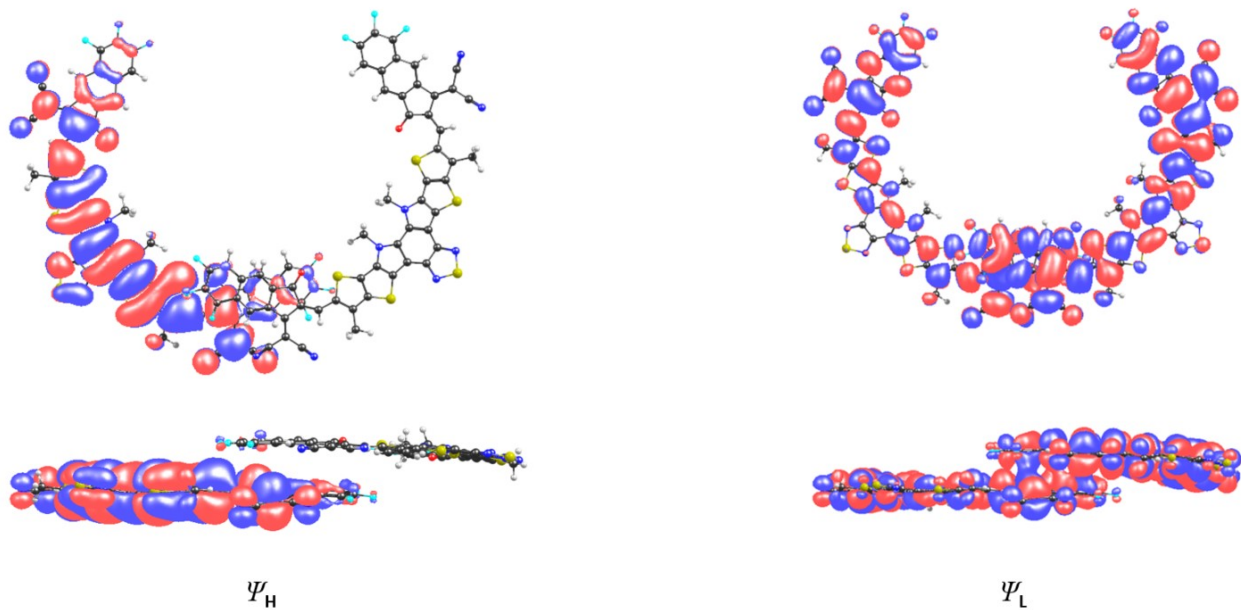
Figure S67. FMO of the dimer AR in the **BTF** single crystal.

Ψ_H

Ψ_L
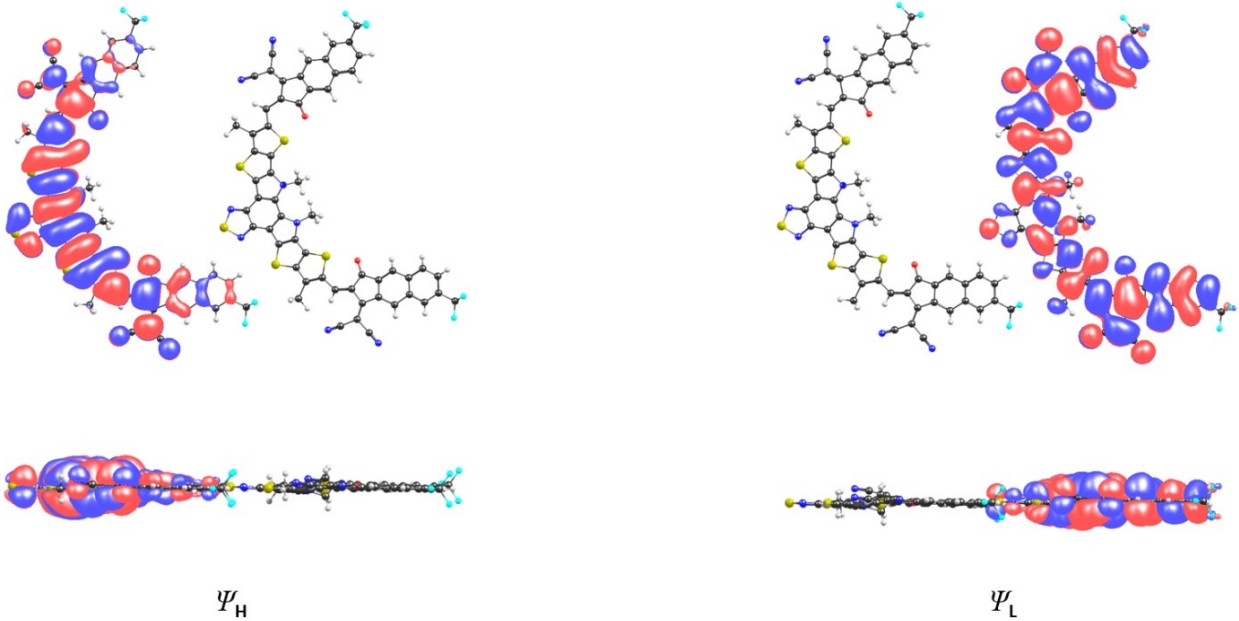
Figure S68. FMO of the dimer AB in the **BTFM** single crystal.

Ψ_H

Ψ_L
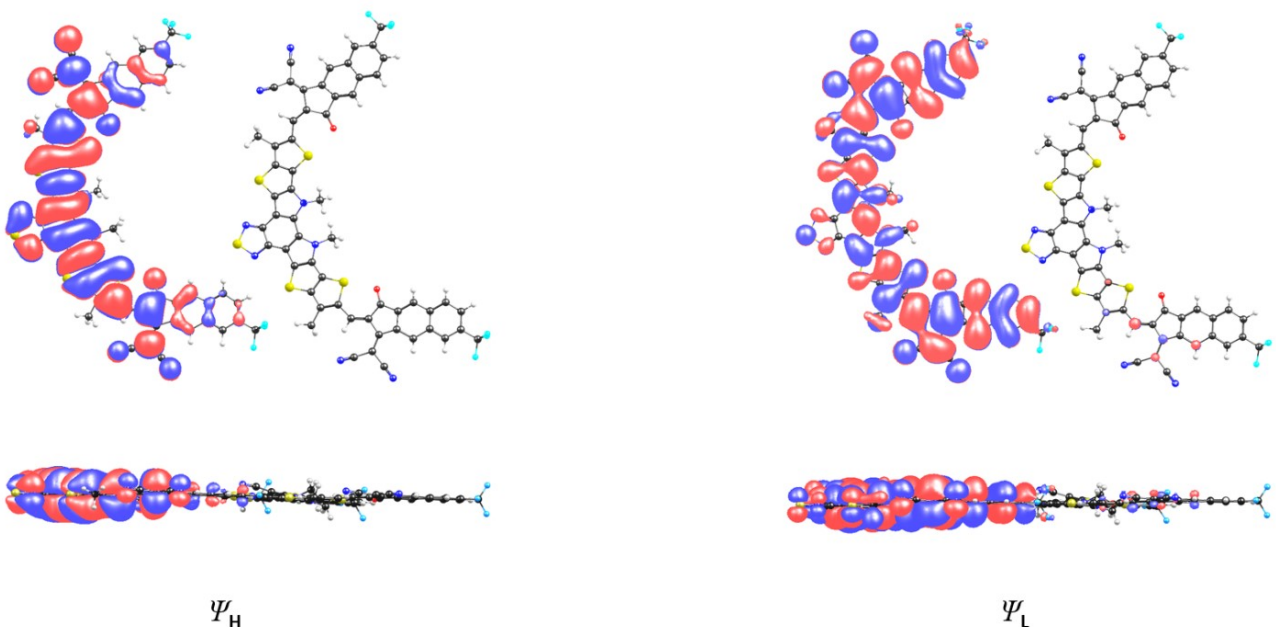
Figure S69. FMO of the dimer AC in the **BTFM** single crystal.

Ψ_H

Ψ_L
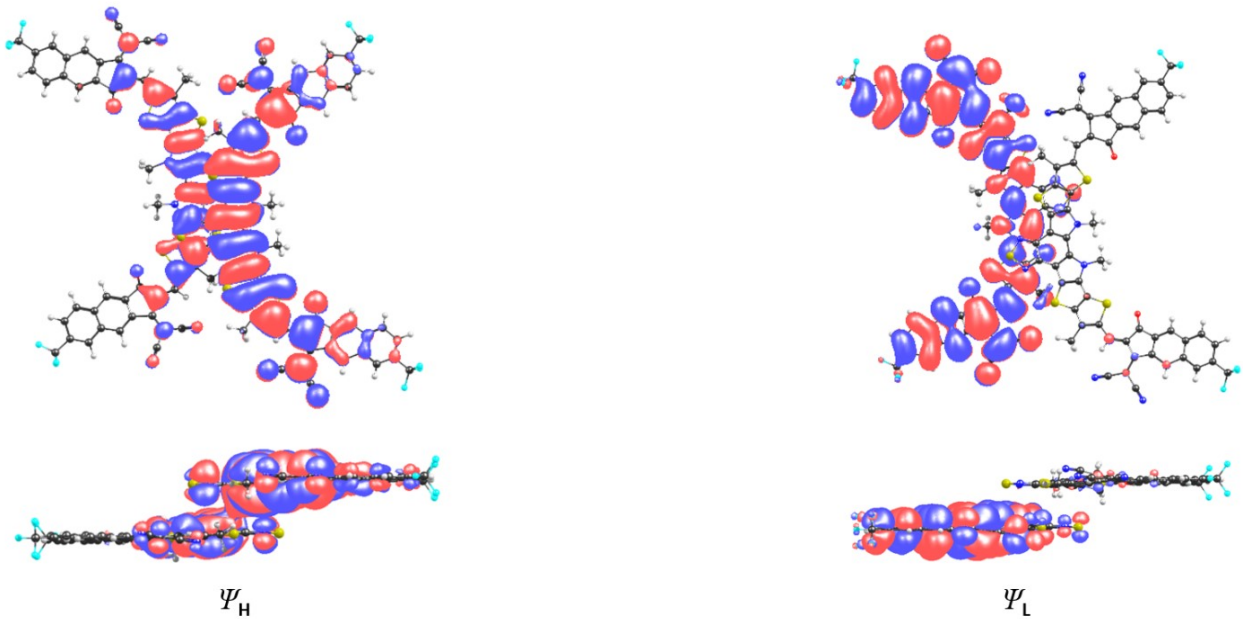
Figure S70. FMO of the dimer AD in the **BTFM** single crystal.

Ψ_H

Ψ_L
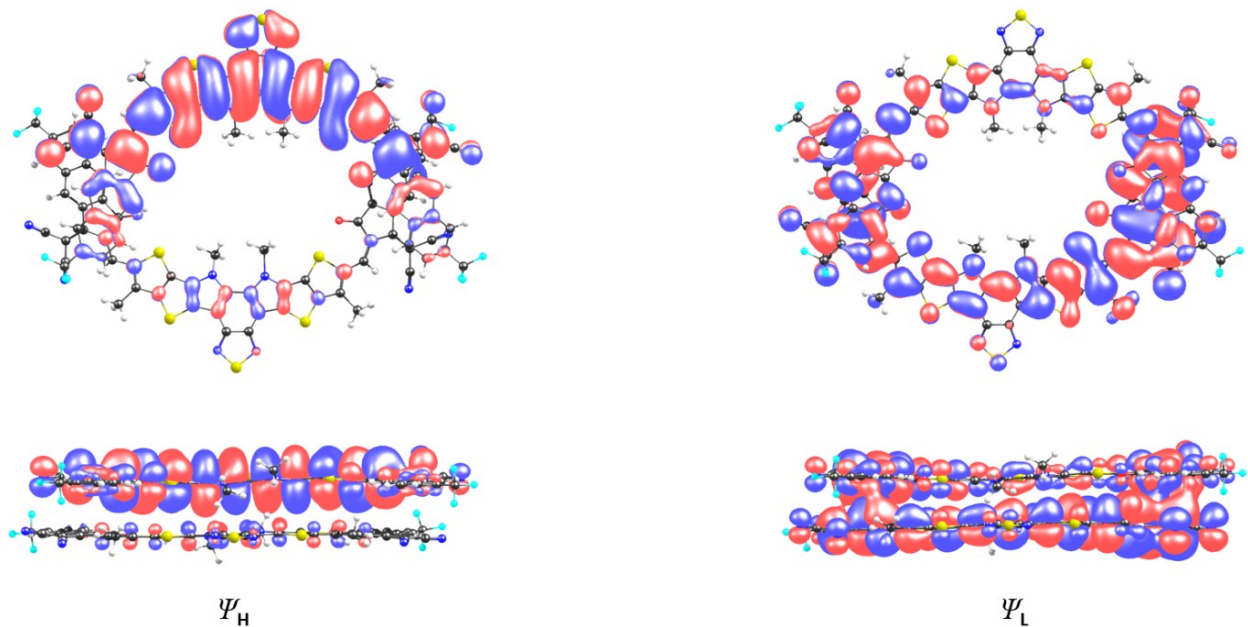
Figure S71. FMO of the dimer AE in the **BTFM** single crystal.

Ψ_H Ψ_L
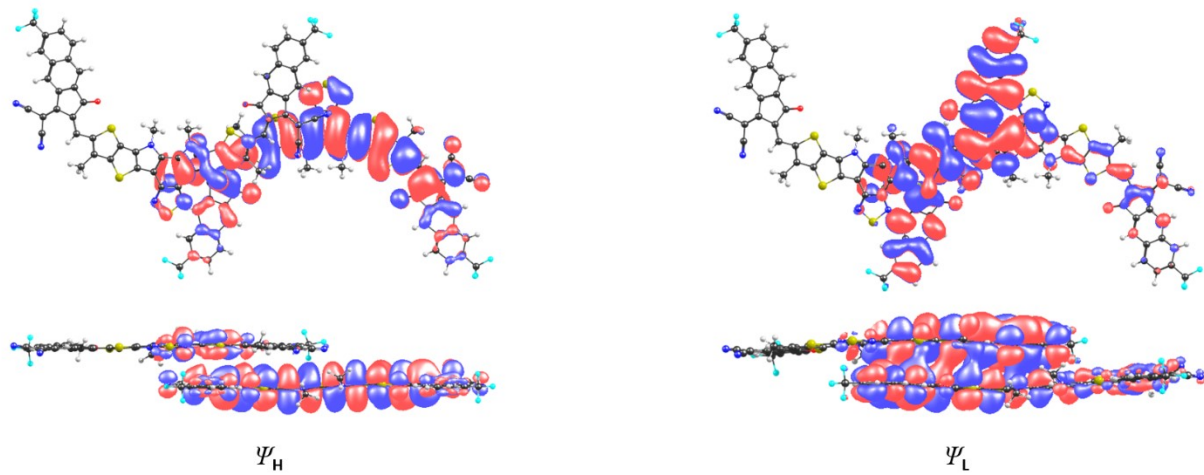
Figure S72. FMO of the dimer AF in the **BTFM** single crystal.

Ψ_H Ψ_L
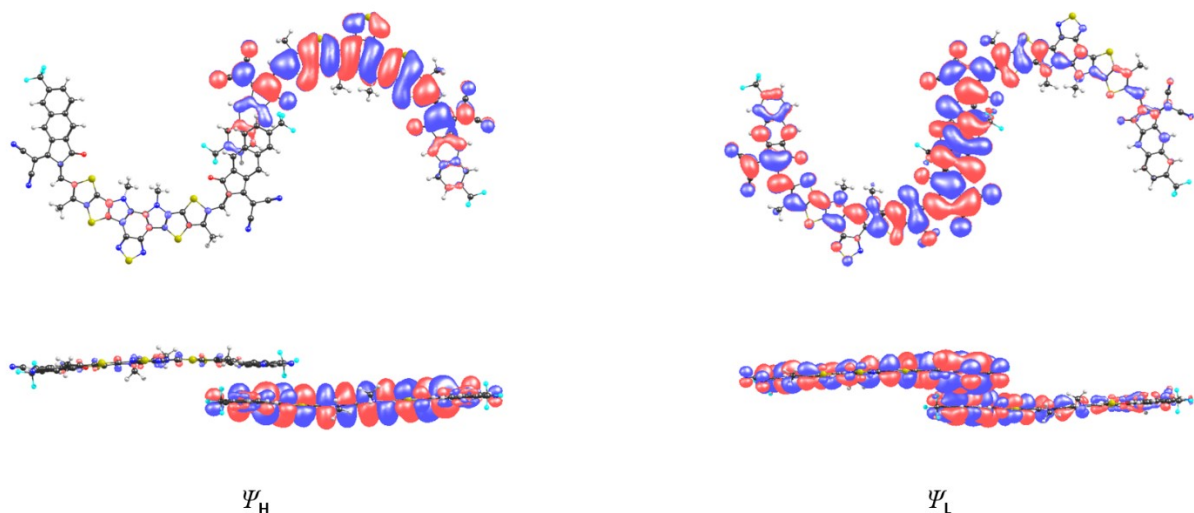
Figure S73. FMO of the dimer AG in the **BTFM** single crystal.

Ψ_H

Ψ_L
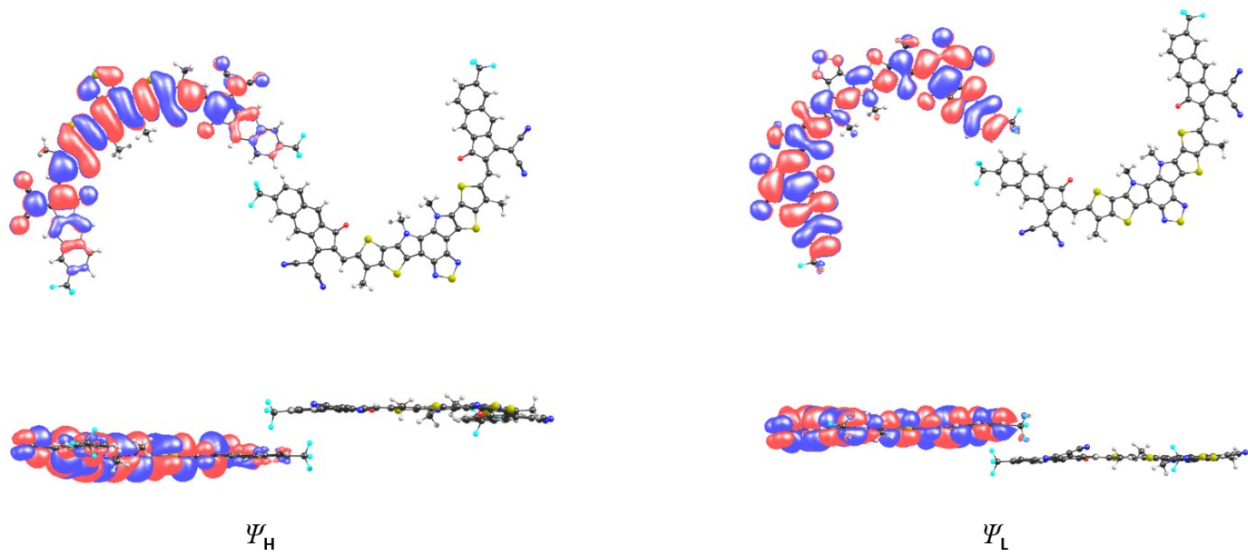
Figure S74. FMO of the dimer AH in the **BTFM** single crystal.

Ψ_H

Ψ_L
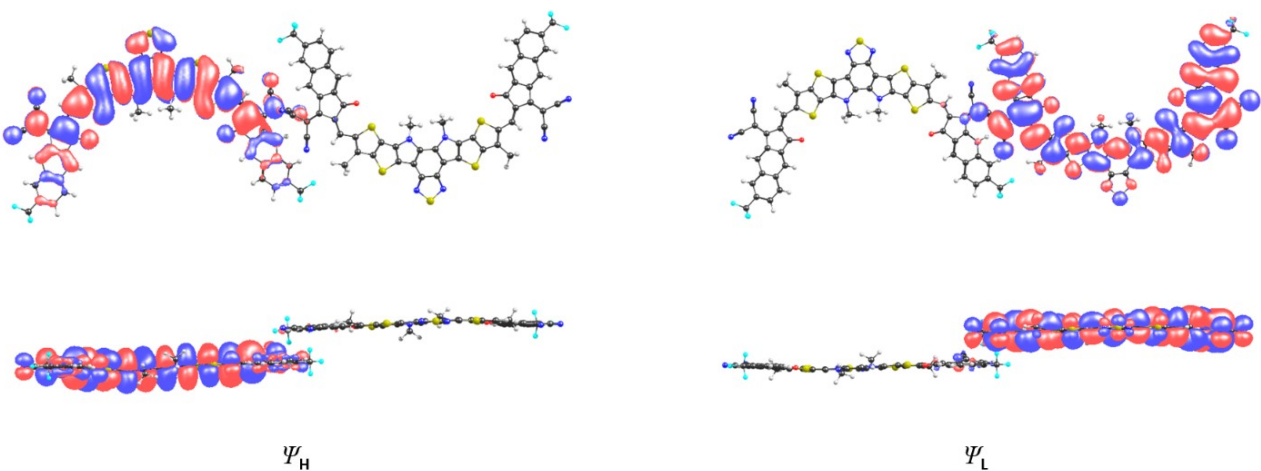
Figure S75. FMO of the dimer AI in the **BTFM** single crystal.

18.5 Cartesian Coordinates

The coordinates are for the methyl-truncated structures (**BTF** and **BTFM**) optimized in vacuum at level of B3LYP/Def2-TZVPP/D3BJ.

Table S19. Cartesian coordinates of the methyl-truncated **BTF** (isomer 1, 2, and 3).

		BTF isomer 1	
F	-22.14492921196328	-5.71970044913106	-1.16431257833695
H	-15.30068114147534	5.68561537281137	0.50186619377116
F	-23.15635442256486	-3.81480956247539	-0.90261361252323
H	-6.02541430162702	1.55828162120038	-2.97519488248381
C	-22.13577479861273	-4.56997090123314	-0.45733278713294
H	-9.64856206236740	0.90682992924095	-1.76572080223398
F	-2.47898462249880	-11.85964466206660	1.69348942193226
H	-21.66321675231187	-1.90902577949714	-0.58798830983118
C	-20.81034402335647	-3.86527243161090	-0.55869525164694
N	-21.25308351166164	2.40320631480171	-0.83693163848511
C	-20.75429210498994	-2.49561764112100	-0.59315888068303
H	-7.68644221787683	1.78850815852296	-2.43767288991702
H	-19.69658823948959	-5.71635973085366	-0.53563931581116
C	-19.62710414597660	-4.63757822271323	-0.56542157893489
C	-20.10790259633633	2.52468677385641	-0.76204829880305
H	-20.37082177363054	0.14038811271651	-0.61505393329094
C	-19.50793158067847	-1.82981724515424	-0.63486032738759
C	-19.44483080605866	-0.41235159098206	-0.63922654607631
C	-18.40674160600459	-4.01990280465285	-0.61847353936620
C	-18.69973850148367	2.69543479984466	-0.66228137835750
C	-18.28526436860643	4.05683958894520	-0.65900541260737
N	-17.96399160158327	5.16588783984878	-0.64962382983525
C	-18.30824441843555	-2.60996858893251	-0.65331507900555
H	0.55388280739175	0.07354855633474	-0.48290975773893
H	-17.49754903507922	-4.60765819853840	-0.62856670032632
C	-18.21877433207227	0.20694147182152	-0.64801308154756
C	-17.82630288808197	1.63259994010027	-0.59253204026326
C	-17.05921460615360	-1.94534748666421	-0.69354094639727
C	-17.03591609203749	-0.58237722219685	-0.68525982100272
C	-16.37198667138693	1.68021484917292	-0.50078470512613
H	-16.20794348032215	3.64785116027778	0.15186314203212
H	-16.13440090546391	-2.50879018849592	-0.71546687364783
C	-15.85602292151244	0.30843195926937	-0.67460357456453
C	-15.63021041482098	2.77787307386148	-0.12368951619608
C	-14.64483661686266	5.25187776019737	1.25957101152883
H	-14.03579774291800	6.05301535996383	1.67667455522908
C	-14.25458292016118	3.00831049909099	0.04490261632584
O	-14.69199295034320	-0.04282630058451	-0.76664527164496

S85

```
C    -13.77465016049234      4.17765239722596      0.68505628825647
C    -12.38299703288892      4.20010473924240      0.72244384302928
S    -12.93296669901800      1.97759085618320     -0.52269587571483
S    -11.21028024268739      5.32129302618143      1.41314195896487
C    -11.78284685573180      3.10673868169645      0.06675083554291
C     -6.75159471045575      1.28935885572176     -2.20770634104765
C     -9.92239821432435      4.32996733437549      0.79772312567043
C    -10.38699540560639      3.20813154001569      0.09953787660459
C     -8.51304330457192      4.26065524373283      0.80866433457500
N     -7.66661207456401      5.99986657996526      2.33204418229674
C     -7.49294202221917      4.97539782133298      1.50530695857743
C     -8.16454206112545      3.10691873274397      0.05636754764188
N     -9.32106525467350      2.45584512291158     -0.34774885436924
N     -6.25890892869416      1.74272453132069     -0.90630831348627
C     -6.80732770052408      2.76301609881497     -0.13819257866914
S     -6.20124428175975      6.36968408405594      2.94460287281363
C     -6.11515591906566      4.53483204777338      1.42003976668913
C     -5.77677773215285      3.43576843601563      0.57049643475646
N     -5.29327217670407      5.24724664656285      2.18372734632562
C     -4.90396709829516      1.73178028958449     -0.63843530617150
C     -4.57218404949961      2.76308926806816      0.24221050723870
C     -9.47083929731409      1.04760527266105     -0.69933206757905
C     -3.83613523189476      0.88303996662649     -0.94732092647579
H     -5.67341434759810     -7.95151329893233      0.14696037944024
S     -3.69070598859303     -0.66689758541077     -1.66187678903487
H     -5.22852560129981     -9.97794876458692      1.47399342981198
H     -4.86448338708336     -5.81185571911919     -0.87583485233195
S     -2.87987001028027      2.76344767182353      0.64904900159177
C     -4.66857701770879     -8.17552072911520      0.48169579121490
C     -2.64692230011421      1.31769457967464     -0.33712908673243
O     -3.81377682340876     -3.33953490411847     -1.91203342874910
C     -4.42276809377975     -9.30477560680943      1.21767941665624
F     -3.94386154213380    -11.21850834148597      3.16029177563377
F    -22.41996987639348     -4.90284877373933      0.82349108011932
C     -3.86570785571760     -6.06973843662469     -0.54586350262249
C     -2.00629123469455     -0.76660348914177     -1.12979560921463
C     -1.58048464183753      0.42660671013410     -0.49655759081022
C     -3.62830347573316     -7.27558177523234      0.15908117115278
C     -2.86056002248168     -3.86184845483449     -1.36188636742710
C     -3.11351287267567     -9.58236911183925      1.66665388299710
C     -2.84958683498484    -10.82282985457734      2.47762565887793
C     -2.82550115279700     -5.21813121422823     -0.77034525819374
H      0.06653795838894      1.73203012639094     -0.16667051526608
C     -0.19606390263369      0.68752764012016      0.01012677157073
C     -1.21836995917182     -1.93393013161674     -1.07388874577674
```

```
C    -2.29782083509038    -7.57347585690437     0.59394719367436
C    -1.52220586535996    -3.27625004104325    -1.13279504227381
C    -2.07357630609322    -8.74677752107085     1.34807417398828
H    -0.20972686301319    -1.71216695347293    -0.75939708865831
C    -1.49579242773113    -5.50793555379145    -0.35529112559049
C    -1.23255900785582    -6.68173053452096     0.30734948692766
H    -1.07246999567400    -8.96529556189241     1.69589386318465
C    -0.63912165658154    -4.34946843495011    -0.68382690563004
H    -0.24398440438256    -6.93961634671853     0.65306774917465
C     0.73339760199181    -4.32952192871740    -0.58692573036219
H   -15.28048385305199     4.86597380417131     2.05881504478571
C     1.51758243023042    -3.18948735752450    -0.91449939429745
N     2.15949802496717    -2.26170442602634    -1.15872504112944
C     1.48651612509719    -5.46240817450387    -0.17204923589359
N     2.10045598916030    -6.38033841985938     0.16261663040891
H   -10.31807427323890     0.63952376399308    -0.15049201680440
H    -6.90111534648816     0.20977069154804    -2.22589095325192
H    -8.58073390476175     0.49999704364526    -0.40267339736609
H    -0.12677486817123     0.50527418169234     1.08679403535019
F    -1.86214164344370   -10.64167397517296     3.37632315467268
```

BTF isomer 2		
F	-23.40165627102177	-4.53685520609208	-1.00097052384681
H	-15.43318485235556	6.08942206082153	-0.91900176648555
F	-3.15830954525177	-12.35478958218914	-0.40883135808921
F	-24.04439776365409	-2.70708631344635	-0.02487257013567
H	-6.35808423490223	-0.28055150146949	-1.54764477818678
C	-23.08104552459748	-3.64487549423462	-0.03730876210421
H	-10.04366805541604	0.35553658813763	-1.15780148571177
H	-22.40095124178933	-1.05304451976258	-0.45934306954883
C	-21.71047782425289	-3.05989700091609	-0.25473357787259
N	-21.69546427753005	3.12679543214457	-1.29592845963215
C	-21.54572244588364	-1.71448854307310	-0.45191867866121
H	-7.89814439416371	0.55906242194622	-1.67634924830229
H	-20.74256009283114	-4.98569915739912	-0.08205102356638
C	-20.59314281316628	-3.92627830100098	-0.24376358185145
C	-20.54217948537240	3.16512969266395	-1.27313221416425
H	-20.96288674574079	0.85467315161450	-0.81477899399315
C	-20.25422355755240	-1.16628028229427	-0.63623918442887
C	-20.08346891939046	0.23042540019618	-0.80960123272117
C	-19.33206413891439	-3.42447554469007	-0.42576910252309
C	-19.12199425987830	3.23942994062205	-1.24244452818327
C	-18.62315525670632	4.55910978355863	-1.42702282092016
N	-18.24322346828891	5.63913147882073	-1.57766106043743
C	-19.12146566580359	-2.03921466313019	-0.62174048018198
H	0.14561157926887	0.61410979206258	0.15694508748603
H	-18.47495063875519	-4.08604826564661	-0.41091452402252
C	-18.81559991378956	0.74419394810816	-0.94026429938809
C	-18.31978030905855	2.13301408421674	-1.06965354148587
C	-17.82722014896875	-1.48579539983620	-0.78183751313945
C	-17.69823232418235	-0.13504673071716	-0.92366904249272
C	-16.86302889228563	2.08056478156350	-1.01436630662976
H	-16.52703380997163	4.11152658173189	-0.73249627238504
H	-16.95030409390191	-2.12158532018624	-0.77181249614077
C	-16.45656139152941	0.66235736018462	-1.03425587856604
C	-16.02646779026561	3.15817522384991	-0.81841641127070
C	-14.86556317963113	5.80641694936557	-0.03074970421075
H	-14.19778680349961	6.62884797145463	0.22208426373419
O	-15.32283939782137	0.22091950117410	-1.11314884427236
C	-14.64079078102742	3.30155927241872	-0.62761863214988
C	-14.08262629909821	4.54639529623777	-0.24391133493981
C	-12.70742478068822	4.44856831945318	-0.05091670930301
S	-13.39992884598817	2.04252579923863	-0.76482593123661
S	-11.48376930901145	5.61056755138949	0.45236356326557

```
C    -12.18512650156482      3.16411687627795     -0.29850949651282
C     -7.19045450253761      0.12438942824708     -0.97510225983700
C    -10.27476888657502      4.37135192577175      0.31808088102190
C    -10.79784868171265      3.13962197282970     -0.08777139728843
C     -8.89316629389393      4.19545640966101      0.52346757354785
N     -7.99854413392256      6.32791872818073      1.38483882628146
C     -7.86997513781063      5.05788701202893      1.01618612329908
C     -8.60078071191469      2.83640266576186      0.20495405775479
N     -9.78774681522029      2.20036042561231     -0.14063418574973
N     -6.67988424905190      1.15399143215784     -0.08338905716066
C     -7.26064855152865      2.36171136946441      0.28579913126660
S     -6.53992804492054      6.81293632462926      1.92769636816550
C     -6.53749530153551      4.54366297867594      1.20415942070000
C     -6.24247963107726      3.20317920788091      0.82346554552211
N     -5.69206691676440      5.43609403538007      1.70768497859765
C     -3.07119582577036    -11.67732544425531      0.75903591649449
F     -4.33492741186701    -11.43185025854227      1.16014635346125
C     -5.34208088621175      1.21448119019839      0.24691385581566
C     -5.04731872290658      2.46165867673978      0.80411340445226
C    -10.08321564382959      0.77538646974833     -0.15341578331707
C     -4.22775004184697      0.36994198991038      0.15045306728818
H     -3.98064363979521     -9.17003117527402      0.37508537636353
S     -3.93872974829966     -1.25195079801107     -0.32374419374035
C     -2.26412458856470    -10.41540943576180      0.60369234293625
H     -3.87356122225236     -6.71381462950985     -0.03361423931620
S     -3.37376570471226      2.63556133209422      1.23215135464754
H     -0.36484811588373    -11.43000952365607      0.80361754376776
C     -3.06829458401150      1.00471121966062      0.63853704744933
C     -2.90015504482312     -9.21881827234704      0.39392009758339
O     -3.63518630791551     -3.90723826685891     -0.41943660684303
F    -23.15595966910487     -4.30949062744776      1.13751972973298
C     -2.79326433007750     -6.78513219219710      0.00520280449292
C     -0.85258664506893    -10.47990574293945      0.63377823331009
C     -2.22711883754006     -1.08430724518735      0.08695489477701
C     -1.92581181243774      0.21046002928196      0.57747620974715
C     -2.15717492595948     -8.03236686787935      0.21200708094022
C     -2.47816842208119     -4.27109665950880     -0.29195522086894
C     -2.02550172997654     -5.66810715617595     -0.13044961261688
H     -0.58339624137012      1.68668392859541      1.35531811595196
C     -0.55755812700807      0.66053558532140      0.99099409693579
C     -1.23382312705740     -2.07203029044021     -0.01949708017311
C     -1.26549793605217     -3.43263187253506     -0.23456243976996
C     -0.72756875445677     -8.08665781313337      0.25408113195173
C     -0.10762543034075     -9.34179718246305      0.46635280365302
H     -0.25368438400228     -1.66158904993169      0.17345363235143
```

```
C    -0.60426358527073      -5.70089193981975      -0.08571790886157
H     0.97381903124416      -9.39019187656404       0.50157706506277
C     0.03943280268742      -6.90137561795900       0.09709904968481
C    -0.10440023603034      -4.31459692596166      -0.23104973667273
H     1.11543419663258      -6.97679206106599       0.14095965189786
C     1.21649525502814      -3.95837762544623      -0.39200580477021
H   -15.58248137816105       5.69736072824710       0.78578741351379
C     1.63908232737765      -2.61677218053699      -0.61381969804873
N     1.98812763351553      -1.53021400115383      -0.78896677117841
C     2.28310572143896      -4.89932310833468      -0.38537207706651
N     3.17201912219627      -5.63552657625930      -0.38311824970670
H   -11.08508050565724       0.62580875341713       0.24535901781151
H    -7.66287773239104      -0.69296185713562      -0.43066178855740
H    -9.38717890094904       0.24738752371210       0.49093930963632
F    -2.52414429541326     -12.52045347832721       1.65830297600566
H    -0.15370917062488       0.03624854474201       1.78977454777866
```

	BTF isomer 3		
F	-21.44523584444233	-4.48503030139836	-3.94199209325634
H	-15.26565888024474	6.02347131939636	-0.22987179293681
H	-8.19920549758670	-0.60030104881181	-1.25432831506560
F	-2.39260824034829	-12.32141198113254	0.78539578152376
H	-23.55737794557021	-2.39046779493365	-2.08823265392694
H	-10.22989299792989	-0.14750714440251	-0.91050118500542
H	-23.00943159466386	-0.16894097665981	-1.17140891460555
F	-23.15414253676792	-4.69562631211205	-2.61878530507908
C	-22.53675144421151	-2.13647385780876	-1.84138758178559
N	-21.90016780213165	3.50752916367192	0.76401281892005
C	-22.22886974992725	-0.90122578404063	-1.33492911286883
H	-21.38374830718319	1.42650781108383	-0.35257404504832
C	-21.83569933358568	-4.42603552092655	-2.64677128058337
C	-21.51621735920294	-3.08781185437226	-2.04089476139530
C	-20.74839829847891	3.43326801342439	0.76464355417197
C	-20.89544472326971	-0.55595982740525	-1.01839090304221
C	-20.57747891724068	0.72720926337897	-0.50647545806290
C	-20.21077559550191	-2.79231659119615	-1.73598551050919
C	-19.86387992999541	-1.52503453085864	-1.22804464867190
C	-19.32764340225643	3.36232448129951	0.76952358241299
C	-19.26934184787981	1.04040388035006	-0.23204377750664
H	-19.43291615770036	-3.52871159918927	-1.89330550064176
C	-18.71156733653117	4.50733126200822	1.34564023396522
C	-18.63502965977352	2.26986219978523	0.29137081116056
N	-18.23758889871833	5.44627591301033	1.82240101831439
C	-18.52095481839030	-1.17323212593656	-0.94644174026266
C	-18.25122219777375	0.07725624808136	-0.47887796374739
H	0.10688062974890	0.23456552953964	-1.10058879738058
H	-17.71729059501123	-1.87900522717560	-1.11786647548034
C	-17.19208841416988	2.06596778489663	0.24299943342169
H	-14.06357987361852	6.38462762890321	1.00952244319239
C	-14.80668216823885	5.65410439810439	0.69099712151466
C	-16.93393570793954	0.67819517824369	-0.18249109509537
H	-16.63842526095026	4.01894813781015	0.66535764365866
C	-16.24071595127104	3.04007692883206	0.44482588641553
O	-15.85136214603747	0.12761280269005	-0.29369713570776
C	-14.15885561816435	4.32017578798798	0.47419808875441
C	-14.83837737333630	3.08264692700277	0.37736406822550
H	-6.62751580709901	-1.29299537043713	-0.89744327401859
C	-12.78846420682442	4.15723206893079	0.31482744841053
S	-11.48123980343361	5.32344532101189	0.22831135238961
C	-7.39850614273423	-0.62563611295650	-0.52044228199973

```
S      -13.71081140968992       1.73450338623867       0.13249983160930
C      -12.37106363550558       2.81715114991131       0.16753124782070
C      -10.37110274164459       4.01373258035661       0.01574566649963
N       -8.05630465844380       6.10797898480754      -0.24821100521765
C      -10.96938456124840       2.75130478489572       0.03193754107461
C       -8.99480057509416       3.83086597133862      -0.15367344651727
C       -7.94616430801797       4.78283193656601      -0.25578686785010
N       -6.80995954808158       0.69213638556787      -0.35311542695741
C       -8.75357029965727       2.42237858585174      -0.20738359989431
S       -6.54351500466112       6.69824470714750      -0.39622710145220
N       -9.98715696607487       1.78319378002051      -0.08424766809207
C       -7.40085834337110       1.95697684252406      -0.33036224203561
C       -6.59856542265414       4.32011907520892      -0.38355165798719
F       -2.72998953127695     -11.66803382376051       2.82598607546400
C       -6.34748648736298       2.92163064013244      -0.39951899208133
C       -5.43677985579860       0.85630399226642      -0.39418580114044
N       -5.70443467864462       5.29995143310072      -0.47065245879052
C       -5.13810903396403       2.21921293453625      -0.44582761295927
H       -2.96601752583098      -9.39235244024291       1.66083512955796
C       -4.28417968718207       0.04718901168718      -0.36219295088701
C      -10.29547511534812       0.37124027606823       0.04503537197259
S       -3.90697217361300      -1.62439566968831      -0.17772521634744
C       -1.78238685374594     -11.79362720268491       1.87224237821035
H       -3.17632690406944      -6.95342894600953       1.12319059360808
C       -1.90402546426161      -9.34502904804603       1.45724653929468
O       -3.28334438885165      -4.17168601386205       0.40454493852053
C       -1.12929155739813     -10.47527059952154       1.55153151581520
S       -3.44569738412230       2.56693912849994      -0.50625101695693
C       -3.12079620830354       0.84162325376647      -0.43356302336361
C       -2.10623609624889      -6.93084628941925       0.95705181301351
H      -11.31225477352238       0.27614258376214       0.41746214132835
C       -1.32868976910577      -8.10747970496193       1.10028070073891
C       -2.17256363620267      -1.26476371168322      -0.24779802202409
C       -2.09458810092069      -4.44246386358516       0.35244411337704
C       -1.48886233253765      -5.76919084568546       0.59966749719413
C        0.25745623798658     -10.41943922791041       1.29876020922840
C       -1.93189992702648       0.12359175613612      -0.38885747542285
H        0.85133360061413     -11.31843039686711       1.38036833767016
C        0.07982907884229      -8.04299117320786       0.85583040141309
C       -1.10032844437063      -2.16894149874207      -0.18553934066097
C       -0.98699999902919      -3.52543853316558       0.02953294107928
C        0.84541830637873      -9.22607787514650       0.96980074878106
C       -0.08516125549624      -5.68388952537927       0.38256303244763
C        0.68884260659497      -6.81088843845954       0.50605876646508
H       -0.16375281367420      -1.65510919261877      -0.33271599107399
```

```
H      1.91055147310979      -9.17799442173714       0.78181646314683
C     -0.57975049602381       0.76187368994129      -0.43967147813966
C      0.25649843424301      -4.28634440266697       0.03684957699928
H     -0.65699496850454       1.79060630339501      -0.78999717395224
H      1.75357098728600      -6.80093692345748       0.33561252126737
H    -15.58726075910398       5.62170161543155       1.45071069851537
F    -21.20453451247107      -5.43284395001018      -2.00830715830929
C      1.53483858436570      -3.84094063531178      -0.22796389603362
C      1.85860536435869      -2.49891485478149      -0.56644909802994
C      2.68470291398166      -4.67761361521428      -0.18405821600682
N      2.16068340373599      -1.41857501664428      -0.84047014265116
N      3.64663985539898      -5.31502964454995      -0.15833164445439
H     -7.77237388054272      -1.02955204591797       0.41974781143162
H     -9.63529657108786      -0.10164171536615       0.76686962849611
F     -0.89596780777895     -12.71144084551403       2.30373472756904
H     -0.11911899704398       0.77667089237152       0.55104022711164
```

Table S20. Cartesian coordinates of the methyl-truncated **BTFM** (isomer 1, 2, and 3).

		BTFM isomer 1	
C	-7.38485745160007	2.28822960839710	0.37292558505489
C	-8.70515944382248	2.78391628645115	0.17648186726178
C	-6.36449359360231	3.16320335027184	0.84362451434089
C	-8.95345187984722	4.18552044893010	0.25443548686470
C	-7.92281016212019	5.07749151299692	0.67626978488702
C	-6.62941906758796	4.55025309900228	1.02972157612307
N	-5.78221128153494	5.47492103407595	1.46882638123443
N	-8.01831455294107	6.39049798906199	0.85151960638851
S	-6.58118248682336	6.89746028637702	1.43044411654864
C	-5.18665044351267	2.40196027162709	0.93294022381094
C	-10.31825129279885	4.37014788244670	-0.03664840637542
C	-5.48889453466944	1.10724196603297	0.49605080158071
N	-6.82355681476457	1.03658542991002	0.14834048778040
C	-4.36811828061357	0.26253167824751	0.45720501035771
C	-3.20833792515750	0.94991096903105	0.86974627721878
S	-3.51480704632253	2.61946916817936	1.33293096261224
C	-2.04884740656715	0.18264281985318	0.82142380254545
C	-2.32643238569458	-1.14192757036470	0.40510965168560
S	-4.04682760469729	-1.38058705306659	0.07031228863439
C	-7.34854575925786	-0.05831844704161	-0.65137435768732
C	-0.68238245563435	0.70052788238261	1.15233216795516
H	-0.73795052331619	1.72348470426984	1.52246869210954
H	-0.03189768621672	0.69134291086330	0.27553430030447
H	-0.19860805707150	0.09669473735400	1.92111672229577
N	-9.90403708569454	2.13567748367202	-0.09624666394802
C	-10.88087215549924	3.10352351363472	-0.23048230695578
S	-11.47696930422195	5.65666395866274	-0.16425113125553
C	-12.26551789920591	3.14243327750475	-0.46039113492224
C	-12.73656336701316	4.46895187884565	-0.47196704449882
C	-10.23698851684362	0.73410134210355	0.11757003390221
C	-14.10346233236540	4.58323273547577	-0.71333858659187
C	-14.71349619958598	3.30929587488910	-0.83659628799851
S	-13.52297198433540	1.99990199500574	-0.70447515308114
C	-14.81854780613775	5.89609773891174	-0.80360216387963
H	-14.11691731867864	6.68555827473714	-1.07354108259996
H	-15.27103853307524	6.16654747425171	0.15448772907349
H	-15.61618390225029	5.89013850572409	-1.54492663240921
C	-1.29365957028280	-2.08356148844154	0.26223028983986
C	-16.10526366247406	3.18437039502446	-0.99553676797236
C	-16.97540089227879	2.11424552579097	-1.01809079981177
H	-16.57293219479435	4.15368992483507	-1.07880267223995
C	-1.25767565381738	-3.44318168188534	0.04526602468041
H	-0.32792127079119	-1.62006200555692	0.39945579933482

```
C    -16.60170015242098      0.69820522718784     -0.85975305428753
C    -17.85870579350664     -0.06797934915295     -0.76177520478421
O    -15.47811080540008      0.22781688756206     -0.79933753306622
C     -2.41745366175054     -4.35360650132090      0.06594414630719
C     -1.86645865299575     -5.72589483524377      0.15784648270586
O     -3.59915080786361     -4.05230164777352      0.04436601485407
C    -18.95828456145317      0.82086456279609     -0.89084574604989
C    -18.43214102319661      2.19058941157765     -1.09697763085518
C     -0.44695871234377     -5.66432026239900      0.09835940771137
C     -0.04634681116258     -4.24874030432757     -0.05155110141982
C    -19.21850157057292      3.29843738643644     -1.32528083537669
C      1.23409617378208     -3.80848773500139     -0.30359101750121
C      1.56053469013359     -2.44227223128178     -0.53383755577521
C      2.35546119814547     -4.67828325621900     -0.39620106328776
C    -18.71116753433003      4.60605374288765     -1.56282568837351
C    -20.64006007311512      3.24500368035277     -1.35131029746157
N    -18.33875528499389      5.68161648539087     -1.75827947055806
N    -21.79383926040177      3.23067114172625     -1.37378601452531
N      3.28949732247179     -5.35128514886806     -0.47643814348616
N      1.84279199682267     -1.33903980434318     -0.72355724012863
C    -18.00541278101626     -1.40379139787698     -0.53752374966890
C    -20.23862649618404      0.33100585010710     -0.78277047500624
C    -19.30750400532565     -1.93916921052316     -0.39888768869906
C    -20.42318775594714     -1.04954364881018     -0.52456885229658
C    -19.52190112111603     -3.30386199552655     -0.10773815601364
C    -21.71596261000008     -1.59135790281299     -0.35414326236929
C    -20.79424547022568     -3.76428337032237      0.06869357674674
C    -21.90991572206832     -2.91342439760458     -0.05360830018188
H    -21.11143492359594      0.95619090138311     -0.86866152849541
H    -17.13452246149053     -2.04014660193493     -0.44158376955168
H    -18.68806351533819     -3.98419441468148     -0.00176038988436
F    -21.02831584170782     -5.04341130116680      0.37761478412585
F    -22.78376324073177     -0.79777837606292     -0.46439738748452
F    -23.13626870279143     -3.40001789544136      0.13206979837268
C      0.29038961101540     -6.81901259739706      0.20688348190335
C     -2.54532567619102     -6.89837486430063      0.31377429910711
C     -0.38801787541512     -8.05082802040082      0.38693083906362
C     -1.81929379384135     -8.10805808652783      0.44132791653337
H     -3.62763433884412     -6.90097714849559      0.35519301066058
H      1.36808909854639     -6.82365204188781      0.17292259227377
C      0.32264324221944     -9.26240888625861      0.53663867409078
C     -2.46911298310132     -9.34879883128305      0.63441637999247
C     -1.72761987808006    -10.48635503151323      0.77431254941950
C     -0.32008225159812    -10.45726711153876      0.72752482680779
H     -3.54817719367310     -9.40559104890282      0.68257580817472
```

F	-2.30841672045239	-11.67570377679722	0.96796889925766
F	1.65790336071391	-9.25595984565454	0.50004216012558
F	0.36736577411553	-11.58853871856278	0.87690474146841
H	-9.54689493900093	0.29644132587917	0.83351498629085
H	-10.21571546403717	0.16187781344113	-0.80881658320954
H	-11.23855340885047	0.67474756828324	0.54019657326556
H	-8.05494553934382	0.32577698033287	-1.38277121167871
H	-7.83179535759948	-0.81920556937377	-0.03826791063781
H	-6.52375990937137	-0.52074148622869	-1.19084407934266

BTFM isomer 2		
H	-15.37266937922792	6.00037157116846	-1.09156458605947
H	-6.62324887045129	-1.05469141031447	-0.93769763950176
H	-10.24579468127446	-0.09160731054205	-0.66881017159293
F	-23.68784869027775	-2.78034458432574	-1.71327870175042
F	-23.16836746825122	-0.20617543051786	-1.12878451295128
C	-22.44041286018630	-2.38872135335269	-1.45705408020709
N	-21.90988214395876	3.72836715466861	-0.10999462681488
C	-22.15989310857998	-1.08132181754302	-1.15899740665405
F	-21.70866208408451	-4.59123605207214	-1.80209024624130
H	-8.16887383590829	-0.27021169496244	-1.22330140722905
C	-21.39222751153498	-3.32844287304170	-1.49736404433950
C	-20.75818500614268	3.65656134683363	-0.08952899343954
H	-21.37638074612861	1.41807674512151	-0.61944791974903
C	-20.84110350364860	-0.64311734254635	-0.90361205113888
C	-20.55714408558319	0.71885403174441	-0.63779181317403
C	-20.10140660243218	-2.96754547112436	-1.24373997689101
C	-19.33680860929427	3.60054820805195	-0.05599248902441
C	-18.74246839628368	4.87348432445061	0.16707998654145
N	-18.30549895431605	5.92718196130565	0.34832900921923
C	-19.79600984939171	-1.62174041630092	-0.94667266684675
H	-0.05932551330980	0.68344126644514	-0.54802147974548
H	-19.32079356211452	-3.71466280640755	-1.28563481868831
C	-19.25121490718525	1.10101380562079	-0.43782520889009
C	-18.63122980982383	2.42644858524970	-0.21123582143632
C	-18.46650574043521	-1.19612409738278	-0.71333844800747
C	-18.22145808111199	0.12265634827503	-0.47678362302939
C	-17.18509974465650	2.22795749732008	-0.17550180095266
H	-16.63429703792876	4.22633220925618	-0.09297945965833
H	-17.64898149604548	-1.90578453996093	-0.74218562420834
C	-16.23526582038790	3.22354047707617	-0.12257570282952
C	-16.91413882528964	0.78343214432862	-0.27704257868981
C	-14.81953991419875	5.83721694400375	-0.16393156086930
H	-14.07780892393626	6.63003319409244	-0.07242443538268
C	-14.82974927157185	3.25525153898216	-0.12742160480711
O	-15.83083763033541	0.22634206415545	-0.21808938541115
C	-14.15247737513951	4.49693880086915	-0.14984842258765
S	-13.69398019410818	1.89044111622837	-0.12592243307155
C	-12.77432394088807	4.32269606347039	-0.16711974343905
S	-11.45580146546769	5.47832923536933	-0.20104802302634
C	-12.35399205328914	2.97478611743964	-0.14531906566869
C	-10.34000486255989	4.15708658894144	-0.17025033550285
C	-7.39983219498267	-0.44778390318597	-0.47690164078378
C	-10.94599014712693	2.89728864322069	-0.14538865337002

```
C      -8.95409647759719        3.96734735679596       -0.10555608479006
N      -7.99199231004568        6.23066701000920        0.02383413616223
N      -9.96182436416318        1.92322212487142       -0.07921220811124
C      -8.72169984253353        2.56030867952103       -0.06641907467617
C      -7.89342647674144        4.90512426937052        0.01316365056739
N      -6.80590752276197        0.81041551337656       -0.05572146556854
C      -7.37324265132486        2.08198469636895        0.01076288546157
S      -6.48251264468311        6.80490451314569        0.25108405265063
C      -6.55462696657941        4.42633500391824        0.19682420900613
C      -6.31300256092897        3.02388991257316        0.18106198069399
N      -5.65894198868863        5.39734356410542        0.34192734983154
C      -5.43869477917812        0.94009606094025        0.10653765900994
C     -10.27568240790448        0.53617571647286        0.22077049106489
C      -5.11883804617849        2.29354801053701        0.25280986438921
C      -4.30372237664863        0.10651348279099        0.12275662022129
F      -3.27331897268117       -9.58995481612712        1.26771354484290
F      -1.70025189507596      -11.77627239252181        1.50446163067293
S      -3.96269819440020       -1.58167603110372        0.05090867854280
H      -3.27334462547716       -7.09122491015358        0.82905209542588
S      -3.42365665207431        2.59863838385553        0.41399106818033
C      -3.12886328247631        0.87207958875925        0.27733119724692
C      -1.94924812860950       -9.46625368799902        1.12287037299231
O      -3.38753785695770       -4.24345801516257        0.31364367908767
C      -1.16487298537955      -10.58256929435403        1.25074317692706
C      -2.19920929615986       -7.03690372957231        0.71452644412733
C      -2.22564580063198       -1.25945094610357        0.16998442042569
C      -1.95656333723558        0.12503601666644        0.29200162281041
C      -1.39859058492657       -8.19750254970390        0.84691667462648
C      -2.19728323996345       -4.50652078911482        0.28141852860133
C       0.23187488737715      -10.46491513081811        1.10838280183540
F       0.95810318088164      -11.57846206653327        1.24882612630187
C      -1.58534453154607       -5.84682508527488        0.44844618888147
H      -0.65422550317702        1.76788414241584        0.71390131296150
C      -0.58944289231157        0.72488273285372        0.40566880262068
C      -1.17095920995478       -2.18516458272985        0.10773873802429
C       0.02266848234734       -8.10546533314162        0.69751134410204
C      -1.08180501284442       -3.55980405641490        0.09018347972959
C       0.82124295764019       -9.26448498362260        0.83887172413475
H      -0.22093435871032       -1.67394049361727        0.09238206700575
C      -0.17628538959630       -5.73431459838242        0.29015610210356
H       1.89575020094840       -9.21066574994365        0.72893454622173
C       0.61533304920345       -6.84956884699819        0.41294112609069
C       0.15785230081948       -4.32118659476383        0.01124319192981
H       1.68703329226169       -6.80966193866798        0.29941564895153
C       1.41593856728442       -3.86075874975684       -0.31507042646674
```

H	-15.53287593647296	5.95104690744589	0.65295010935927
C	1.70027710919689	-2.50998968885385	-0.65946119260834
N	1.95704703017633	-1.42027359321225	-0.94214835873361
C	2.56593722788508	-4.69618966857215	-0.37101977609422
N	3.52293849848745	-5.33934752703168	-0.42430443678036
H	-11.27823826758434	0.49296219034641	0.64067027614359
H	-9.58631899517283	0.14761554172233	0.96627619305166
H	-7.82371752914766	-1.00222061148493	0.36030822454115
H	0.02623027766550	0.20015550846585	1.13561800137075

	BTFM isomer 3		
H	-15.28232120343624	6.11743185862599	-0.15906974724497
H	-6.55894320608984	-0.71396482384721	-1.31478940782545
H	-10.14127035755072	0.17207101670708	-0.91350867594564
F	-23.50764764153315	-2.93251094786215	-1.82045091851692
H	-22.81761050819400	-0.50991991513246	-1.19361657260520
C	-22.25489559408162	-2.50401827521111	-1.63291653586849
N	-21.81231987106411	3.50502166057691	-0.21403098566966
C	-21.99780526698454	-1.20605724912977	-1.30683291434415
F	-21.50651275909883	-4.70191810063773	-2.10419841051780
H	-8.07749716131946	0.15268851286154	-1.48269982526852
C	-21.21415461211550	-3.44219356156476	-1.78413721258977
C	-20.65872269975992	3.47144234183054	-0.19203461802145
H	-21.21607447894784	1.24190043860997	-0.68279700554179
C	-20.66239060302833	-0.77932253309978	-1.12580079807781
C	-20.38225290750533	0.56977489790015	-0.80077511258400
C	-19.91475284751194	-3.04313965224918	-1.60441133396192
C	-19.23681885782111	3.45370243525287	-0.15389962593106
C	-18.68018355460249	4.73660870070551	0.10412146168785
N	-18.27511398379140	5.79757345026769	0.31547731071748
C	-19.58619053819431	-1.71064001137687	-1.27922419614874
H	-0.02261213071568	0.67823623915689	-1.02434723390955
F	-18.93892308418955	-3.94909691039746	-1.74425690406261
C	-19.08005030702679	0.98017783794799	-0.65554576488345
C	-18.49725992328829	2.30598178978239	-0.35393341575722
C	-18.24888039254245	-1.26993445753153	-1.12424598628461
C	-18.02467080122418	0.04346653401661	-0.82853700000636
C	-17.04989090607393	2.14676956460991	-0.33176680569030
H	-16.58295409838224	4.09567230073398	0.20308746685159
H	-17.42211530340121	-1.95574294176684	-1.24978394033361
C	-16.14226064921418	3.13745665790801	-0.02504059823914
C	-16.73044662781829	0.74360828232991	-0.65759015371051
C	-14.82612488449385	5.71093169618634	0.74582156713332
H	-14.12626717651747	6.45019336213805	1.13359392084663
C	-14.74562025819388	3.20621558794299	0.09116723883918
O	-15.62111824321460	0.25096922797285	-0.77491082937152
C	-14.11814338753363	4.41937389786155	0.47079520631950
C	-12.73854362690486	4.27323231491664	0.54469161317119
S	-13.56263296223624	1.91224986979571	-0.17786945289828
S	-11.45684914946768	5.41338638478926	0.92216462909124
C	-12.27455189058863	2.97830016863204	0.23681581848112
C	-10.29652652687555	4.15717944993531	0.65145848338351
C	-7.33847947552691	-0.19225426646547	-0.76404677817465
C	-10.87102322013618	2.92725116217491	0.31694395865815

C	-8.90508163746524	3.98110270832213	0.67646169469755
N	-7.96653906541049	6.15812977616286	1.33561526737597
N	-9.87413020004012	1.98418252414650	0.15529720601162
C	-8.64732433439040	2.61739779665699	0.34728116753544
C	-7.84904588788235	4.88165144185692	0.98413832245372
N	-6.73467400385665	0.93911194231920	-0.08048912892762
C	-7.29418558209914	2.16428000293867	0.26826416732561
S	-6.45595355598702	6.70393417298518	1.61508708021675
C	-6.49107167262129	4.41311206162161	0.96025061152242
C	-6.22794175260410	3.06428706630601	0.58148193129735
N	-5.60592175809067	5.34634041057386	1.29863496490672
C	-5.36421006352348	1.05073589634911	0.02812711698872
C	-10.18935048153990	0.56657120559545	0.10063378745486
C	-5.02736165474590	2.34941909004589	0.41658835586887
C	-4.24964111499358	0.21573774907480	-0.15401112433143
F	-3.56755316499247	-9.08860570636059	1.96547942103920
F	-2.10976929285286	-11.31416476933875	2.41676803259810
S	-3.96932653414746	-1.45496839943645	-0.43530073136080
H	-3.49486277301922	-6.74396126297382	0.98889554333269
S	-3.31404055004567	2.60729496732880	0.51584316379611
C	-3.05120455743744	0.93112103380719	0.04398667188389
C	-2.27584332621940	-9.11059229533892	1.61143952721943
O	-3.53361713694957	-4.08677269513377	-0.09989964640717
C	-1.54889512034162	-10.24814859545699	1.84614149638847
C	-2.44093714889381	-6.79604310541000	0.75312653845163
C	-2.22171071389580	-1.19330020041290	-0.37178955606605
C	-1.90127591078065	0.16306250779308	-0.12334048249368
C	-1.69717091179097	-7.97062188139541	1.01472935353289
C	-2.35527241726409	-4.39734374216131	-0.12845737122586
C	-0.18883869005728	-10.28569092037612	1.47618304441642
F	0.48045694317917	-11.41989804126909	1.70777901778434
C	-1.79540797972561	-5.72346879585785	0.21156074453388
H	-0.51891918235395	1.74225810725529	0.29402897200720
C	-0.50798295842238	0.70761930531574	-0.04635004946299
C	-1.21442394406877	-2.16401383505444	-0.51850002637965
C	-0.30728770570076	-8.02289960288881	0.67061899563531
C	-1.20689517646418	-3.54157450232372	-0.48815641542046
C	0.42623325490847	-9.20856920901569	0.90745415809708
H	-0.24172141533981	-1.70266262265904	-0.60625306885130
C	-0.40538801315719	-5.73198788170315	-0.08789169626691
H	1.47267350690670	-9.27166049724878	0.64147728599824
C	0.32312339555290	-6.87874950385149	0.11534777233862
C	-0.01883023867817	-4.38401993881707	-0.56292359820247
H	1.37397034064481	-6.94103619454890	-0.12058487852561
C	1.23839788389400	-4.02732757792151	-0.99951107460525

H	-15.62731437388915	5.59571285918233	1.47653261092462
C	1.56087086241550	-2.73034955159194	-1.49018056917251
N	1.84466305335049	-1.68296500872931	-1.88476773347520
C	2.34812660635221	-4.91759687623395	-0.99932715281997
N	3.27498878178065	-5.60560009207774	-1.00457606977627
H	-11.20032512519219	0.42671385166172	0.47706202045734
H	-9.51753776296261	0.00666005566378	0.74389805080175
H	-7.79781080493628	-0.89526494904218	-0.06996761234660
H	0.11717166854131	0.13699805496950	0.64048933572955

19. Integrated Photocurrent Device Analysis

D18-Cl:BTFM and **D18-Cl:BTF** solar cells with and without 1-CN additive were studied, characterized by integrated photocurrent device analysis (IPDA) under an inert N_2 environment. Illumination intensity was varied approximately 30 to100 mW/cm^2 using a simulated AM 1.5G light source and neutral density filters. All IPDA measurements were performed using previously discussed fully automated system.[1, 7, 10] Impedance and photocurrent measurements were conducted on a Solartron 1260 impedance analyzer using an AC amplitude of 100 mV operating in the frequency range of 100 Hz to 5 MHz (Figs. S72, S73). Photocurrent and chemical capacitance data from Figures S76 and S77 were used to calculate device parameters in Figure 9. All calculations and data analyses were conducted using a publically available IGOR software, Flexible Electronics Data Management System (FlexEDMS), https://github.com/MikeHeiber/FlexEDMS.
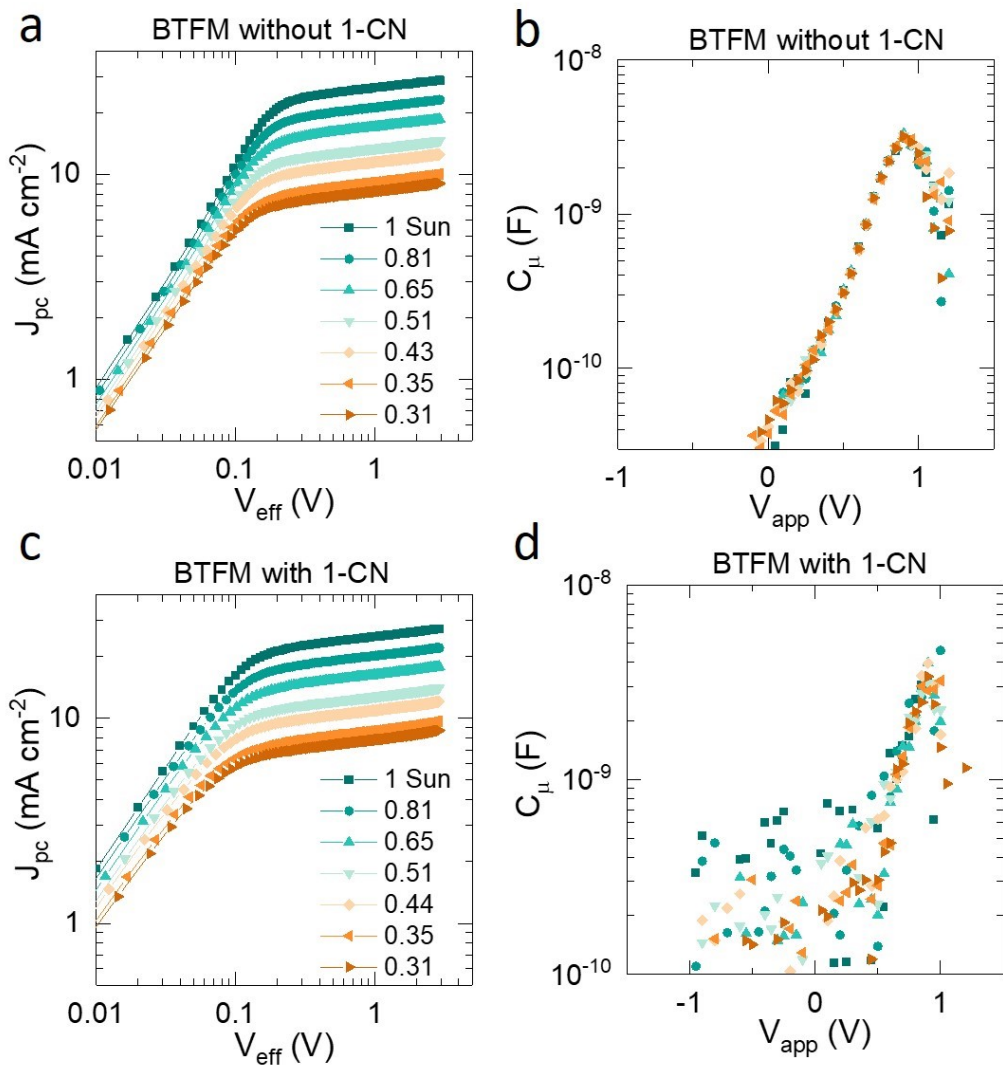
Figure S76. (a) Photocurrent (J_{pc}) versus effective voltage ($V_{eff} = V_{OC} - V_{app}$) for a **D18-Cl:BTFM** cell without 1-CN additive at different illumination intensities, where V_{app} and V_{OC} are applied voltage and open-circuit voltages, respectively. (b) Chemical capacitance (C_μ) versus V_{app} for the same BTFM cell without 1-CN additive at different illumination intensities shown in the legend in (a). (c), (d) $J_{pc} - V_{eff}$ and $C_\mu - V_{app}$ plots for a BTFM cell with 1-CN additive at different illumination intensities shown in the legend in (c), respectively.
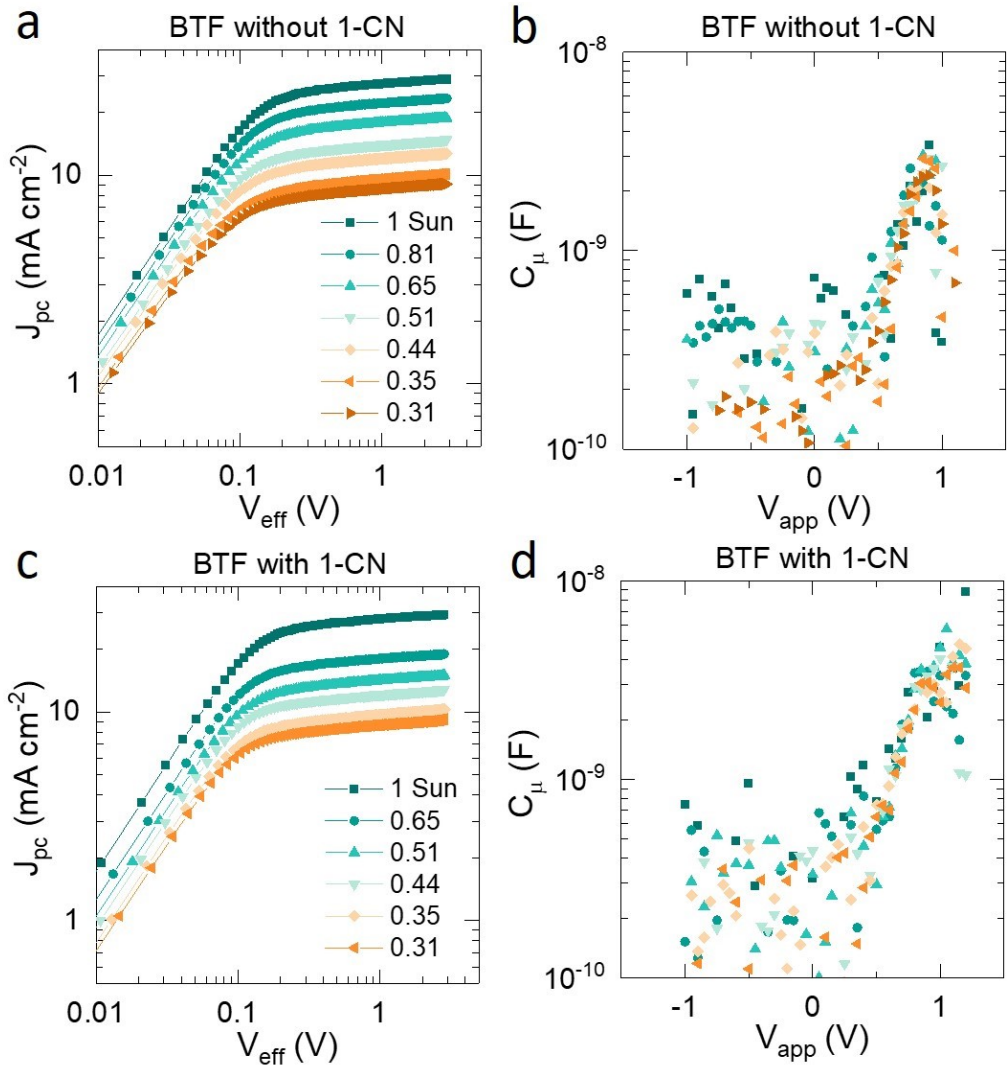
Figure S77. (a), (b) $J_{pc} - V_{eff}$ and $C_\mu - V_{app}$ plots for a **D18-Cl:BTF** cell without 1-CN additive at different illumination intensities shown in the legend in (a), respectively. (c), (d) $J_{pc} - V_{eff}$ and $C_\mu - V_{app}$ plots for a BTF cell with 1-CN additive at different illumination intensities shown in the legend in (c), respectively.

20. References

1. N. Su, R. Ma, G. Li, T. Liu, L.-W. Feng, C. Lin, J. Chen, J. Song, Y. Xiao, J. Qu, X. Lu, V. K. Sangwan, M. C. Hersam, H. Yan, A. Facchetti and T. J. Marks, *ACS Energy Lett.*, 2021, **6**, 728-738.

2. O. V. Dolomanov, L. J. Bourhis, R. J. Gildea, J. A. Howard and H. Puschmann, *J. Appl. Crystallogr.*, 2009, **42**, 339-341.

3. V. Elakkat, C.-C. Chang, J.-Y. Chen, Y.-C. Fang, C.-R. Shen, L.-K. Liu and N. Lu, *Chem. Commun.*, 2019, **55**, 14259-14262.

4. N. Lu, W.-H. Tu, Y.-S. Wen, L.-K. Liu, C.-Y. Chou and J.-C. Jiang, *CrystEngComm*, 2010, **12**, 538-542.

5. N. Lu, V. Elakkat, J. S. Thrasher, X. Wang, E. Tessema, K. L. Chan, R.-J. Wei, T. Trabelsi and J. S. Francisco, *J. Am. Chem. Soc.*, 2021, **143**, 5550-5557.

6. G. Li, X. Zhang, L. O. Jones, J. M. Alzola, S. Mukherjee, L.-W. Feng, W. Zhu, C. L. Stern, W. Huang, J. Yu, V. K. Sangwan, D. M. DeLongchamp, K. L. Kohlstedt, M. R. Wasielewski, M. C. Hersam, G. C. Schatz, A. Facchetti and T. J. Marks, *J. Am. Chem. Soc.*, 2021, **143**, 6123-6139.

7. L. W. Feng, J. H. Chen, S. Mukherjee, V. K. Sangwan, W. Huang, Y. Chen, D. Zheng, J. W. Strzalka, G. Wang, M. C. Hersam, D. M. DeLongchamp, A. Facchetti and T. J. Marks, *ACS Energy Lett.*, 2020, **5**, 1780-1787.

8. J. Schindelin, I. Arganda-Carreras, E. Frise, V. Kaynig, M. Longair, T. Pietzsch, S. Preibisch, C. Rueden, S. Saalfeld, B. Schmid, J. Y. Tinevez, D. J. White, V. Hartenstein, K. Eliceiri, P. Tomancak and A. Cardona, *Nat Methods*, 2012, **9**, 676-682.

9. J. Ilavsky, *J. Appl. Crystallogr.*, 2012, **45**, 324-328.

10. W. G. Zhu, A. P. Spencer, S. Mukherjee, J. M. Alzola, V. K. Sangwan, S. H. Amsterdam, S. M. Swick, L. O. Jones, M. C. Heiber, A. A. Herzing, G. P. Li, C. L. Stern, D. M. DeLongchamp, K. L. Kohlstedt, M. C. Hersam, G. C. Schatz, M. R. Wasielewski, L. X. Chen, A. Facchetti and T. J. Marks, *J. Am. Chem. Soc.*, 2020, **142**, 14532-14547.

11. E. Gann, T. Crofts, G. Holland, P. Beaucage, T. McAfee, R. J. Kline, B. A. Collins, C. R. McNeill, D. A. Fischer and D. M. DeLongchamp, *J. Phys.: Condens. Matter*, 2021, **33**, 164001.

12. R. M. Young, S. M. Dyar, J. C. Barnes, M. Juricek, J. F. Stoddart, D. T. Co and M. R. Wasielewski, *J. Phys. Chem. A*, 2013, **117**, 12438-12448.

13. F. Neese, *J. Comput. Chem.*, 2003, **24**, 1740-1747.

14. K. Raghavachari, *Theor. Chem. Acc.*, 2000, **103**, 361-363.

15. N. D. Eastham, J. L. Logsdon, E. F. Manley, T. J. Aldrich, M. J. Leonardi, G. Wang, N. E. Powers-Riggs, R. M. Young, L. X. Chen, M. R. Wasielewski, F. S. Melkonyan, R. P. H. Chang and T. J. Marks, *Adv. Mater.*, 2018, **30**.

16. Y. Firdaus, V. M. Le Corre, S. Karuthedath, W. Liu, A. Markina, W. Huang, S. Chattopadhyay, M. M. Nahid, M. I. Nugraha, Y. Lin, A. Seitkhan, A. Basu, W. Zhang, I. McCulloch, H. Ade, J. Labram, F. Laquai, D. Andrienko, L. J. A. Koster and T. D. Anthopoulos, *Nat. Commun.*, 2020, **11**, 5220.
17. R. Izsák and F. Neese, *J. Chem. Phys.*, 2011, **135**, 144105.
18. F. Weigend and R. Ahlrichs, *PCCP*, 2005, **7**, 3297-3305.
19. S. Grimme, S. Ehrlich and L. Goerigk, *J. Comput. Chem.*, 2011, **32**, 1456-1465.
20. F. Neese, *Wiley Interdisciplinary Reviews: Computational Molecular Science*, 2012, **2**, 73-78.